ONLINE SORTING OF WOOD TREATED WITH CHROMATED COPPER ARSENATE USING LASER INDUCED BREAKDOWN SPECTROSCOPY

By

THOMAS M. MOSKAL

A THESIS PRESENTED TO THE GRADUATE SCHOOL
OF THE UNIVERSITY OF FLORIDA IN PARTIAL FULFILLMENT
OF THE REQUIREMENTS FOR THE DEGREE OF
MASTER OF SCIENCE

UNIVERSITY OF FLORIDA

2001

Dedicated to the memory of Angela Smith, or as known by a little boy that could never figure out how to say Nana, she was simply Na. In addition to being a beloved grandmother, she was a caregiver, protector, role model and one of my first teachers. Her love and guidance played a profound role in shaping the character of that little boy and the man he grew up to be.

ACKNOWLEDGMENTS

I would like to thank Dr. David Hahn, for the guidance, enthusiasm and leadership he provided during my course of study. His teaching abilities in the classroom, his lab or in the field were invaluable. He has been an advisor, mentor and friend.

I would also like to express my gratitude to the United States Navy, Civil Engineer Corps, for providing me with this opportunity to attend the University of Florida. They are an organization that pursues excellence through vision and a "can do" spirit that I am deeply proud to be associated with.

Most of all, I want to thank my wife, Beth, for her support and encouragement during this past year. Her ability to take care of the family while working full time was truly amazing. While an often tiring and sometimes thankless role, her efforts are deeply appreciated.

TABLE OF CONTENTS

LIST OF TABLES

LIST OF FIGURES

Abstract of Thesis Presented to the Graduate School
of the University of Florida in Partial Fulfillment of the
Requirements for the Degree of Master of Science

ONLINE SORTING OF WOOD TREATED WITH CHROMATED COPPER ARSENATE USING LASER INDUCED BREAKDOWN SPECTROSCOPY

By

Thomas M. Moskal

August, 2001

Chairman: Dr. David W. Hahn
Major Department: Mechanical Engineering

The use of the CCA chemical as a wood treatment to protect against insect and fungal deterioration has had commercial application for the past twenty-five to thirty years. While CCA treated wood has several benefits, with perhaps the most important being the saving of an estimated 225 million trees annually due to its longer service life, there are growing concerns that the handling and disposal of CCA treated wood may have negative impacts on human health and the environment. Because CCA treated wood has a service life of nearly thirty years, the amount of CCA treated wood that will be disposed of is expected to dramatically rise in the near future. The disposal of the metals contained within CCA treated wood by incineration, land applications as landscape mulch or disposal in a landfill will all fail to meet leaching protocols established by the EPA. While there is an exemption in place for CCA treated wood to be disposed of in unlined construction and demolition landfills, there is a need to detect and sort CCA treated lumber from untreated lumber quickly and accurately with an online method.

Sorting would allow the continued disposal of untreated wood as landscape mulch and in biomass combustors while easing the burden on landfills.

This work details the design and evaluation efforts to develop an online detector using laser induced breakdown spectroscopy (LIBS) technology. By forming a plasma on the surface of the wood, the detector analyzed the spectral emission from the plasma to identify the metals present in the wood sample. This analytical process was performed twice per second with the demonstrated potential to increase to ten times per second. In addition to this rapid sampling and analysis, the results of this work demonstrated accuracies approaching 100%.

With the cost effective development of an online LIBS detector for CCA treated wood, regulators and industry have a useful tool to meet the challenges of CCA treated wood disposal.

CHAPTER 1
INTRODUCTION AND BACKGROUND

The use of preservative treatment processes to extend the useful service life of wood products by protecting them from insect and fungal deterioration dates back to the 19th century. The first treatment was an oil based preservative named creosote that emerged prior to 1900. Creosote is a distillate of coal tar that is comprised of a mixture of over 100 chemical compounds. In addition to being carcinogenic, this treatment produced a surface that was unattractive, difficult to paint and released odors, yet it was the predominant process until the commercial introduction of Chromated Copper Arsenate (CCA) in the1970's (Solo-Gabriele *et al.* 1998). However, since the introduction of CCA, creosote market share has fallen from over 50% of treated wood products to 14.6% while CCA has risen to over 70% by volume of all treated wood products sold in 1996 (American Wood Preservers Institute [AWPI] 1996). Additionally, the overall volume of treated wood has increased. During the period from 1970 to 1996, the volume of treated wood has increased from 248 to 591 million cubic feet (AWPI 1996).

The benefits of CCA treated lumber are numerous. The CCA treatment produces virtually no odor once the wood is dry, the chemicals do not corrode standard mechanical fasteners, decrease the strength of the wood nor reduce the climability of utility poles (Solo-Gabriele *et al.* 2000). Furthermore, since it is a waterborne preservative the surface of the wood can easily be painted or stained. The most significant advantage claimed by

the industry is that while untreated southern pine lumber exposed to the weather has a service life of only a few years, CCA treated wood has a useful life of at least 25 years, saving approximately 225 million trees annually (Matus 2001, March 25). This is particularly important in the southeastern United States where wood has the greatest deterioration potential due to a climate that promotes fungi and insect proliferation along with the coastal requirements for marine grade products (Solo-Gabriele *et al.* 1998).

The process used to pressure treat lumber with CCA involves placing a load of lumber on racks into the treatment chamber, evacuating the atmosphere and adding the waterborne CCA chemical. The water carries the CCA into the wood fibers by diffusion under high pressure and is then evaporated either through natural processes or kiln drying, leaving behind the CCA chemical (Solo-Gabriele *et al.* 2000).

The arsenic in CCA protects the wood from insects while the copper acts as a fungicide. The role of the chromium is to "fix" the copper and arsenic in the wood to maintain an effective chemical concentration within the wood for the duration of its useful life. The CCA retention level specified is dependent on the application of the wood. Common recommendations are a retention value of 0.25 pounds of CCA per cubic foot of wood (pcf) for above ground, 0.40 pcf for ground/freshwater contact, 0.60 pcf for salt-water splash and wood foundations and 2.50 pcf for saltwater immersion (American Wood Preservers Association [AWPA] 1996).

The CCA chemical comes in three formulations, types A, B and C. Type C, the most common formulation, is composed of 47.5% CrO_3, 18.5% CuO, and 34.0% As_2O_5. Type A contains 65.5% CrO_3, 18.1% CuO, and 16.4% As_2O_5 while type B contains 35.3% CrO_3, 19.6% CuO, and 45.1% As_2O_5. Therefore, since the average density of

southern pine is approximately 34 lbs/ft^3, and taking into consideration the three formulations and the range of four retention levels, elemental metal concentrations may range from 1400 to 25,000-ppm for chromium, 1100 to 11,600-ppm for copper and 800 to 21,600-ppm for arsenic. To determine average values, in 1996 28.3 x 10^6 ft^3 of CCA treated wood was sold in Florida and Georgia containing 6.0 x 10^6 lbs of CrO_3, 2.3 x 10^6 lbs of CuO and 4.3 x 10^6 lbs of As_2O_5 (Solo-Gabriel *et al.*1998). Therefore, the average piece of CCA treated lumber contained elemental metal concentrations of approximately 3200-ppm chromium, 1900-ppm copper and 2900-ppm arsenic.

1.1 Environmental Concerns

The concerns regarding CCA treated wood began with the realization that the CCA preservative was responsible for elevated toxic metal concentrations in the wood ash from biomass combustors (Atkins and Fehrs 1992; Fehrs 1995; McGinnis 1995). The quantities of arsenic and chromium present in the ash were sufficient to result in failure to meet the Toxicity Characteristic Leaching Procedure (TCLP) levels required by the EPA (Gaba and Steever 1995). The failure to meet these levels requires the ash to be treated as a hazardous waste, greatly increasing the disposal costs. It is important to note that while the disposal of CCA treated lumber by the end user has a hazardous waste exemption in the code of federal regulations under 40 CFR 261, the ash produced from the combustion of wood is not exempt (Solo-Gabriele *et al.* 1999). Due to the metal emissions, CCA producers do not recommend the combustion of CCA treated wood.

Further research by Solo-Gabriele *et al.* established that if CCA wood and untreated wood were mixed, CCA wood treated at the 0.25 pcf retention level could make up no more than 2 % of the wood combusted in order for the resulting ash to meet the

federal limits for arsenic of 41 mg/kg. Wood at the 0.6 and 2.5 pcf retention levels could make up no more than 0.9% and 0.2% of the mixed wood respectively, while still meeting federal limits. They also concluded that with the stricter requirements present in the state of Florida, wood fuel would have to be free of CCA wood to meet the State limits. The actual metal concentrations for unmixed CCA treated wood ash were found to be 4%, 13% or 39% for 0.25, 0.60 and 2.50 pcf respectively. It is estimated that Florida burned 2.5 million of the 3.7 million cubic feet of CCA treated wood disposed of in 1996 (Solo-Gabriele *et al.* 1998).

In order to allow the continued burning of wood for an energy source while reducing the landfill burden of disposed wood, Solo-Gabriele *et al.* (1999) investigated the use of solvents to extract the metals from the mixed wood ash with the intent to reduce the TCLP results below regulatory limits while also reclaiming the metals for reuse. While their tests proved successful in recovering between 41%-100% of the three metals, CCA manufacturers demand relatively pure metal solutions for their treatment processes. As a result, it is questionable whether extraction is a viable economic alternative at this time. This left three choices regarding burning of wood waste:

1. Sort the wood waste prior to shredding to remove the treated wood from the fuel stream.

2. Continue burning mixed fuel and dispose of the ash as hazardous waste.

3. Stop burning wood waste and divert to other disposal methods.

While the third option places an increased burden on landfills, it is the primary option currently chosen. However the land disposal of CCA treated wood has also received attention from the Florida Department of Environmental Protection (FDEP) and

researchers in the last two years since the primary disposal paths for discarded wood are construction and demolition (C&D) debris landfills and C&D debris recycling facilities. CCA treated wood makes up between 6% and 30% of the wood in the C&D wood waste stream. Unlike municipal solid waste landfills, C&D landfills are unlined, allowing rainwater to migrate through the landfill creating leachate that has the potential to migrate through the soil below to the groundwater. Some of the CCA wood that is sent to C&D recycling facilities is visually sorted out for reuse or landfill disposal, however this can be quite difficult since weathered CCA wood is virtually indistinguishable from untreated wood. The result is that CCA wood still makes up a portion of the wood that ends up as landscaping mulch or boiler fuel (Townsend *et al.* 2001).

While recognizing the current exemption in 40 CFR 261, investigations into the leaching characteristics of unburned CCA treated wood were undertaken. Although the Environmental Protection Agency (EPA) states in their Resource Conservation and Recovery Act (RCRA) Manual that,

> Discarded arsenically treated wood or wood products that are hazardous only because they exhibit certain toxic characteristics (e.g. contain harmful concentrations of metal or pesticide constituents), are excluded from the definition of hazardous waste. Once such treated wood is used, it may be disposed of by the user (commercial or residential) without being subject to hazardous waste regulation. This exclusion is based on the facts that the risks posed by the use of such wood products on the land is identical those posed by the woods disposal . . . (EPA 2001, p. III-17)

The results of TCLP tests indicated that half of the samples exceeded the regulatory limits for arsenic and would be classified as hazardous waste if the exemption was not in place. While the TCLP test is intended to simulate leaching process of the wood subjected to the acidic conditions experienced in a landfill, additional Synthetic Precipitation Leaching Procedure (SPLP) tests were also performed to simulate the

effects of precipitation on wood that is surface applied to the land. All of the results exceeded Florida's Ground Water Cleanup Target Levels (GWCTL) for each of the three metals (0.05 mg/l, 0.10 mg/l and 1 mg/l for arsenic, chromium and copper, respectively) (Townsend *et al.* 2001). These results demonstrate that while the chromium may "fix" the copper and arsenic in the wood from a performance standpoint, sufficient leaching occurs resulting in the failure of standardized EPA tests. Due to the size reduction in mulch, resulting in a much greater surface area for leaching, mulch made from wood waste must contain at least 99.9% untreated wood to meet Florida's industrial soil cleanup target levels of 3.7 mg/kg. Mulch meeting Florida's residential soil cleanup target levels of 0.8 mg/kg must be CCA free (Solo-Gabriele *et al.* 2000). Therefore, the researchers suggest that CCA treated wood not be allowed to be used in mulch and to prohibit the disposal of CCA treated wood in unlined landfills (Townsend *et al.* 2001).

1.2 Public Policy and Awareness

Since chromium and arsenic are two of the seven listed RCRA metals (As, Be, Cd, Cr, Pb, Hg and Se), it is also important to examine public policy and perceptions along with their impact on political decisions. While the EPA considered banning CCA treated wood nearly twenty years ago because "potential dermal exposure and inhalation exposure may occur to persons involved in handling and sawing pesticide treated wood, contacting treated playground equipment or other treated structures with unprotected skin," they determined "the economic impact which would result from across the board cancellation would be immense" (Hauserman 2001, March 11). Instead, after lobbying by the wood treatment industry, the EPA instituted a voluntary consumer awareness program where fact sheets detailing proper handling and disposal methods were to be

distributed at retail locations selling CCA treated wood. However since even the industry concedes that most consumers do not receive the sheets, United States Senator Bill Nelson, after unsuccessfully urging the Director of the EPA Christine Todd Whitman to make the warning labels mandatory, recently filed legislation to require warning labels on every piece of CCA treated lumber sold in the United States (Matus 2001, April 5, April 9, May 9).

Lawmakers also recently debated lowering the federal drinking water standards for arsenic from 50 parts per billion to 10 parts per billion, requiring landfill liners at C&D landfills and a ban on CCA lumber at playgrounds (Matus 2001, February 22, April 5, May 4). Each of these restrictions ultimately failed after intense lobbying from the CCA treatment companies, which constitute a $4 billion industry.

Since the beginning of this year in Florida, over twenty-five articles on CCA wood were published in the *Gainesville Sun* and *St. Petersburg Times*. In addition to covering the regulatory decisions, they also detailed several cases of the 40 reported incidents where people working with CCA treated wood were treated for arsenic poisoning after sawing wood, getting a splinter, burning treated wood in a stove or simply handling the wood. The results of poisoning ranged from amputation of fingers infected with CCA splinters to massive hair loss and neurological disorders including seizures, blackouts, partial paralysis and memory loss after burning CCA wood in a stove (Matus 2001, March 25, April 1). However, the primary focus was on leaching of arsenic from local playground equipment resulting in elevated arsenic concentrations in the playground soil. Some of the results showed concentrations ninety-six times higher than the residential soil cleanup target level standards of 0.8 mg/kg (Hauserman 2001, March

15). After conflicting statements and internal disagreement within the FDEP and Florida Department of Health on the risks posed by the soil, over a dozen playgrounds were closed in April and May 2001 (Hauserman 2001, March 11, March 15, March 16; Matus 2001, March 17, March 19, March 22, March 23). As a result of these public concerns, the EPA is currently conducting a comprehensive evaluation of CCA treated wood use including an assessment of children's exposure to CCA treated wood in playgrounds (Fields 2001).

The arsenic leaching from the CCA treated playground structures should not come as a surprise. Stilwell and Gorny (1997) found arsenic concentrations in soil averaging 76 mg/kg below treated decks in Connecticut while the background concentrations (i.e., control samples) were only 3.7 mg/kg on average. While these findings were attacked by the industry, Townsend *et al.* also found soil concentrations of arsenic averaging 28.5 mg/kg below treated decks in Florida while the background concentrations were only 1.4 mg/kg on average (Townsend *et al.* 2001; Matus 2001, May 12). Townsend's research also established that the decks impact on the soil extended to a depth of 4-8 inches, and that the elevated concentrations were not limited to sawdust deposited during deck construction. Furthermore, this research estimated that of the 565 million cubic feet of CCA treated wood sold in Florida, containing over 28,000 tons of arsenic, 36% was used for deck construction resulting in 25,000 acres of decks and an impact on 60 million tons of soil.

1.3 Alternative Treatment Processes

There are alternatives to CCA treated wood. In addition to woods that have natural resistances such as teak, cedar and mahogany, there are alternative waterborne treatments that are safer than CCA or creosote. These treatments include Alkaline Copper Quat (ACQ), Borates, Copper Boron Azole (CBA), Copper Citrate (CC), and Copper Dimethyldithiocarbamate (CDDC). Of these, ACQ and CBA have similar beneficial performance characteristics to CCA and may be cost competitive if produced at the same volume of CCA (Solo-Gabriele *et al.* 2000). In general, there are alternative treatment processes and standards for use in 80% of typical CCA applications including outdoor decks, landscaping, fences and highway construction (Townsend *et al.* 2001).

In addition to numerous individual lawsuits that have recovered damages for those people affected by the arsenic in CCA, currently there is a lawsuit filed in U.S. District court that lawyers are seeking to have certified as a class action lawsuit (Matus 2001 March 14, April 21). Targeting the three largest producers of CCA, the suit claims the product is "defective and unsafe" with the proposed remedy requiring defendants to remove structures built with CCA wood, clean up contaminated soil and pay for the monitoring of people who may have been exposed to the arsenic (Matus 2001, March 14).

1.4 Future Disposal Projections

As a result of these findings and media attention, customers are inquiring about the safety of CCA and alternative products prompting companies to shift greater production volume to alternative treatments already marketed in other countries (Matus

2001, May 6). However, even if CCA was banned in the United States as it is in Switzerland, Vietnam and Indonesia, restricted as in Japan, Denmark, Sweden, Germany, Australia and New Zealand or simply ceased production due to market forces, disposal of the existing inventory of CCA will be problematic. Considering the product has at least a 25-year lifespan and was first introduced just 30 years ago, the current issues of metal concentrations in ash or leaching from landfills are in their infancy. Solo-Gabriele and Townsend's inventory of CCA treated wood in the state of Florida predicts a dramatic increase in disposal quantities from 3.7 million ft^3 in 1996 to 31 million ft^3 in 2016 (Solo-Gabriele and Townsend 1999). As shown in Figure 1.1, this amount is expected to peak around 2020 before returning to current levels in 2030 if alternative chemicals were in use by 2002. Assuming there will not be a change in CCA use, there would be over 30 million cubic feet of CCA treated lumber disposed in Florida annually (Solo-Gabriele *et al.* 2000).

Townsend *et al.* also performed a mass balance analysis for arsenic, estimating that as of 2000, 28,600 tons had been sold in Florida with 1600 tons of arsenic continuing to be imported annually. They also estimated that 2900 tons were lost through in service uses and that 1600 tons have been disposed of to date. Of the 28,600 tons imported into Florida, 24,100 tons remain to be disposed of. To get a better understanding of the potential impacts of this amount of arsenic,

> this quantity . . . has the potential to increase 6.5×10^9 tons of soil (which is equivalent to the soil within the upper 1" of the entire state) by 4 mg of arsenic per kilogram of soil [the residential soil cleanup target levels are 0.8 mg/kg]. It has the capacity to increase 6.5×10^{14} gallons of water (equivalent to 650 times the size of Lake Okeechobee) by 10 μg/l which is the proposed federal drinking water limit. (Townsend *et al.* 2001, pg. 54)

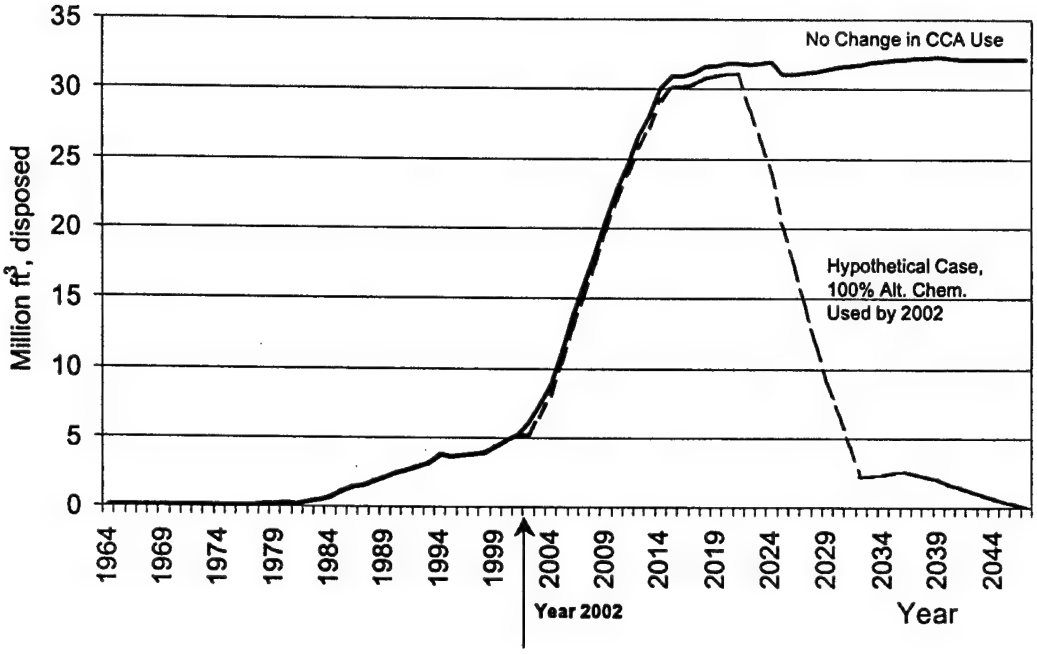

FIGURE 1.1: Long Term Disposal Forecast for CCA Treated Wood Waste in Florida

1.5 Sorting of CCA Treated Wood

Therefore, considering all of these factors, the one solution that satisfies both regulators and industry representatives is the sorting of wood waste streams to segregate CCA treated lumber (Holton 2001). The untreated wood can be burned for energy or chipped for reuse as landscaping mulch. The CCA treated wood removed from the waste stream can then be disposed of in a landfill. An ongoing debate still centers on the need for disposal in lined landfills.

1.5.1 Visual Methods

The important characteristics for a sorting system are the ability to sort large volumes of wood quickly and accurately at a reasonable cost. One method currently in

use at construction and demolition (C&D) reuse facilities is visual sorting (Biocycle 1996). Unfortunately, as mentioned earlier, dirty or weathered CCA treated wood can be very difficult to distinguish from untreated wood. Solo-Gabriele *et al.* (2000) experimentally confirmed this during visual sorting trials with highly trained sorters that showed accuracies ranging from 59% to 94%. While these results are actually quite good considering the difficulties, accuracies between 98% and 100% are required to meet the regulatory leaching requirements for mulch and ash discussed earlier. It is unlikely that visual sorting accuracy could be improved to this level.

Another sorting technology involves the use of chemical stains that react with the metals to change color. The three types tested by Solo-Gabriele *et al.* are rubeanic acid, Chrome Azurol S and PAN indicator, all prepared in accordance with AWPA, 1996 standards. Chrome Azurol S is a water based organic compound that reacts with several metals, including copper and aluminum, that turns a blue color in the presence of copper (Sandell and Onishi 1978; Solo-Gabriele *et al.* 1999). Chrome Azurol S takes approximately one minute to soak into the wood and change color. PAN Indicator is a reagent that reacts with nearly all metals except alkali (Sandell and Onishi 1978). Solo-Gabriele *et al.* found that the PAN Indicator quickly turns a magenta color when applied to CCA treated wood and an orange color when applied to untreated wood. Rubeanic acid requires the application of two separate chemicals to the wood before the compound reacts with the copper to produce an olive green color. In laboratory experiments all three stains were able to correctly identify most wood samples. However, when applied to wood collected from C&D recycling facilities there were some interference reactions noticed that may have been due to weathering or dirt.

Field trials conducted by Solo-Gabriele *et al.* of these three stains also revealed some other inherent weaknesses. Rubeanic acid was found to be inconvenient and time consuming due to the two applications required and the color produced was not easy to distinguish when applied to weathered wood. Chrome Azurol S was slow to react with the CCA (63 seconds) while the quick acting (12 seconds) PAN indicator depended on the sorters ability to distinguish between shades ranging from orange to bright red to magenta. Furthermore, weathered wood often needed to be cut with a knife to expose a clean surface to prevent interference reactions. PAN indicator also needs to be refrigerated to prolong the life and sensitivity of the chemical. The common conclusion that applied to all stains was "their use is labor intensive and may be too time consuming for sorting very large quantities of wood waste" (Solo-Gabriele *et al.* 1999, pg. 61).

Another weakness with the stains currently in use is their inability to distinguish between various types of treated wood. The benefit of alternative chemicals such as ACQ, CBA, CC and CDDC described earlier is their ability to be burned or mulched without adversely affecting human health or the environment. The problem with the stains is that they would all show positive results for these alternate chemicals since the alternate chemicals all contain copper, which is the metal the stains react with. This would in effect place the same regulatory restrictions on the alternate chemicals since they would be indistinguishable from CCA. Therefore a sorting system also needs to detect the chromium or arsenic since these metals are unique to CCA.

1.5.2 X-Ray Fluorescence

One system that is sensitive to chromium and arsenic is X-Ray Fluorescence (XRF). XRF utilizes either a radioactive source or an x-ray tube to produce x-rays that

are absorbed by electrons of the elements in the wood promoting them to higher energy levels. As these excited electrons return to their ground state the electrons release the electromagnetic energy through fluorescence at distinct wavelengths unique to each element (Van Hecke and Karukstis 1998; Williams 1987).

Solo-Gabriele *et al.* (1999) conducted experiments with an ASOMA model 200 XRF system utilizing a curium 244 source at the headquarters of ASOMA Instruments, a supplier of XRF equipment. ASOMA employees conducted two of the experiments while the researchers conducted a third. The first experiment consisted of placing the probe in direct contact with the solid wood sample or a plastic bag containing wood mulch for 100 seconds. The second experiment consisted of placing the probe in direct contact with the solid wood sample or the plastic bag containing wood mulch and moving the probe head across the sample. The third experiment was to repeat the detection limit study.

The initial results of these experiments estimated that XRF technology could detect CCA in mulch samples if at least 20% to 25% of the mulch contained 0.25 pcf CCA treated wood. The experimental results from the first trial showed detection at 50% and failure at 10%, prompting retesting in trial three to better define the limit. After extensive recalibration they estimated detection limits as low as 5% but noted some outliers that did not conform to their calibration line. The researchers also established that the XRF detector was most sensitive to arsenic followed by copper and chromium, while noting the weathering process decreased the sensitivity. Solo-Gabriele *et al.* claimed an analysis time as short as 2 seconds and the ability to position the probe up to 1" away from the sample through a protective plastic shield. The shield is required to

protect the beryllium window that collects the x-rays. The detector also performed very well at identifying CCA in dimensional lumber.

Overall, the XRF detector proved to be able to identify CCA treated lumber and did a fair job of detecting CCA in wood mulch. Some additional issues to consider are the $100,000 estimated cost for an online system, the requirement to have a license for the radioactive source, shielding to prevent workers from x-ray exposure, and the 1" standoff distance. Furthermore, the XRF detector design utilizes a stationary time-averaged measurement to quantify the metal concentrations present. This would require the wood to remain stationary for several seconds while the analysis took place or mounting the detector on an industrial robot to track a moving piece of wood. To overcome this limitation, Solo-Gabriele and Townsend are currently investigating the ability to use a stationary XRF detector to take a time-averaged measurement over the length of a moving piece of wood. However it is also important to consider the characteristics of the waste stream when designing the detector. Common wood waste includes ½" plywood, 1" x 4", 2" x 4" and 4" x 4" lumber. With a 1" standoff distance an XRF detector placed above the wood would have to constantly identify the size of the next piece of wood and adjust position accordingly to accommodate the various wood sizes. A detector placed below the wood traveling on a roller conveyor would have debris accumulate on the detector optics.

1.5.3 Laser Induced Breakdown Spectroscopy

As a result of these challenges, the Florida Department of Environmental Protection funded research into the development of an online sorting system based on the Laser Induced Breakdown Spectroscopy (LIBS) diagnostic technique through an

innovative recycling grant to Sarasota County. Sarasota County subsequently entered into a contract with the University of Florida and the University of Miami to develop an online CCA detector based on LIBS technology.

LIBS utilizes a pulsed laser to produce high intensity pulses of collimated monochromatic light focused into a medium to form a nearly totally ionized gas (plasma) through dielectric breakdown (Andrews 1997; Radziemski and Cremers 1989). The experimental custom is usually the observation of a plasma flash (e.g., spark) in the focal region. This process uses a laser pulse of a trivial amount of energy, as little as 10 mJ for solids, but for an extremely short duration, i.e. 10 ns. Due to this timescale the resultant power is immense, on the order of megawatts, for the 10 ns duration of the pulse. This low energy, high power pulse focused to a tight spot is characterized by a term referred to as the energy density with units of energy divided by area (e.g., mJ/cm^2). Once the energy density reaches the breakdown threshold for the medium, a seed electron is formed through multiphoton ionization (Radziemski and Cremers 1989). The number of photons required for the formation of the seed electron is dependent on wavelength, with longer wavelengths requiring more photons; yet once the threshold is surpassed, wavelength is of little importance. The seed electron initiates a cascade process that increases the electron concentration within the focal volume exponentially, provided the electrons continue to acquire energy from the laser exceeding the band gap of a solid or ionization energy of a gas. The threshold for this cascade to occur can range from as low as 10^6 W/cm^2 in some solids to usually in excess of 10^8 W/cm^2 (Radziemski and Cremers 1989).

The plasma is a transient process that can reach temperatures up to 20,000 K and initially consists primarily of free electrons and excited ions for first few microseconds. During this time, the plasma releases energy characterized by broadband radiation known as continuum made up of recombination and Bremsstrahlung emissions. Recombination emission is the result of ions recapturing electrons. Since the free electrons are not quantized in atomic shells, energy is released across all wavelengths. Bremsstrahlung emission is the process where a free electron passes an ion without capture yet releases energy in the form of a photon equal to the difference in free quantum levels. At timescales greater than approximately 5 microseconds, ions and neutrals begin to relax back to their groundstate resulting in atomic emission at discrete wavelengths that are unique to each element. The intensity of this atomic emission peak is directly proportional to the number of atoms of analyte in the plasma (Radziemski and Cremers 1989).

Typically, a spectrometer and a Intensified Charge Coupled Device (ICCD) are temporally optimized to record the energy emitted from the plasma. The optimization consists of delaying the beginning of spectrometer integration to allow the plasma to cool and the continuum to decrease in intensity. As the plasma cools the atomic emission peaks increase in relation to the continuum baseline. The spectrometer is then calibrated to record emission during this period of maximum peak-to-base ratio (Radziemski and Cremers 1989).

For most elements, the atomic emission is independent of the source of the atom or the other species undergoing breakdown and recombination in the plasma (Hahn and Lunden 2000). However, matrix effects are atomic interactions within the plasma that

can affect the emission peaks. Solids can have particularly strong matrix effects due to varying laser penetration depths within the solid medium (Radziemski and Cremers 1989). Some of these effects present in wood will be discussed in later chapters as well as in other researchers findings.

1.6 Prior LIBS Research

A review of the scientific literature revealed little information regarding the application of LIBS to wood or use in an online sorting process. The only comparable study was by a German team of researchers who gave an oral presentation at the LIBS 2000 international conference regarding their research into detection of wood preservers containing various metals. Their approach was to apply a commercial laser plasma spectrometer to the analysis of wood preservers in an off-line process. This process measured the concentration of metals present after several seconds of analysis with a commercial system consisting of an Nd:YAG laser operating at 1064 nm, 10 Hz and with a 5 ns pulse. The light was collected through a telescope into a fiber optic cable to a spectrometer and ICCD camera. A computer then analyzed the spectra by applying a correction factor compensating for the matrix effects of different species of wood and reducing the systematic error when compared to Inductively Coupled Plasma (ICP) results (Uhl *et al.* 2001).

While neither elemental arsenic or chromium nor the CCA chemical were the primary focus of this research, the researchers demonstrated the ability to apply LIBS to the detection of wood preservers as well as the quantitative analysis of metal concentration levels within the wood. Furthermore, they concluded that LIBS could be applied to wood recycling facilities. The difficulties with their system were the detection

times on the same order as x-ray fluorescence, and the off-line nature of analysis. The wood sample had to be placed inside a sample chamber at a fixed focal distance for analysis; hence this time consuming process precludes the rapid sampling of 100% of the waste stream.

Due to the minimal published research into the application of LIBS to on-line sorting or wood analysis, a review of LIBS applications to arsenic or chromium detection, *in situ* applications and rapid processing was undertaken. One such application was the use of LIBS for the on-line determination of the elemental composition of encrusted sandstone and stained glass (Klein *et al.* 1999). This method used a 240 mJ KrF excimer laser ($\lambda = 248$ nm) with a 30 ns pulse focused at a distance of 300 mm in a laser ablation process. The plasma spectral emission was monitored 0.5 μs after the laser pulse by a spectrograph and optical multichannel analyzer with an intensified photodiode array detector. The detector was triggered using a fast photodiode that detected the laser pulse and signaled an oscilloscope and a high voltage pulser that in turn triggered the detector array. A fiber optic cable without any focusing optics was placed adjacent to the plasma plume for light collection. Ablation depth was gauged by monitoring the decrease in Mg and Fe(II) for sandstone and the increase in Mg and Si with the concurrent decrease in Ca for glass. Once the ratios for these analytes passed a predetermined value, the computer signaled an X-Y translation stage holding the sample piece to move to a new position. The translation stage movement pattern and overlap protocols were established before beginning the ablation cleaning process (Klein *et al.* 1999). It appears that the KrF excimer laser, with relatively shallow penetration depth, was used to minimize the potential destructive thermal damage to the underlying

sandstone and stained glass. This is not a concern in the sorting of wood and would allow the use of a less expensive laser.

A similar feature of Klein's system to an online detector for treated wood is the need to trigger an output once the analytes exceeded predetermined levels at a similar focal distance from the sample. However, a CCA sorting system must be able to analyze the spectra with a less complicated triggering method and less expensive detection equipment in order to be economically feasible.

Another application was the use of LIBS for the analysis of metals in soils. Soil samples were mechanically compacted in a press and rotated in front of a Nd:YAG laser with an unstable resonator operating at the third harmonic (λ =355 nm). This rotation minimized crater effects on the surface of the sample and partially compensated for surface inhomogeneities (Barbini *et al.* 1999). The laser energy was from 20-40 mJ and was focused using a seven mirror optical arm that terminated with a 250 mm focusing lens. The pulse repetition rate was 18 Hz while the pulse width was 8 ns. A fiber optic bundle collected spectral emission from the plasma plume to a monochromator and ICCD detector with an acquisition time of three minutes and an elaboration time of five minutes. The information processing was accomplished with a Pentium 166 MHz computer running LabView software. The information processing included the estimation of the plasma temperature that allowed application of a correction factor to the emission data. This correction factor improved the LIBS to ICP correlation from 0.64 to 0.87 (Barbini *et al.* 1999).

While the online detector for treated wood would have to detect the presence of the analyte (i.e. arsenic or chromium), it is not necessary to accurately quantify the

concentration nor estimate plasma temperatures or apply correction factors. The wood detector would therefore analyze much quicker using commercial software and current computer equipment since in addition to the plasma temperature estimation, the slow elaboration times are likely the result of a relatively slow computer. The choice of a third harmonic Nd:YAG laser was also unusual. Since wavelength is of little importance once the threshold for breakdown is surpassed, the very inefficient reduction from 1064 nm to 355 nm appears to be unnecessary unless the researchers found that it reduced matrix effects within the sample.

LIBS has also been applied to the analysis of liquid samples. Since the laser pulse can cause splashing or ripples on the surface of a liquid, one technique is to evaporate the analyte solution on a graphite substrate followed by LIBS analysis of the substrate surface. Vander Wal *et al.* (1999) used a 300 mm focal length lens but placed the focus 1 cm behind the surface resulting in an power density of 4.4 GW/cm^2. Focusing behind the surface was undertaken to prevent breakdown prior to reaching the sample surface. The 1064 nm Nd:YAG laser was also pulsed at 2 second intervals to eliminate particulate induced breakdown. While not an *in situ* or online process, this research provides insight into prebreakdown phenomena, as well as sample placement outside the laser focus. It also touched upon an alternate method that uses two laser pulses in an *in situ* process within the liquid medium. The first pulse creates the plasma within the fluid while a time delayed second pulse acts as an excitation pulse providing further heating of the initial plasma and enhancement of line intensities (Vander Wal *et al.* 1999; Samek *et al.* 2000).

Samek *et al.* abandoned this two-laser pulse approach during their study of *in situ* LIBS analysis of liquids. Instead, they used a 1064 nm Nd:YAG laser at 20 Hz with a

pulse width varying from 4 to 8 ns. A Glan polarizer was used to adjust the beam energy rather than adjusting the power supply. This allowed the laser to operate at optimum conditions while allowing control through angular adjustments to the polarizer. The relevant aspect of their research was their three methods of focusing the laser and collecting the atomic emission. The first method used telescope combinations to transmit the laser beam up to 30 m before focusing on the target. This method used off axis collection optics to focus light into the fiber optic cable. The second method used a single telescope that also acted as the focusing optic that allowed a standoff distance of 3 to 5 m and off axis collection of the spectra similar to the first method. The problem with off axis spectra collection is that any misalignment of the sample can cause the focused spectra to miss the fiber optic cable. The third method used the same telescope/focusing optics as the second method but collected the emission axially back through the telescope to a fully achromatic beam separator that used an optical switch based upon the principle of frustrated total internal reflection (FTIR). This beam separator directed the collected emission off axis to the spectrometer, overcoming the alignment problems of typical off axis collection schemes while still diverting the collected spectra to the spectrograph and intensified photodiode array detector (Samek *et al.* 2000). While a novel collection approach that overcame off axis collection limitations, the FTIR modulator was a complex solution to a challenge that could be met with simple optics and mirrors.

One study that looked into issues of metal analysis in solid samples is the quantification of metal accumulation on teeth using LIBS. Similar to applications in art restoration, as laser ablation for plaque removal and micro drilling is finding greater applications in dentistry, scientists are examining the resultant plasma emissions for

metal analysis (Samek *et al.* 1999). Similar to his later work described previously, Samek *et al.* used a Glan polarizer to modify the energy of a 1064 nm Nd:YAG laser from 10 to 100 mJ. The pulse widths ranged from 4 to 6 ns while operating at 20 Hz. The same spectrograph, intensified photodiode array detector was used for emission collection with a delay generator to optimize the timing. They confirmed previous researchers findings that higher pulse energies result in hotter plasmas and increased emission. They were also able to observe deposition of the whitening additive aluminum from toothpaste on the tooth surface as well as several other metals including the migration of mercury from fillings a couple of millimeters across the tooth. One very interesting finding was the matrix effects of the biological samples behaving differently than solid metal samples. This was seen for the strong emission of phosphorous lines while phosphorous emission is very difficult to detect as an additive in steels (Samek *et al.* 1999).

The final topic of review was the development of an *in situ* continuous emissions monitor (CEM) by a team from Sandia for the Department of Energy (DOE). They used a 1064 nm Nd:YAG laser with a pulse width of 10 ns and a pulse energy of 350 mJ. The high energy was required to initiate the plasma breakdown in the exhaust gasses from incinerators and controlled burn facilities. They used a beam expander and a 50 mm diameter, 75 mm focal length lens to focus the beam sharply to maximize the energy density. The 50 mm diameter lens also served to collect the spectral emissions in an axial arrangement that simply used a pierced mirror to redirect the collected spectra into the fiber optic. The mirror was pierced to allow the laser to pass unimpeded. A similar arrangement was used in the online treated wood detector as detailed in Chapter 2. The

researchers used a novel conditional data analysis approach that produced an ensemble average of all shots recorded as hits above a predetermined threshold rather than the traditional method of ensemble averaging all shots (Hahn *et al.* 1997; Buckley *et al.* 2000). This approach solved the typical poor detection limits resulting from low particle loading present at stack temperatures. The conditional analysis approach combined with calibration curves resulted in successfully enhancing the peak-to-base ratios of chromium, cadmium and yttrium. However, they found that arsenic could not be monitored due to interference with the strong arsenic emission line at 228.81 nm from cadmium at 228.80 nm. They identified the emission line at 189.04 nm as a suitable alternative but their detection equipment did not extend to this short of a wavelength (Buckley *et al.* 2000). French *et al.* (2000) also noted during a review of the four CEM technologies under development, that while a high resolution spectrometer would detect these wavelengths, fiber optics are not efficient transmitters below 200 nm. Similar difficulties in detecting arsenic were also experienced with an alternative CEM developed for the DOE (Monts *et al.* 1998).

1.7 Objectives

This thesis details the research, design and implementation of the online LIBS detector that meets the requirement for a rapid, on-line, *in situ* detector that can reliably discriminate between both untreated wood and wood treated with the CCA chemical. The key characteristics of this design include the following:

1. The construction of a field deployable unit and housing that is robust enough to operate continuously outdoors at a C&D landfill or recycling facility.

2. An *in situ* system that can quickly process the large quantities of wood present in the waste stream at C&D landfills and recycling facilities. This wood is often weathered and dirty.

3. Predictive accuracies from 98% to 100% in order to meet the environmental requirements to allow the wood identified as untreated to be used as fuel or landscaping mulch.

4. The ability to quickly analyze wood of varying dimensions as it passes on a conveyor.

5. The design must employ current technology at an affordable cost that can be an economical sorting alternative for C&D landfills and recycling facilities.

6. Completion of research, design, testing and implementation within twelve months to meet the contractual terms with the FDEP and Sarasota County.

CHAPTER 2
DESIGN AND CONSTRUCTION

The design effort began with the investigation of plasma breakdown initiation on the surface of wood over varying distances from the focusing optic. A 50 mJ, Q-switched, Nd:YAG laser operating at 1064 nm was focused using 50.8 mm diameter lenses with focal distances of 200, 250 and 300 mm. The focusing lens was placed approximately 250 mm from the shutter of the laser. The advantages of longer focal lengths are that the laser is a safe distance from the wood passing underneath and that the beam gradually changes area as it approaches and departs the focal region. By using a narrow beam and focusing over a long distance, the focused beam was expected to result in an energy density above the breakdown threshold over the widest distance from the lens. The long focal lengths would therefore allow the laser to fire down at pieces of wood of various sizes without adjusting the position of either the wood or laser and without the need to have an adjustable focus system.

During initial testing, it was determined that the 300 mm lens was unable to focus the beam enough to induce breakdown, and the 200 and 250 mm lenses produced only a very weak breakdown at a point beyond the focal spot. Two factors were identified as the causes of these problems. While no laser produces entirely collimated light, the laser beam divergence of 6.21 mrad was greater than typically encountered in higher energy lasers. Since the nominal focus of a lens is based upon a collimated source, the divergent beam resulted in the focus being shifted further away from the lens. The more pressing

problem was that the narrow 2.63 mm diameter laser beam resulted in a reduced focusing efficiency of the lens. The narrow diameter beam combined with reduced curvature of the longer focal length optics resulted in very little effective curvature and difficulty focusing. After measuring the area of the beam as a function of distance, this effect was plotted as shown in Figure 2.1.

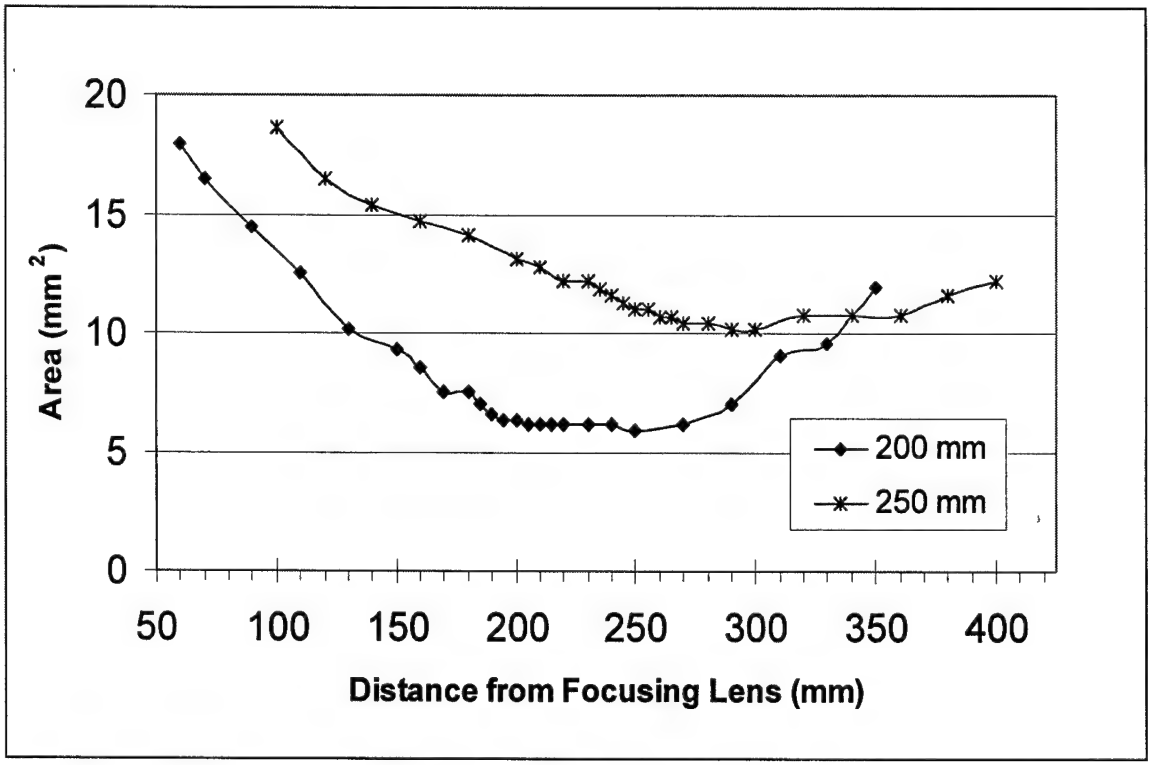

Figure 2.1: Lens Performance

2.1 Telescope Design

To improve the focusing ability of the 250 mm and 300 mm lenses, telescopes were constructed to expand the diameter of the incident beam and to eliminate the beam divergence. The telescopes were constructed and tested at 1.6x, 2x, 2.2x, 2.4x, 2.7x and 3.4x powers. The telescopes were constructed by placing a double concave lens with a

virtual focus of -25 mm in the beams path to cause the beam to diverge. A second convex lens was then used to collimate the expanding beam. To correct for the divergence of the original beam, the separation distance between the two optics was adjusted to produce a nearly collimated expanded beam. While this had varying effects on the effective telescope power, depending on the convex lens used, the results were very satisfying. The telescopes improved the focusing ability of the focusing optic through beam expansion, while the correction of the beam divergence resulted in more symmetrical focusing around the focal spot. The results for four selected telescopes are shown in Figure 2.2 while the complete results are in Appendix A.

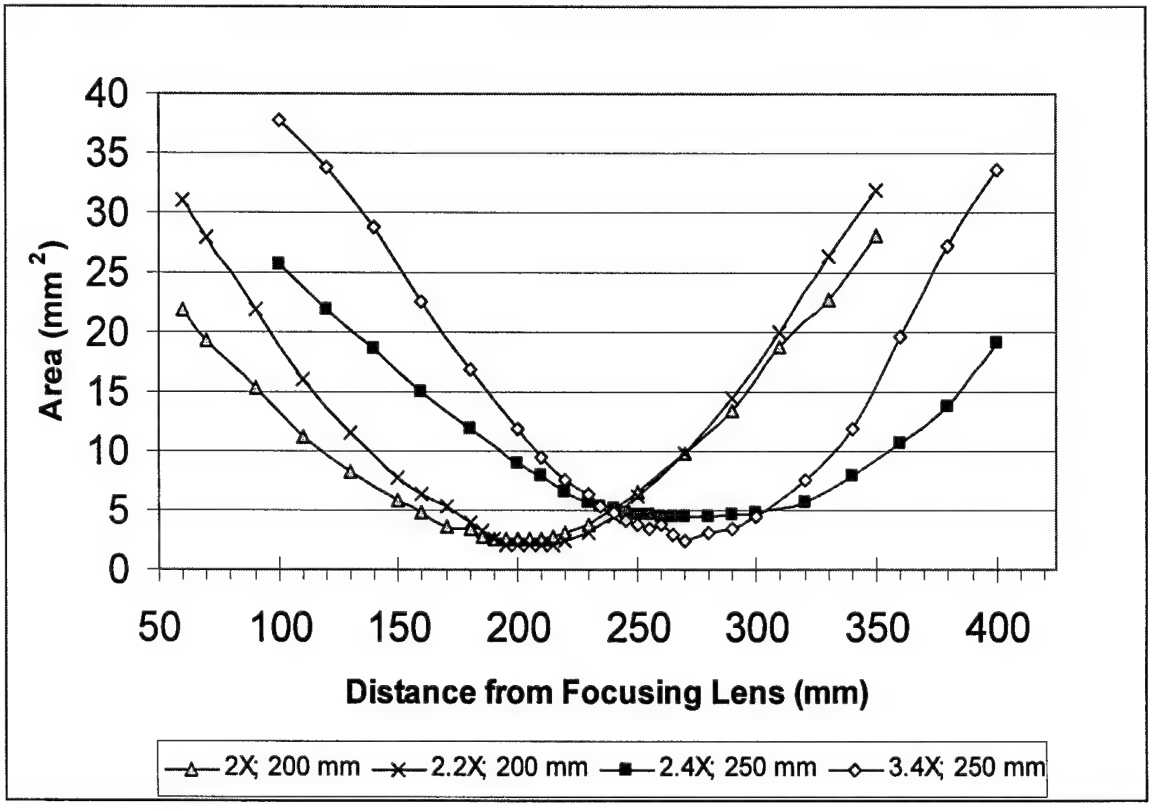

Figure 2.2: Selected Telescope Performance

As seen by comparing Figures 2.1 and 2.2, the telescopes effectively reduced the beam area from over 10 mm^2 down to less than 4 mm^2 for the 250 mm lens and from approximately 6 mm^2 down to almost 2 mm^2 for the 200 mm lens. This reduction in area increased the energy density and enhanced the formation of plasmas on the wood sample surfaces.

2.2 Detection Equipment

2.2.1 Design Apparatus

Schematic diagrams of the apparatus used during these design experiments are provided in Figures 2.3 and 2.4 with a listing including manufacturer, model and description of the individual components provided in Table 2.1. Note that several plano-convex spherical lenses used during the design experimentation are listed in Table 2.1. The first group of lenses includes optics with two different anti-reflective coatings at varying focal lengths. The optics with the 1064 nm anti-reflective coating were used to focus the 1064 nm laser beam and collect the spectral emission of the plasma. The optics with the 355 - 532 nm anti-reflective coating were used to couple the collected light into the fiber optic cable. The anti-reflective coating on these lenses closely matched the wavelengths of the spectra recorded by the spectrometer. The second group consists of 25.4 mm diameter lenses, coupled with the double concave lens, that were used to create the telescopes of varying powers.

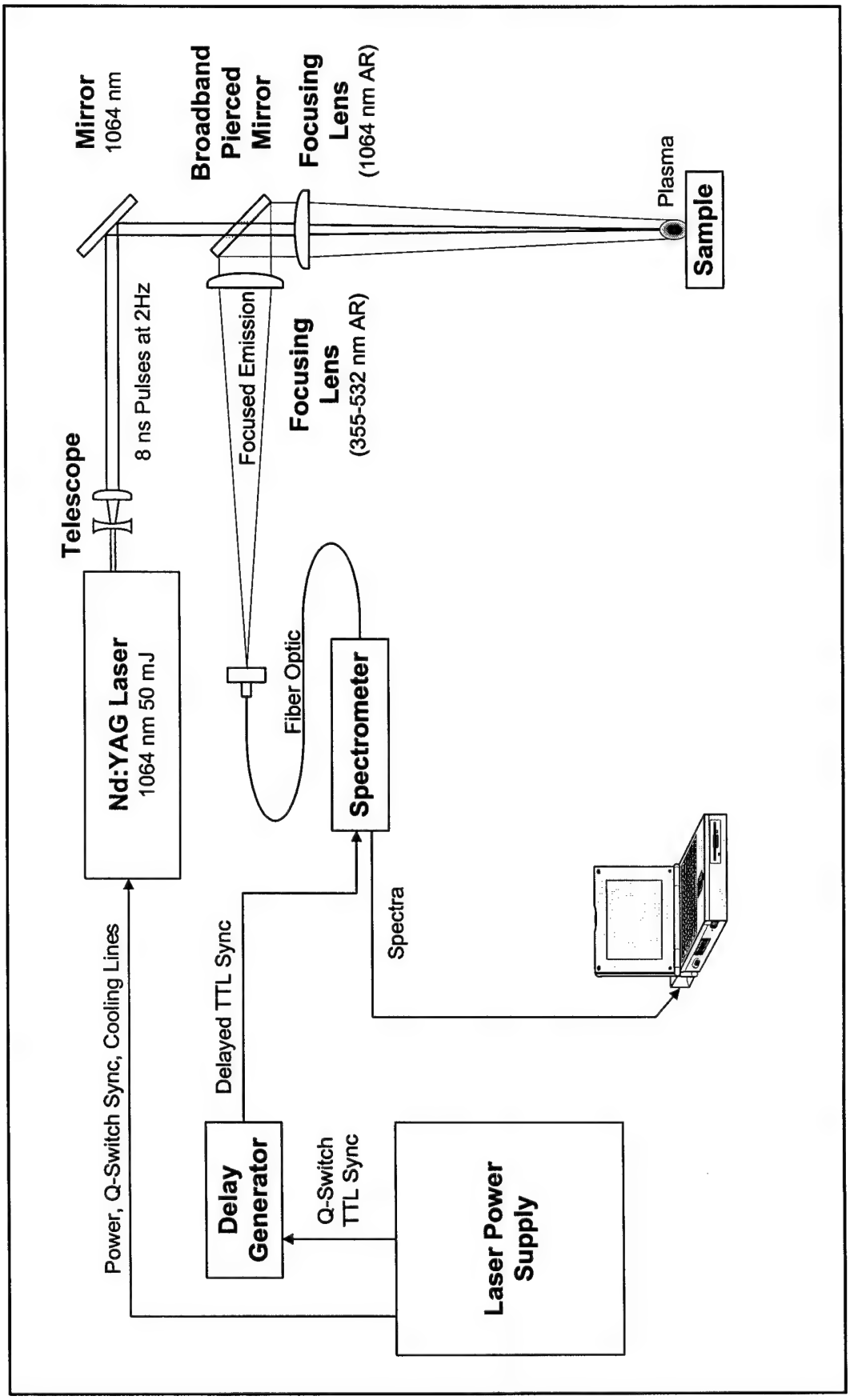

Figure 2.3: Initial Apparatus for Laser Induced Breakdown Spectroscopy System Design

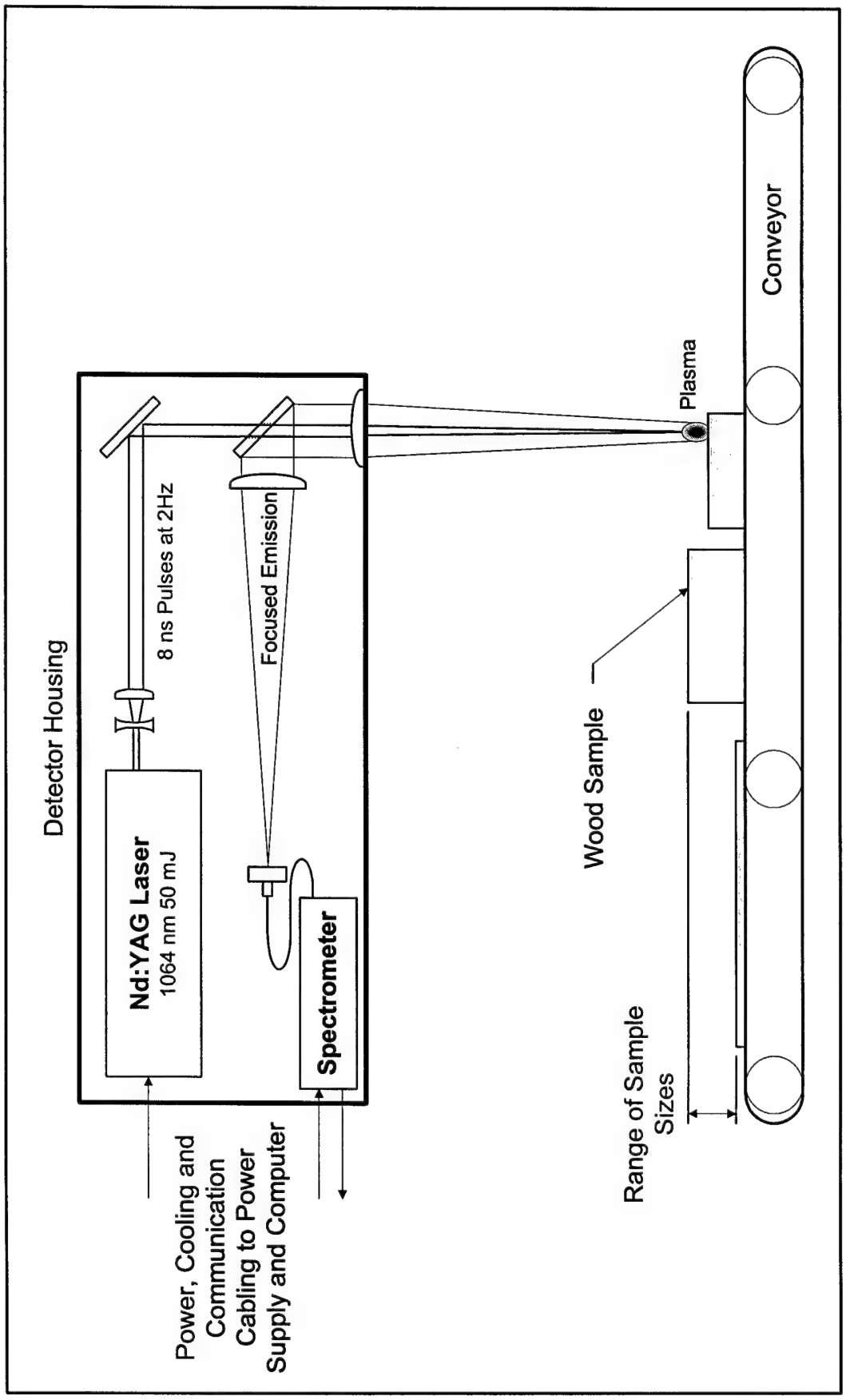

Figure 2.4: Schematic of Detector Mounted above Conveyor

Table 2.1: Description of Design Components for LIBS System

Device	Manufacturer	Model	Description
Laser and Electronics			
Nd:YAG Laser	Big Sky Laser	Ultra CFR	50 mJ, Q-Switched 1-20 Hz, 1064 nm Full Width Half Maximum Pulse Width = 7.53 ns Stable Resonator Near Field Beam Diameter = 2.63 mm Divergence = 6.21 mrad
Laptop Computer	Gateway	9300 xl	Pentium III 700 MHz, 128 MB RAM Running Customized LabView Software
Spectrometer	Ocean Optics	S2000	330-510 nm, 10 μm Slit - 0.37 nm Resolution 500 kHz A/D Board
Delay Generator	Stanford Research Instruments	DG 535	Programmable Delay Generator
Optics			
Plano Convex Spherical Lenses (6)	CVI Laser	PLCX-UV	1064 nm AR Coated, 50.8 mm Diameter Nominal f = 300.0 mm Nominal f = 250.0 mm Nominal f = 200.0 mm 355-532 nm AR Coated, 50.8 mm Diameter Nominal f = 300.0 mm Nominal f = 250.0 mm Nominal f = 200.0 mm
Laser Plane Mirror	CVI Laser	Y1	1064 nm AR Coated, 50.8 mm Diameter Incidence Angle = 45 Degrees Minimum Unpolarized Reflectance = 99%
Pierced Mirror Aluminum; Plane	CVI Laser	PAUV PM	355-532 nm AR Coated, 50.8 mm Diameter Incidence Angle = 45 Degrees Minimum Reflectance = 85%
Double Concave Spherical Lens	CVI Laser	BICC	1064 nm AR Coated, 25.4 mm Diameter Nominal f = -25.4 mm
Plano Convex Spherical Lenses (6)	CVI Laser	PLCX-UV	1064 nm AR Coated, 25.4 mm Diameter Nominal f = 45.8 mm Nominal f = 50.5 mm Nominal f = 57.4 mm Nominal f = 61.0 mm Nominal f = 68.7 mm Nominal f = 85.8 mm
Fiber Optic Cable	Ocean Optics	P-600-UV-VIS	600 μm diameter, 200-750 nm

2.2.2 Light Collection and Processing

Simultaneous with the telescope experiments was the development of the light collection optics, detector equipment and data processing. As schematically represented in Figure 2.3, an axial collection method was used where the 50.8 mm diameter lens, in addition to focusing the laser, collected the spectral emission. The emission was collimated by the focusing lens, split off axis by the pierced mirror and focused with another 50.8 mm diameter lens with an anti- reflective coating optimized for 355-532 nm wavelengths. A fiber optic coupled this light into the spectrometer. As described in Chapter 1, the advantage of the axial collection is that while breakdown can occur at varying distances from the focusing lens, the same lens will collect the spectral emission and direct the light to the fiber. As the breakdown occurs farther away from the focal spot, the light striking the fiber will become defocused resulting in less light collected by the fiber, but will not be translated away from the fiber as with off axis collection methods. The spectrometer then diffracts this light across a CCD array and transmits the relative intensity recorded on each pixel to the computer. Since each pixel represents a discrete wavelength of light, the LabView software then ratios the intensity recorded at the known chromium emission peaks to the baseline and compares this result to a user defined threshold to determine if a "hit" has occurred. Chromium was selected as the analyte since it is unique to CCA treated wood and the research team experienced the same difficulties detecting arsenic as the other researchers discussed in Chapter 1. Complete details regarding threshold selection are presented in Chapter 3.

2.2.3 Equipment Timing

As discussed previously, the laser-induced plasma process must be synchronized with the spectrometer integration and temporally optimized to maximize the chromium emission signal. To accomplish this, a TTL pulse is generated by the laser power supply as the Q-switch fires and releases a laser pulse. This TTL pulse is received by the programmable delay generator, which waits the preset time before sending a new TTL pulse to the spectrometer to initiate integration. However, the integration does not actually begin until 11 μs after the TTL signal is received by the spectrometer due to internal delays in the circuitry. Therefore, even with the delay generator set to zero delay, the internal electronic delays within the spectrometer cause the integration to occur after the plasma has cooled significantly, resulting in missing the temporal window for collecting chromium emission lines. Triggering the integration on the preceding laser pulse solved this problem. By setting the delay generator to wait 499.96 μs, and adding the internal spectrometer delay of 11 μs, the integration begins while the chromium emission is at its maximum in relation to the continuum. Temporal optimization is discussed later in this chapter. It was also required to set the width of the spectrometer trigger pulse short enough that the trailing edge would end before the next Q-switch sync from the laser. If the trailing edge extends beyond the next TTL sync, the delay generator will skip the next trigger. The spectrometer integration was also reduced to the minimum 8.8 ms by removing internal jumpers. This results in the integration continuing well beyond the plasma lifespan, however the expense of a gated ICCD array was not justified since the detector essentially integrates dark current during the remaining integration

period. The timing system is graphically represented in Figure 2.5 and is not to scale because the timescales range from nanoseconds to milliseconds.

Initially the goal was to operate the laser at 10 Hz; however the spectrometer, with a serial cable connection to the computer, would lose synchronization with the software at frequencies above 2 Hz. Another similar spectrometer by Ocean Optics, using a USB connection cable, was identified as capable of running at 10 Hz. Such a system is owned by the Chemistry Department at the University of Florida, where this performance was verified. This enhancement is discussed in Chapter 4.

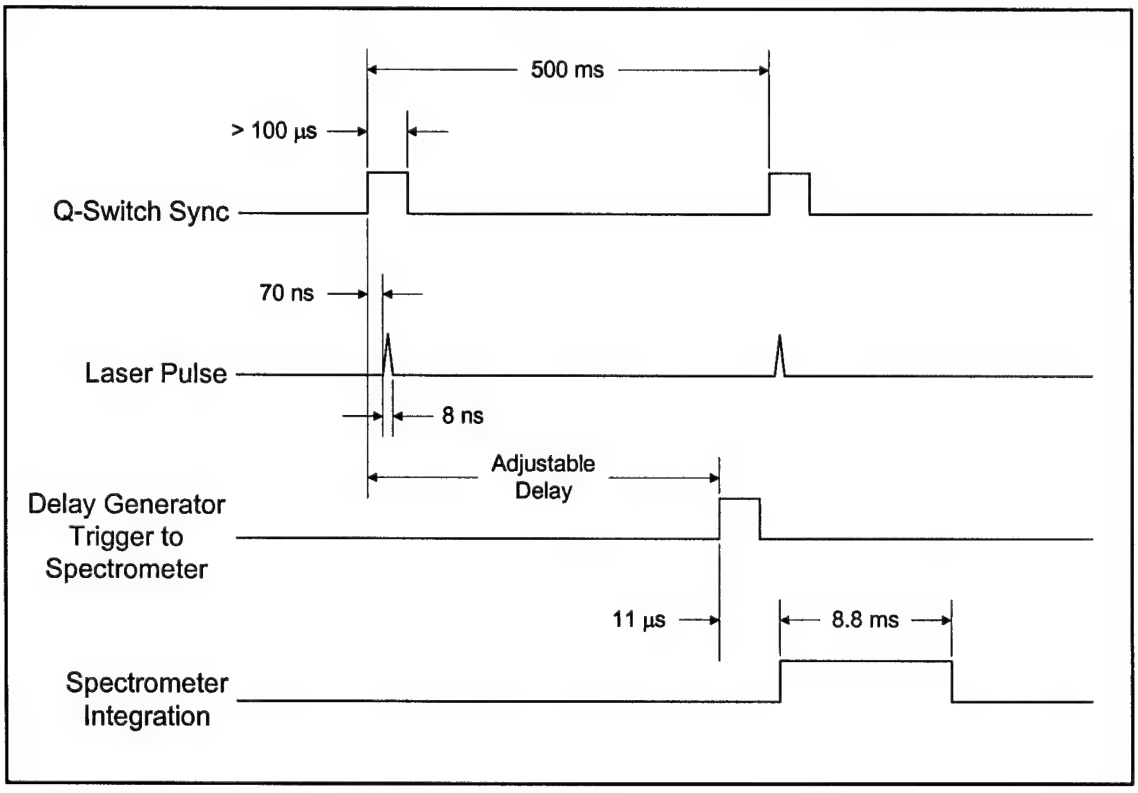

Figure 2.5: Timing Diagram of Design Apparatus

2.3 Breakdown Thresholds of CCA Treated and Untreated Wood

The next step was to characterize the breakdown threshold for various species of untreated wood and CCA treated lumber treated at varying retention levels. These thresholds, combined with the energy densities calculated from the beam areas, would allow the approximation of the distance over which breakdown would occur. A total of 27 wood samples were collected with 12 CCA treated and 15 untreated samples. Seven wood species were represented along with six engineered sheet products and three CCA retention levels. Three trials were conducted on the each of the 27 samples to visually determine the laser energy level for each sample such that at least 50% of the pulses induced a breakdown spark. The variation of energy level was accomplished by adjusting the laser flashlamp pump energy. Once the threshold was visually determined, the spot area was measured with flash-paper and the pulse energy was measured with a Vector S310 power meter manufactured by Scientech. The use of the power meter negated any effects of variation in the laser power supply settings.

The results of the 81 data points show that the mean threshold for treated wood is 6.87 mJ/mm^2 with a standard deviation of 2.35 mJ/mm^2. The threshold for untreated wood was slightly higher at 8.44 mJ/mm^2 with a standard deviation of 1.97 mJ/mm^2. It was observed, as expected, that wood treated at the 2.5 pcf retention value had the lowest threshold, due to the sharply increased metals concentrations that would aid the formation of the seed electron. The lower threshold levels for metals is due to their partially filled electron shells. The earlier formation of the seed electron allows greater absorption of the pulse energy by the free electrons in the plasma, thereby enhancing the cascade process. A similar interesting observation was the effect weathering had on the induced

breakdown of treated lumber. Rather than diminishing performance, as seen with visual methods or x-ray fluorescence, weathering actually enhanced the breakdown process. Similar to metals, the light dirt and weathering provided micro-sites with a lower breakdown threshold to trigger the cascade process earlier with the same enhanced plasma formation as seen in metals. The complete results of the three trials are presented in Appendix B.

In order to reach the predictive accuracies required of the online LIBS detector, the required threshold for all samples was determined to be the mean threshold of untreated lumber plus two standard deviations, 12.39 mJ/mm^2. This value ensures consistent breakdown over a wide variety of wood species and retention levels with breakdown statistically occurring over 98% of the time. This threshold level was then compared in Figure 2.6 to the calculated energy densities from the telescope experiments to determine the optimum optics package that would exceed this threshold over the greatest distance.

As shown in Figure 2.6, the combination of results predicted only a 50 mm distance over which breakdown would occur reliably. Even though these results were considerably better than the 1-inch distance achieved by x-ray fluorescence, a wider sampling distance is required for the expected range of wood sizes. While slight improvements could be achieved using a best-form optic optimized for 1064 nm, it was determined that enhancing the optics package further would not markedly improve performance.

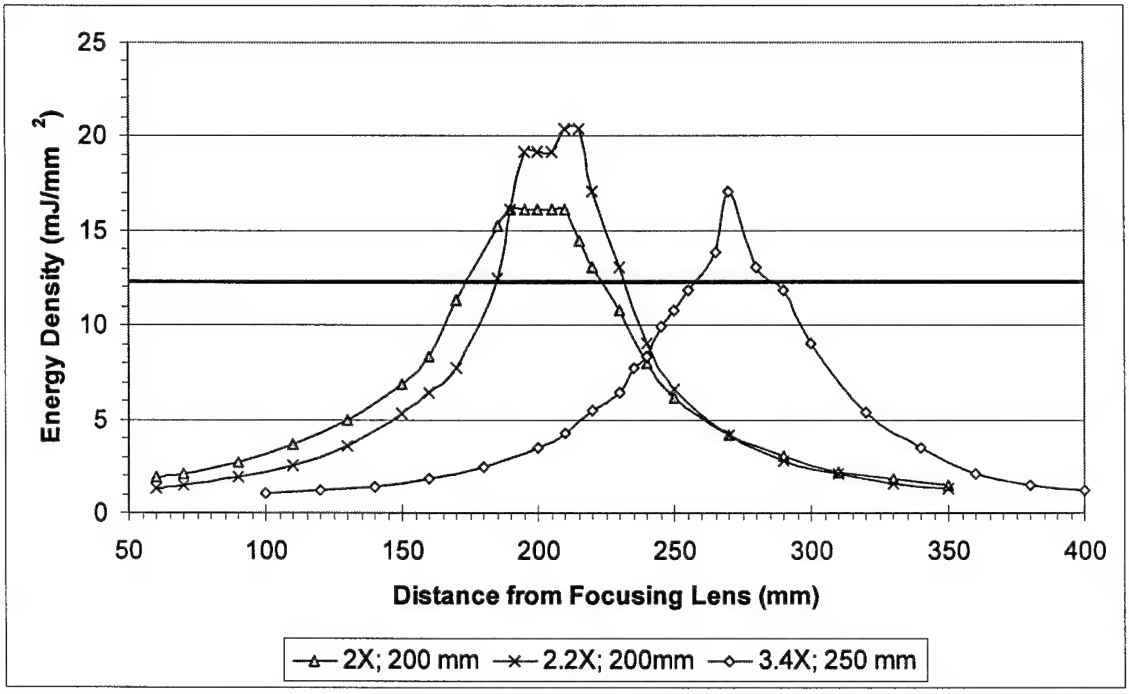

Figure 2.6: Combined Energy Density and Threshold Results

The solution lay in delivering more energy into the plasma to enhance the breakdown process. Initially, a multiple laser system was considered similar to the process described in Chapter 1 for *in situ* analysis in liquids. Two pulses timed to arrive simultaneously would induce breakdown and energize the cascade process. While possible, this approach was complicated and ill suited for a field application. It was primarily considered because there was a possibility of acquiring another 50 mJ laser, while the purchase of a larger laser was beyond the research budget.

2.4 Final Detector Design

2.4.1 Increased Laser Energy

A 200 mJ, Nd:YAG laser operating at 1064 nm was provided on loan to the research team from Sandia National Laboratories, Livermore, California. This laser provided several advantages over the 50 mJ laser, notably four times the beam energy, beam divergence of 4.1 mrad, and near field beam diameter of 5.8 mm. This wider and less divergent beam eliminated the need for the telescope while still easily surpassing the required breakdown threshold. The focused beam diameter was measured as a function of distance for a 200 mm lens using ink on glass slides. The ink is ablated by the laser beam, producing a clear demarcation of the beam diameter. The energy density was calculated and compared to the previous results in Figure 2.7. As shown in Figure 2.7 with the superimposed breakdown threshold, these experiments predicted breakdown over 135 mm, more than sufficient for the online detector.

2.4.2 Improved Resolution and Timing Sequence

Receipt of the new laser prompted simultaneous refinements in various apparatus components. The spectrometer was replaced with a similar model capable of operating at 2 Hz, that provided a high-resolution spectral region of 325-452 nm. The narrower range of spectral operation had the positive effect of increasing resolution from 0.37 nm to 0.20 nm per pixel while still covering the three chromium peaks of interest, namely 425.40, 427.50 and 428.90 nm. The enhanced resolution aided in separating the chromium emission peaks from adjacent non-chromium peaks.

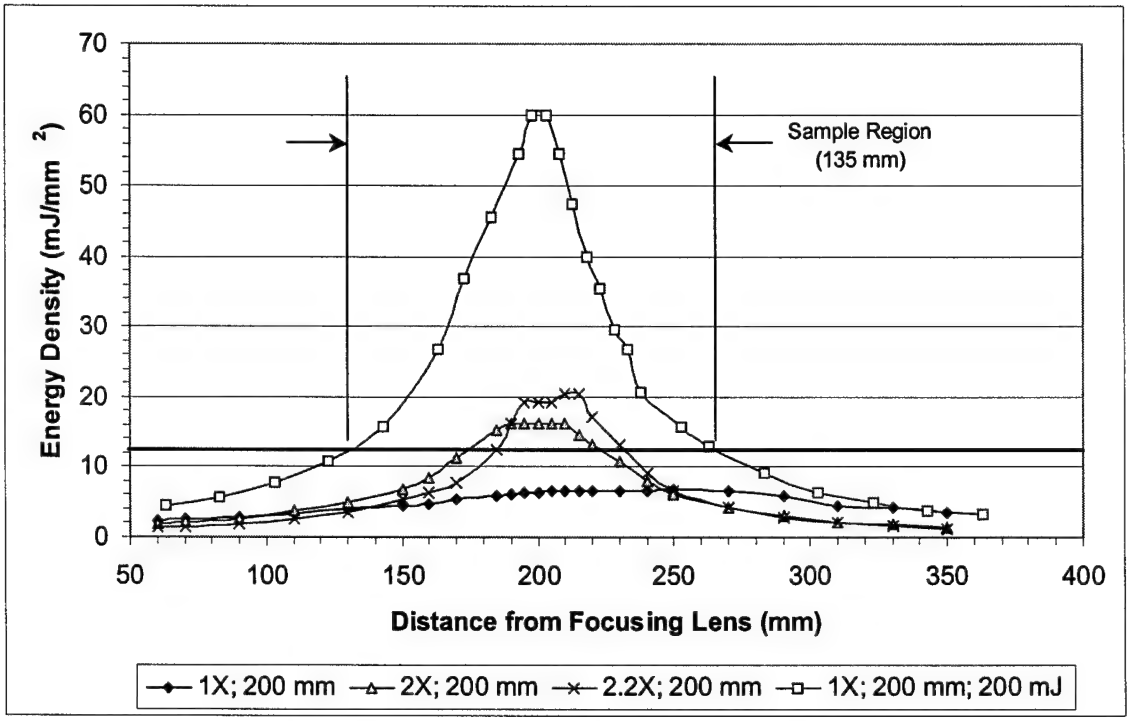

Figure 2.7: Energy Density Comparison of the 200 mJ and 50 mJ Lasers

Another refinement involved reconsideration of the timing arrangement as shown in Figure 2.8. Rather than triggering the spectrometer on the preceding pulse, it was determined that triggering on the flashlamp sync from the laser supply would be easier. This was possible because the delay between the flashlamp firing and the Q-switch firing is 41 μs, while the internal delay of the new spectrometer was 17 μs between receipt of the trigger and integration. The inherent delay of 17 μs required the use of an additional delay generator to be triggered by the flashlamp sync. The output pulse of the delay generator then triggered the spectrometer. An appropriate delay was introduced between these two pulses.

While the process of optimizing the delay time will be fully explained later in this chapter, the new delay was set at 28 μs. This method also eliminated the possibility of

the trailing edge of the delayed pulse interfering with the next TTL sync as explained earlier. The electronics shop at the University of Florida's Chemistry Department is constructing an adjustable delay circuit for use with the field instrument. This circuit fully meets the requirements of the system and will be much smaller and less expensive than the full feature delay generator used for preliminary measurements. Also shown is the digital output from the computer used to fire the strobes as discussed later.

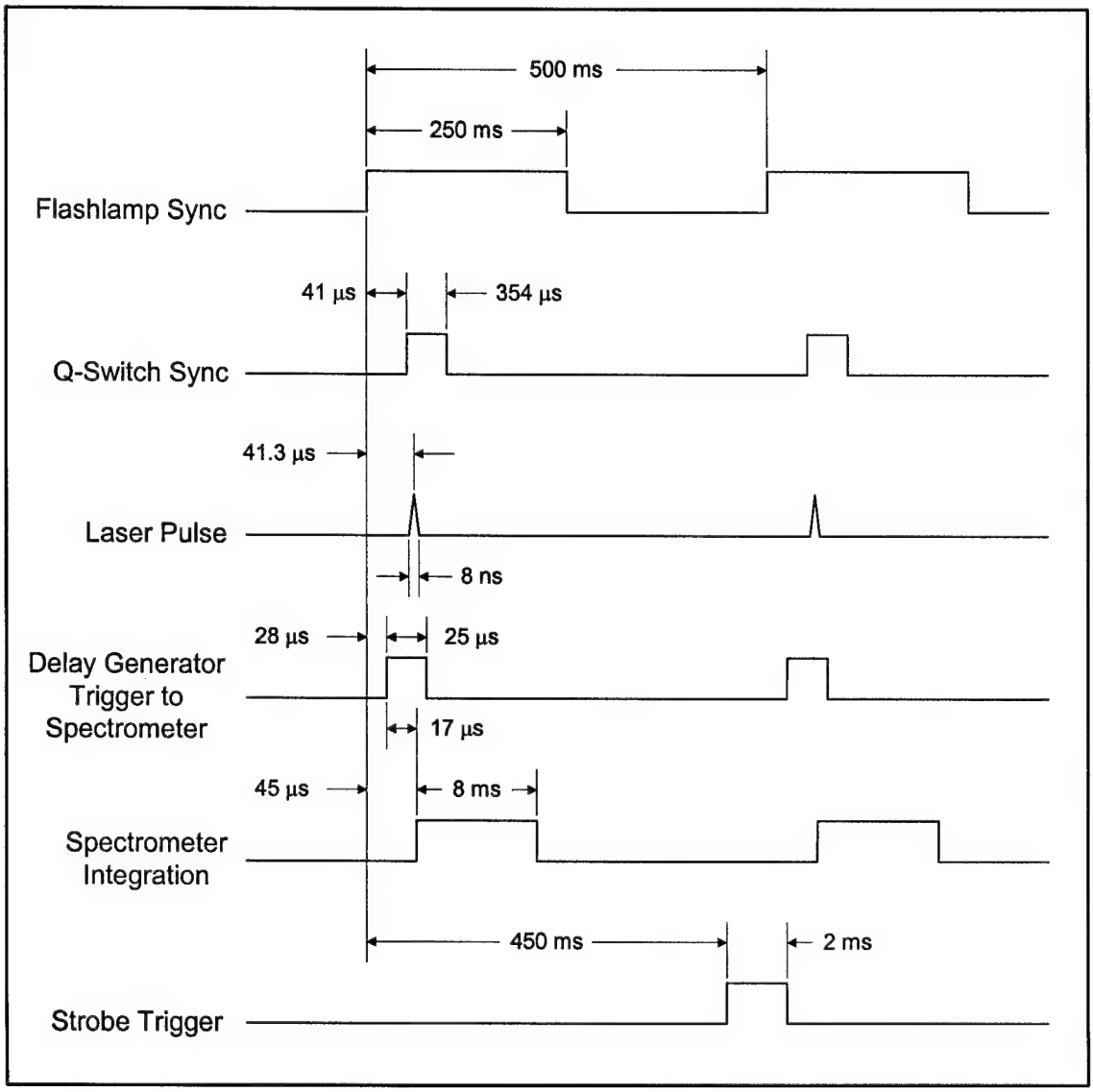

Figure 2.8: Timing Diagram of LIBS Online Detector

2.4.3 Collection Optics

With this new equipment and timing, experiments were conducted to determine the collection efficiency of the design. This was necessary because while breakdown will occur over 135 mm, the collected light may be insufficient due to the distance of the collection lens away from the plasma, inefficiencies in the collection optics or excessive defocusing of the collected light when the sample is far from the focal spot. Preliminary results when using 200 mm focusing lenses for both the plasma collection and focusing to the fiber optic revealed a detection limit of less than 50 mm, even though the induced plasma remained intense over a much wider distance.

A new fiber optic cable was obtained to increase the diameter of the fiber from 600 μm to 1000 μm. 1000 μm is the maximum useful diameter because this is the height of the entrance slit to the spectrometer. Since the spectrometer has a 10 μm entrance slit that will shield most of the optic, a 65% enhancement was expected rather than the full increase in fiber area. Figure 2.9 shows the average signal increase achieved with the new fiber by plotting a fraction of the spectra to aid in distinguishing between the two fibers. The results exceeded expectations. Rather than a 65% increase, the average increase for emission lines was 100% as is shown on the right side of the figure. As an unexpected benefit, the new fiber also revealed emission lines that were previously lost in collection and transmission. An example of this are the three lines on the left of Figure 2.9.

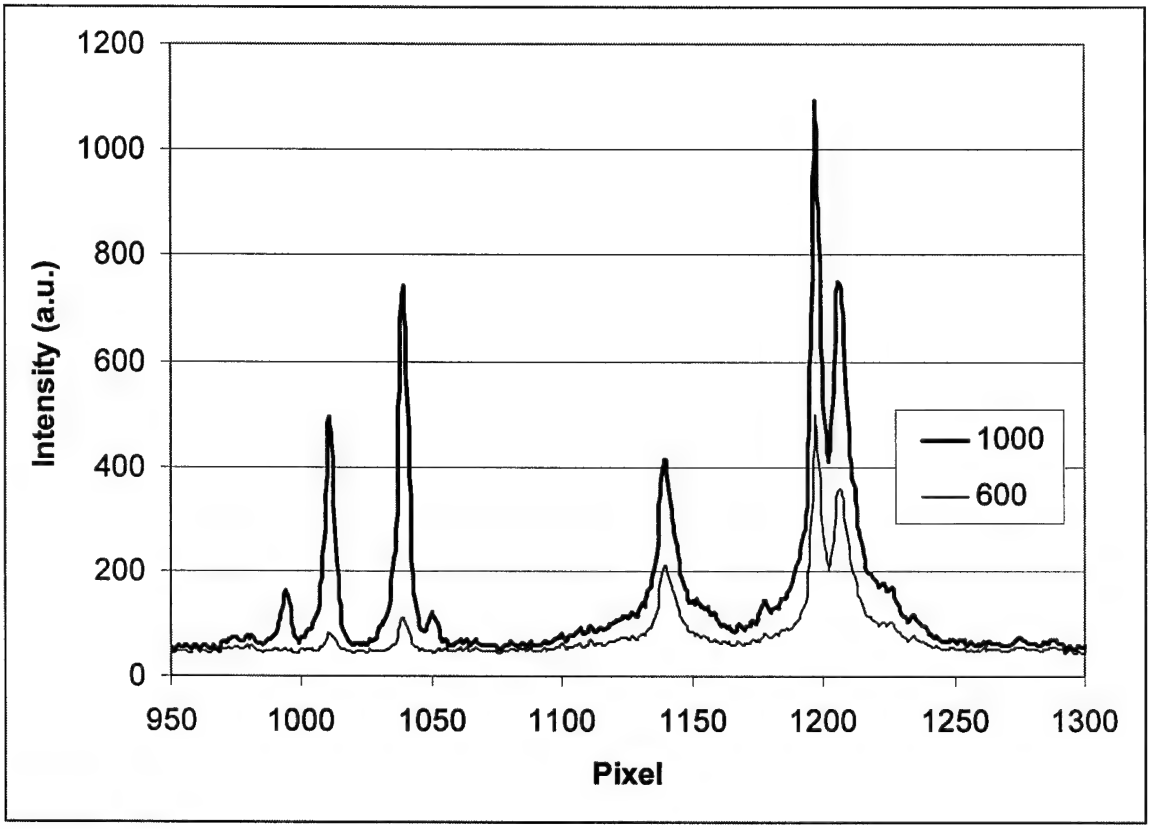

Figure 2.9: Spectral Comparison of 600 μm and 1000 μm Fiber Optics

To further increase performance, measurements were conducted by placing a 2 x 4 piece of CCA lumber treated at the 0.4 pcf retention level in the lasers path at measured distances from the 200 mm focusing optic. 25 shots were recorded at each distance. The collected spectra were then analyzed to compare the peak-to-base ratio of the average of nine pixels centered on pixel 1538 (corresponding to the 425.40 nm chromium emission line) to an average baseline of 40 pixels located away from any atomic emission lines. A hit was recorded if this peak-to-base ratio exceeded 1.60. Both the hit percentage and ratio of all shots were recorded at varying distances to characterize the collection performance. The use of the 200 mm focusing lenses for both the plasma collection and

coupling to the 1000 μm fiber optic improved the spatial detection limit to 65 mm. The advantage of using a 200 mm lens to collect the emission spectra is simply that by being nearer the plasma more light is collected. The disadvantage of using a matched 200 mm lens to couple the emission to the fiber is more rapid defocusing away from the focal spot than a longer lens. While matching the two lenses is common to enhance the focusing of plasma formed on fixed samples, the online detector would rarely have a sample exactly at the focal spot. With the variety of wood pieces analyzed, most of the plasma emission would be defocused to some extent. Therefore, a 250 mm lens was used to focus the light onto the fiber optic. This would keep the focused light narrower over a longer distance from the focal point, which improved the spatial detection region to slightly over 77 mm ($3\ ^{1}/_{16}$"). This is nearly twice the detection range experienced prior to optimization. Figure 2.10 plots the peak-to-base ratio with units of inches as the distance from the lens with the detection threshold overlaid at 1.60 while Figure 2.11 plots the hit percentage. Inches were used for these measurements to directly correlate to the English system of measurement used in the construction industry. The span of $3\ ^{1}/_{16}$" closely matches the expected range of lumber from the true 3 ½" height of a 4 x 4 to a ½" sheet of plywood. One interesting feature of both plots is the steepness of the profiles, especially with the hit percentage. This feature was to later prove useful in differentiating treated from untreated wood based upon hit percentage.

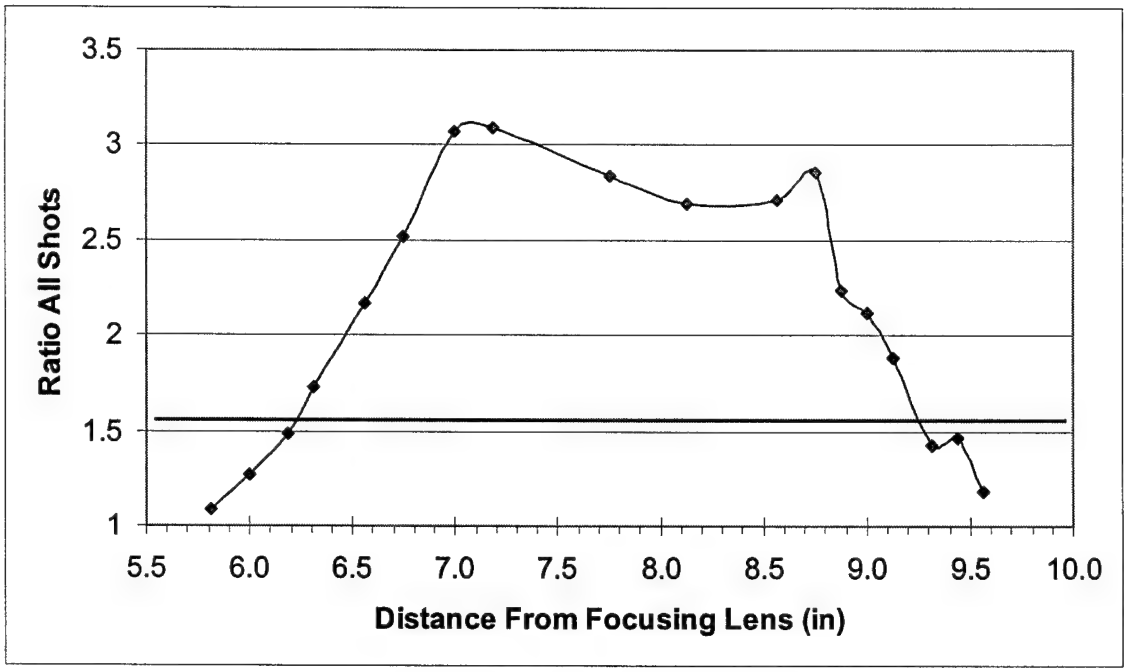

Figure 2.10: Average Chromium Emission (Peak-to-Base) for Optimized Collection Optics Trial

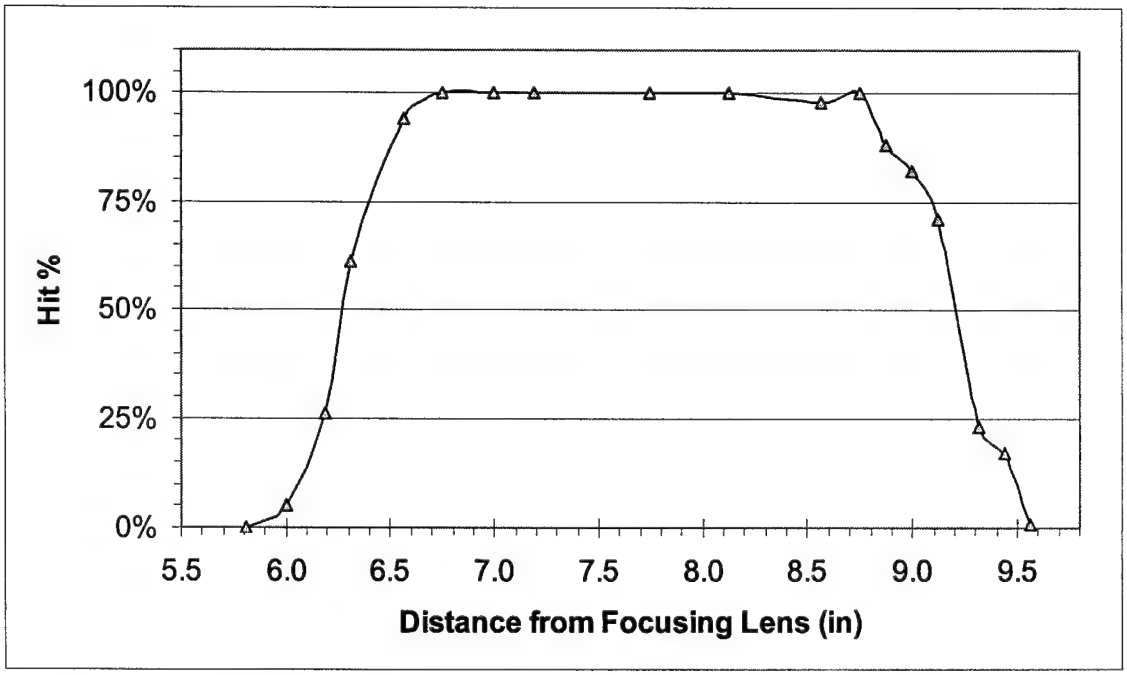

Figure 2.11: Percentage of Laser Pulses Exceeding the Chromium Emission Threshold for Optimized Collection Optics

The concave profile at the top of Figure 2.10 was attributed to the proximity to the focal spot. As the sample is placed near the focus of the lens the intensity of the plasma increases dramatically. This amplification of visual intensity is due to increases in the plasma temperatures due to greater energy density. However, the delay timing is optimized for the temperatures reached by samples closer to the edges of detection rather than the increased temperatures at the center of the plot. This allows the maximum detection range, while the concave feature does not affect detection since it is well above the peak-to-base threshold set.

2.5 Timing Optimization

Examining the timing optimization process provides further insight into the relationship between temperature, time, and peak-to-base ratios within plasma formation and cooling. To determine the correct setting for the optimal delay, treated wood samples were passed under the detector at varying delay times from 23 to 30 μs, in 1 μs increments. Figure 2.12 shows the average spectra of forty shots for all eight delay times. While it is difficult to see the individual plots, especially at longer times, 23 μs is the highest intensity plot with each lower plot sequentially falling for each time increase. The flattening of the peaks near pixel 1000 for the 23 μs plot is due to saturation of the CCD detector. The rapid decay of the plasma emission is apparent in the figure. Figure 2.13 examines only the chromium emission peaks of interest at pixel 1539, 1576 and 1603, which correspond to wavelengths 425.40, 427.50 and 428.90 nm respectively.

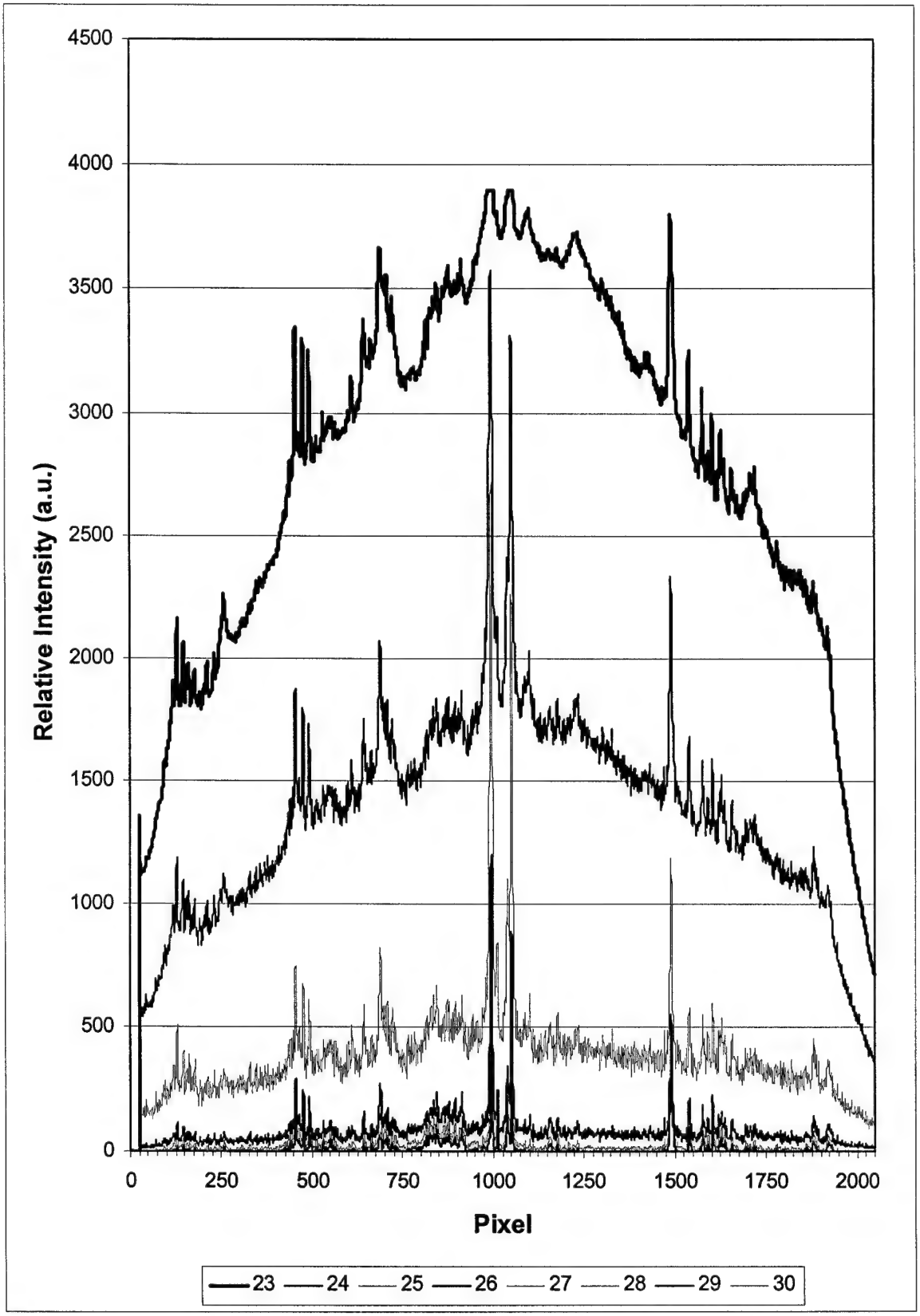

Figure 2.12: Spectral Intensity as a Function of Delay with Respect to the Flashlamp Sync. (delay is in μs)

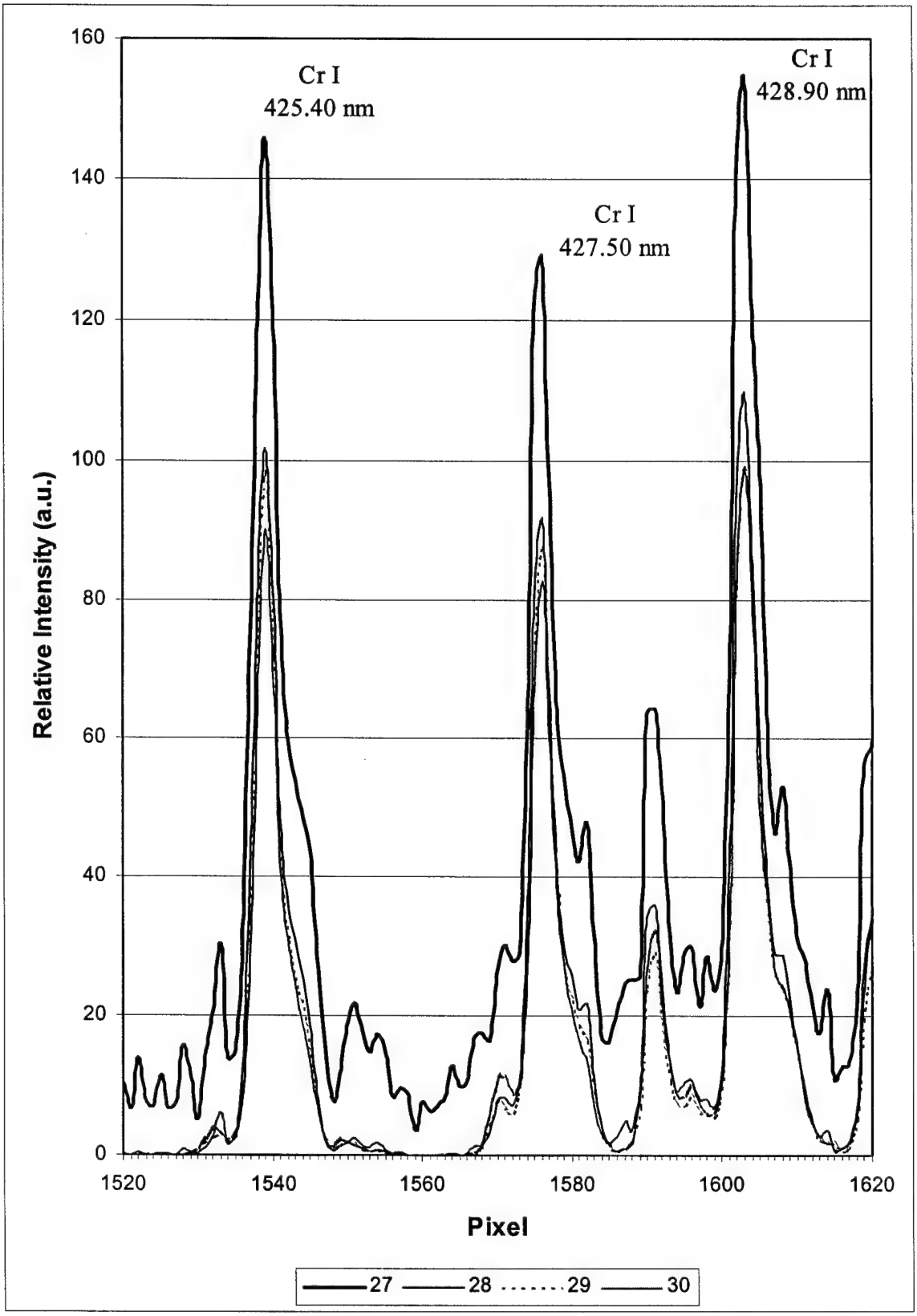

Figure 2.13: Chromium Emission as a Function of Delay with Respect to the Flashlamp Sync. (delay is in μs)

The temporal plots shown in Figure 2.12 directly correlate to the temperature within the plasma. As time passes, the plasma cools, releasing less energy and spectral emission. As discussed previously, the peak-to-base ratio of the analyte also varies as a function of time. This ratio is initially very low, as the initial hot plasma consists primarily of free electrons and ions. As the plasma cools, the continuum (recombination emission) diminishes as the atomic emission from the relaxing atoms increases, resulting in enhanced peak-to-base ratios. With further cooling, electrons begin to reach their ground state, atomic emission is reduced resulting in decreasing ratios. Peak-to-base ratio as a function of time for the three chromium peaks is shown in Figure 2.14. An additional benefit of using a peak-to-base ratio as opposed to *absolute* chromium emission is the effect of signal normalization. With the strong defocusing effect resulting from varying wood thickness, the absolute signal levels fluctuate widely. However, peak-to-base ratios are very consistent, hence they provide an excellent metric for chromium detection.

The peak-to-base ratio was calculated by averaging nine pixels centered on each of the three peaks, and dividing by the 40 base pixels representing the continuum. The forty pixels chosen to represent the continuum were 1385-1404 and 1958-1977. An offset of 2 counts was added to both the peak and base to eliminate division by zero errors as the baseline approached zero at longer delays. Figure 2.14 indicated an optimum delay for chromium emission at 28 μs. These results were used to set the timing as discussed in section 2.4.2.

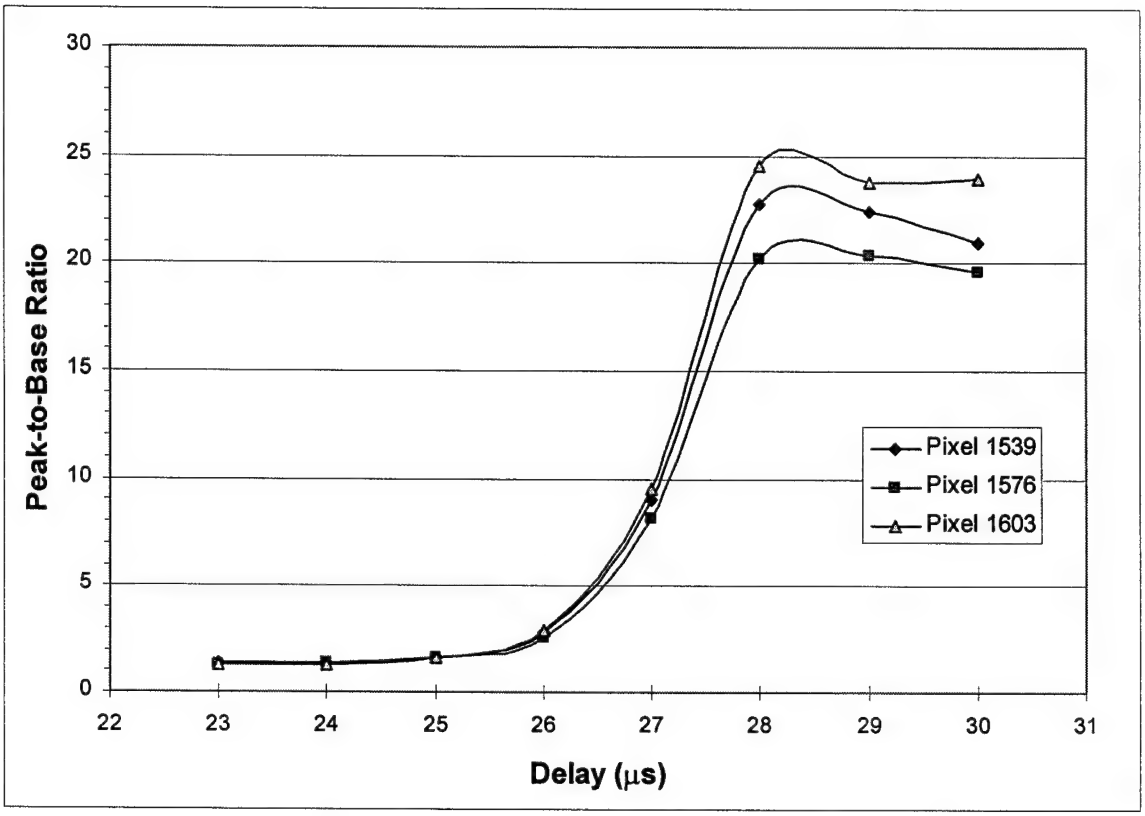

Figure 2.14: Chromium Emission Peak-to-Base Ratio as a Function of Time

2.6 Detection Signaling

The final design requirement was to activate mechanical sorting equipment or signal the operator when CCA treated wood was detected. This was accomplished by modifying the LabView software to provide an output whenever the peak-to-base ratio of all six detection channels exceeded the user programmable thresholds. The six channels could analyze the three chromium lines as well as the strong calcium peaks at 392.64, 395.86 and 423.56 nm corresponding to pixels 995, 1051 and 1490 respectively, as shown in Figure 2.13. The combination of the chromium and calcium lines verified that the laser had struck treated wood and not just a metal fastener (i.e. nail) containing

chromium. All six channels could also monitor a single emission line if it was determined that the extra capability was not required.

The software output was routed through a PCMCIA digital input / output card to a 24 channel circuit board with connector terminals. Each pair of terminals could be individually assigned to produce a 5V TTL pulse for 2 ms. The software was programmed for three of the channels to provide the TTL pulse when triggered by LabView.

One channel was dedicated to activating a shear arm on the conveyor to remove the wood, one was to be used for an alarm, and the final channel was for triggering a strobe light. This TTL pulse is the strobe trigger identified in Figure 2.8. Unfortunately, the shear arm had a 16-second cycle time to extend and retract. Because the laser operates at 2 Hz, the shear arm would never be able to keep pace with the detector system's ability to sort wood. While automated mechanical sorting is still the preferred option, further development of the conveying system is required before integration with the laser detector. The speed of sampling also raised difficulties with an audible alarm system. After searching numerous vendors, no alarms were found that could cycle on and off at 2 Hz. After similar difficulties in finding strobe lights that could be triggered for a single flash and operate at up to 120 flashes per minute, Nova Electronics offered to produce a custom strobe power supply that could take the 5V TTL pulse and trigger an array of 2 - 4 compact strobe heads. This was the only detection signal output used in the design.

2.7 Construction of the Field Unit

With the design completed, a schematic diagram of the final LIBS detector and signaling equipment is provided in Figure 2.15. A listing including manufacturer, model and description of the individual components is provided in Table 2.2.

The laser head, optics package and spectrometer were mounted on aluminum plates with a plexi-glass cover as shown in Figures 2.16 and 2.17. The overall dimensions were 24" x 12" x 6". This detector head was placed on a steel strut bridge constructed over the conveyor. The laser power supply, computer, and delay generator were located in a control room approximately 10 feet away. The detector head was linked to the power supply and processing equipment through 30 feet of cooling lines, power and communication cabling.

With the design complete and the field unit installed at a landfill, field-testing at the Meyer and Gabbert C&D Recycling Facility at the Sarasota County landfill began to determine appropriate threshold values, predictive accuracy of the detector, as well as any limitations in the design.

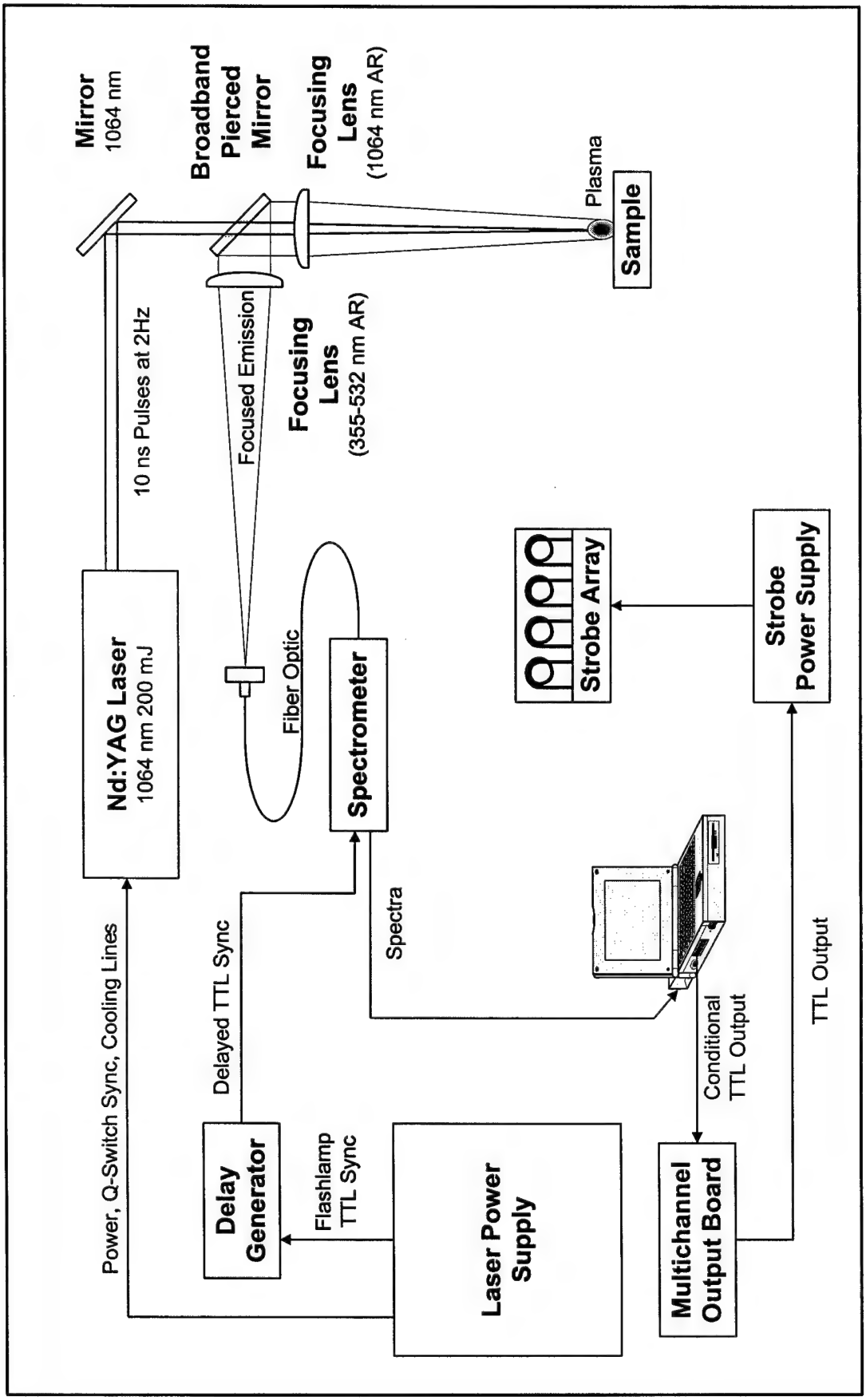

Figure 2.15: Apparatus for Final Laser Induced Breakdown Spectroscopy Online Detector

Table 2.2: Description of Components for LIBS Detector

Device	Manufacturer	Model	Description
Laser and Electronics			
Nd:YAG Laser	Big Sky Laser	CFR 200	200 mJ, Q-Switched 1-20 Hz, 1064 nm Full Width Half Maximum Pulse Width = 10 ns Stable Resonator Near Field Beam Diameter = 5.75 mm
Laptop Computer	Gateway	9300 xl	Pentium III 700 MHz, 128 MB RAM Running Customized LabView Software
Spectrometer	Ocean Optics	S2000	325-452 nm, 10 μm Slit - 0.20 nm Resolution 1 MHz A/D Board
Delay Generator	Stanford Research Instruments	DG 535	Programmable Delay Generator
PCMCIA Digital I/O Ca	National Instruments	DAQCARD DIO-24	Multichannel Digital I/O Card
Strobe Power Supply	Nova Electronics	Micro-Pak 404	40 W Custom Power Supply that is TTL Triggered, up to 180 FPM
Strobe Heads (4)	Nova Electronics	Hide A Flash	Compact Xenon Stobe Tube
Optics			
Plano Convex Spherical Lenses (2)	CVI Laser	PLCX-UV	1064 nm AR Coated, 50.8 mm Diameter Nominal f = 200.0 mm 355-532 nm AR Coated, 50.8 mm Diameter Nominal f = 250.0 mm
Laser Plane Mirror	CVI Laser	Y1	1064 nm AR Coated, 50.8 mm Diameter Incidence Angle = 45 Degrees Minimum Unpolarized Reflectance = 99%
Pierced Mirror Aluminum; Plane	CVI Laser	PAUV PM	355-532 nm AR Coated, 50.8 mm Diameter Incidence Angle = 45 Degrees Minimum Reflectance = 85%
Fiber Optic Cable	Ocean Optics	P-1000-UV-VIS	1000 μm diameter, 200-750 nm

Figure 2.16: Photograph of the LIBS Online Detector Mounted at the Sarasota County C&D Sorting Facility

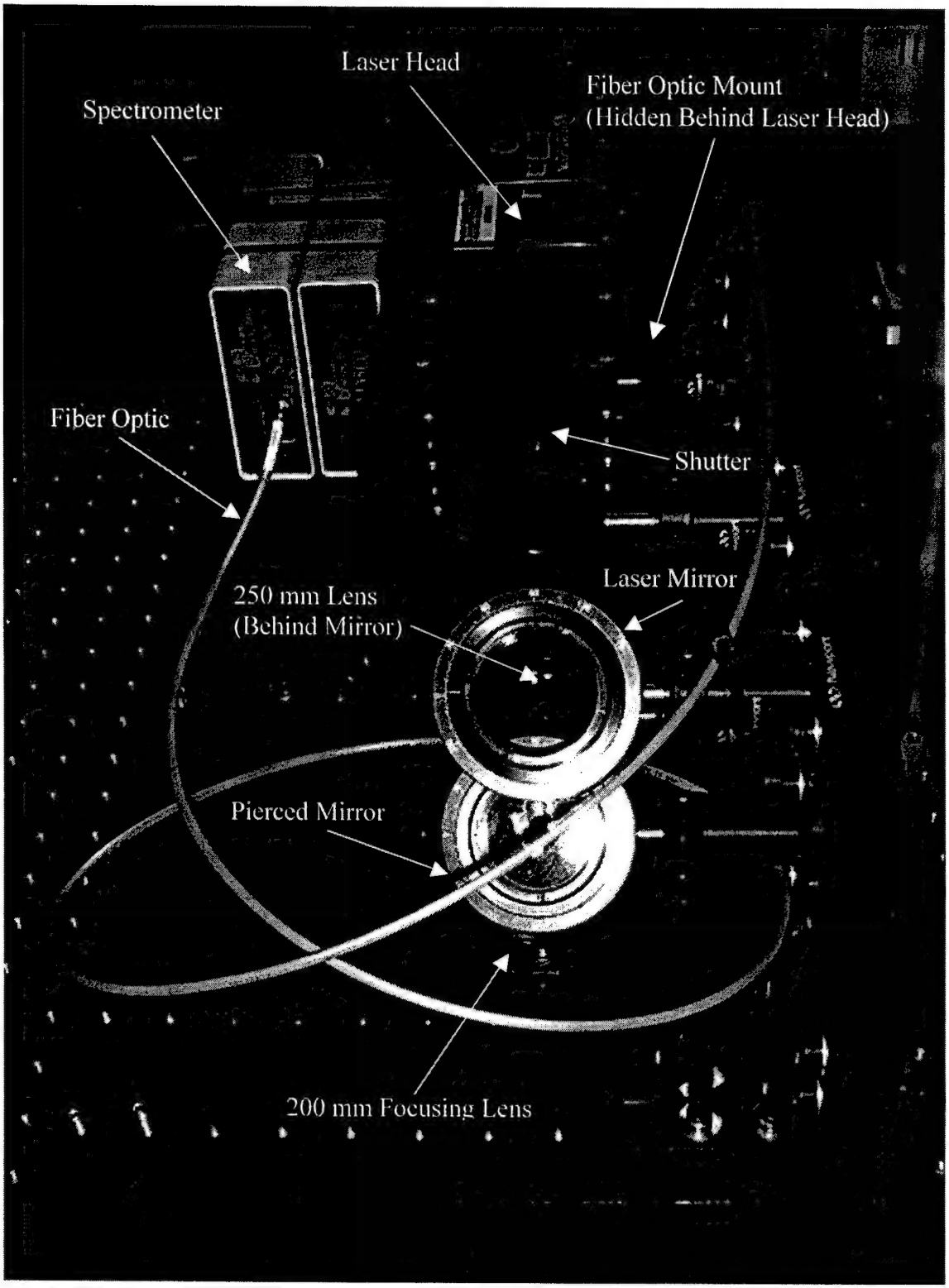

Figure 2.17: Detector Photograph with Components Labeled

CHAPTER 3
RESULTS AND DISCUSSION

The first field-test of the detector was performed at the Meyer and Gabbert C&D recycling facility located at the Sarasota County landfill during the latter portion of the design phase of the LIBS detector development. While the design was progressing well in the lab, checks were needed to ensure that the design would perform as well with weathered, dirty wood encountered at landfills. Another reason for field-testing was due to an interesting phenomenon occurring in the lab. Occasional pre-breakdown of the air above the wood sample occurred after repeated shots when the sample was located at the focal spot. The cause of this pre-breakdown was the amount of fine material ejected from previous sparks present in the air above the sample. This material, with a lower breakdown threshold, would initiate the cascade process just prior to the pulse reaching the surface of the wood. It was assumed that the speed of the samples moving along the conveyor and the naturally occurring winds at the landfill would quench this process and alleviate any need to alter the frequency of pulses or mechanically disturb the air above the wood samples.

3.1 Design Stage Field Trial

The first field trial was performed on April 20, 2001 with the settings as shown in Table 3.1. The laser output shown is the measured output for the flashlamp output setting of 11.5 J. Peak 1 is a conditional data analysis channel corresponding to the chromium

emission pixel. LabView software was utilized to average the intensity of the nine pixels centered on peak 1, namely pixel 1538, the location where the chromium emission line with the least interference was visually observed. This peak was then divided by the average intensity of the 20 pixels in each of the conditional analysis channels labeled base 1 and base 2. These areas were visually chosen to represent the plasma continuum characterized by a lack of atomic emission lines. The other two chromium lines were not used during this initial trial. The peak-to-base threshold of 4.0 was set after preliminary trials that day indicated that ratios above this value would accurately predict the presence of CCA, while values below 4.0 accurately predicted untreated wood.

Table 3.1: Settings for Field Trial 1 in Sarasota County, April 20, 2001

Setting	Value
Flashlamp Energy	11.5 J
Laser Output	188.5 mJ
Frequency	2 Hz
Spectrometer Delay	28 μs
Peak 1	Pixels 1534-1542 (~ 425 - 426 nm)
Base 1	Pixels 1385-1404 (~ 417 - 418 nm)
Base 2	Pixels 1958-1977 (~ 448 - 449 nm)
Threshold	4.0
Offset Correction	-4.5

The spectrometer offset is the CCD array output when no light is present on the array. This dark current, applied to all pixels of the array, increases both peak and baseline values. The offset has the effect of diminishing the peak-to-base ratio by adding a constant value to both the peak and the base. This offset is corrected within the analysis software by adding the offset correction entered by the operator. The offset correction is subtracted from both the peak and the base values, and is set to approximately 5 counts

less than the actual offset to avoid division-by-zero errors when the baseline continuum signal approaches zero.

The presence of the CCA chemical on wood samples was confirmed by using Chrome Azurol S and PAN Indicator chemical stains. As detailed earlier in Chapter 1, the stains were slow to act and often required shaving the outer surface away to prevent interference reactions.

With these settings in place, two sorting trials were conducted using 40 pieces of mixed lumber. The established protocol was to identify a piece as CCA treated if 5 or more of the 10 shots from the laser were above the set threshold. The research team did not know which pieces were treated with the CCA chemical until after reporting their observations to the other project team members.

The results for the two sorting trials were impressive. Figure 3.1 identifies each sample as well as the average peak-to-base ratio of all 10 shots. Samples 1-40 were from the first trial while samples 41-80 were from the second trial. Of the 80 combined samples, only three were misidentified. Sample 37 had only 4 of the 10 shots exceed the threshold even though the ratio of all shots was 4.4. Sample 61 had 10 shots exceed the threshold and the ratio of all shots was 4.1.

Sample 34 was identified by the stains as treated yet the laser had only 1 of the 10 shots exceed the threshold, and the ratio of all shots was only 2.9. Upon further analysis of the stains, it was uncertain whether the stain indicated treated or untreated. Since it appeared that the stains were undergoing interference reactions and based upon the laser results, this piece was determined to be untreated.

Even before design completion, the laser proved to be 97.5% accurate based upon this preliminary trial. Additionally, as expected, the pre-breakdown events observed in the lab did not occur in the field. Areas requiring additional effort were the desire to increase the spread between the average peak-to-base ratios for the treated and untreated wood samples, and optimizing the collection optics to accurately predict treated versus untreated wood over a greater distance with respect to the focal point. This led to the optimization efforts detailed in section 2.5.3 Collection Optics.

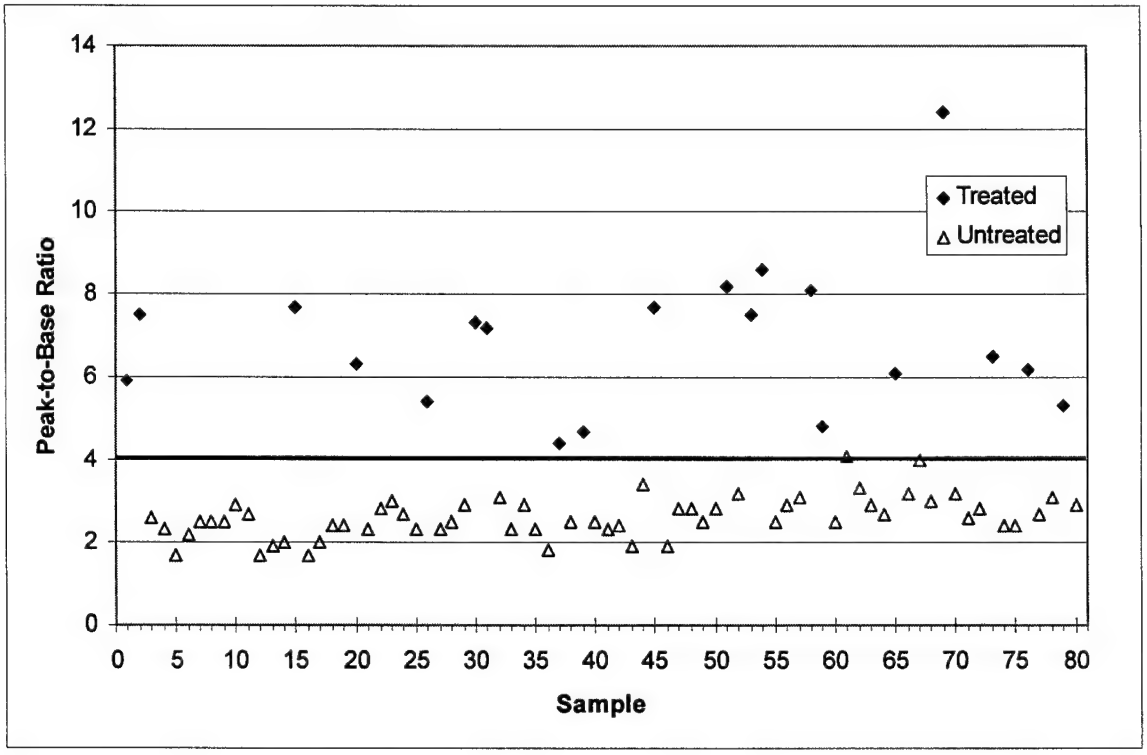

Figure 3.1: Peak-to-Base Ratios for Trial 1 Based on the Chromium 425.40 nm Emission Line. Detector Threshold is Equal to 4.0

Just as the optics optimization process was ending, the laser head had to be returned to the manufacturer for repair. As a result of these repairs, several new components were installed, including a replacement flashlamp that differed slightly from the original specifications. This replacement lamp was used due to the specified flashlamp requiring 8 weeks for delivery. The use of the replacement lamp allowed the project to complete on schedule, and would only have a detrimental effect on the lifespan of the new lamp. The other feature that changed was the laser output as a function of flashlamp energy. This is the cause for the lower flashlamp energies in later trials.

3.2 Calibration Field Trials

The second field trial took place on June 11, 2001, after receipt of the repaired laser. By examining individual spectra at varying delay times, this trial verified the 28 μs delay resulted in the maximum peak-to-base ratio. These results were displayed in Figure 2.14. Additional analysis of the spectra established pixel 1539, rather than pixel 1538 used in trial 1, as the peak of the chromium emission line at 425.40 nm.

The third field trial was conducted on June 20, 2001 to collect single-shot spectra for various wood samples, including CCA treated, untreated, treatment with alternate chemicals, painted and stained surfaces. This data was then taken back to the lab for statistical analysis. The analysis sought to determine the optimum peak-to-base threshold considering both the mean values and standard deviation of the peak-to-base ratios. Also examined was the optimum number of pixels around the chromium peak to average. The laser settings for this trial are shown in Table 3.2.

Table 3.2: Settings for Field Trial 3 in Sarasota County, June 20, 2001

Setting	Value
Flashlamp Energy	10.7 J
Laser Output	184.5 mJ
Frequency	2 Hz
Spectrometer Delay	28 μs
Base 1	Pixels 1385-1404 (~ 417 - 418 nm)
Base 2	Pixels 1958-1977 (~ 448 - 449 nm)
Offset Correction	1

Note that the threshold and peak information are not listed since this information would be calculated after data analysis. It was also noticed that the spectrometer offset was at zero during these tests but would be later corrected by adding 1 during analysis.

400 single-shot spectra were collected for CCA treated wood, while 300 single-shot spectra were collected for untreated wood. The peak-to-base ratio was calculated at two chromium and two calcium peaks. The third chromium peak at pixel 1603, corresponding to 428.90 nm, was not analyzed since it was readily apparent that while a strong emission line for treated wood, it also suffered from strong interference lines in untreated wood resulting in false positive hits.

As shown in Table 3.3, the mean and standard deviation were calculated for the peak-to-base ratios of pixels 1539 and 1576, corresponding to 425.40 and 427.50 nm respectively, with the peak value based on an average of 3, 5 or 7 pixels centered about the peak. The overlap is the calculated result of the mean peak-to-base ratio plus one standard deviation for untreated wood, while subtracting the mean minus one standard deviation for CCA treated wood. This factor provides insight into the separation of the peak-to-base ratios for treated and untreated wood by considering both mean values and deviation from the mean and is represented in Figure 3.2. Increased separation of the

peak-to-base ratios results in improved accuracy of the detector. Table 3.3 also shows that while the 427.50 nm line centered on pixel 1576 was a strong emission line that had less interference than the 428.90 nm line discarded earlier, there were enough interference lines in the spectra of untreated wood to reduce the effectiveness of this line to indicate the presence of chromium. Therefore, the 427.50 nm line corresponding to pixel 1576 was not used in future analysis.

Table 3.3: Trial 3 Statistical Results

Peak	Width	CCA Treated		Untreated		Overlap	Threshold
		Mean	σ	Mean	σ	μ+/−σ	P/B Ratio
1539	3 Pixels	31.02	19.32	6.75	5.45	0.50	11.70
	5 Pixels	25.31	16.01	5.73	4.51	0.94	9.30
	7 Pixels	20.83	13.37	4.97	3.85	1.36	7.46
1576	3 Pixels	30.80	18.70	9.68	7.44	5.02	Not Used
	5 Pixels	25.07	15.57	8.08	6.23	4.81	Not Used
	7 Pixels	21.06	13.24	7.17	5.53	4.88	Not Used

Peak	Width	CCA Treated Wood Accuracy			Untreated Wood Accuracy		
		1 Shot	5 Shots	10 Shots	1 Shot	5 Shots	10 Shots
1539	3 Pixels	84.8%	95.0%	100.0%	82.3%	93.3%	90.0%
	5 Pixels	85.0%	95.0%	100.0%	78.7%	86.7%	93.3%
	7 Pixels	86.0%	95.0%	100.0%	74.0%	81.7%	83.3%

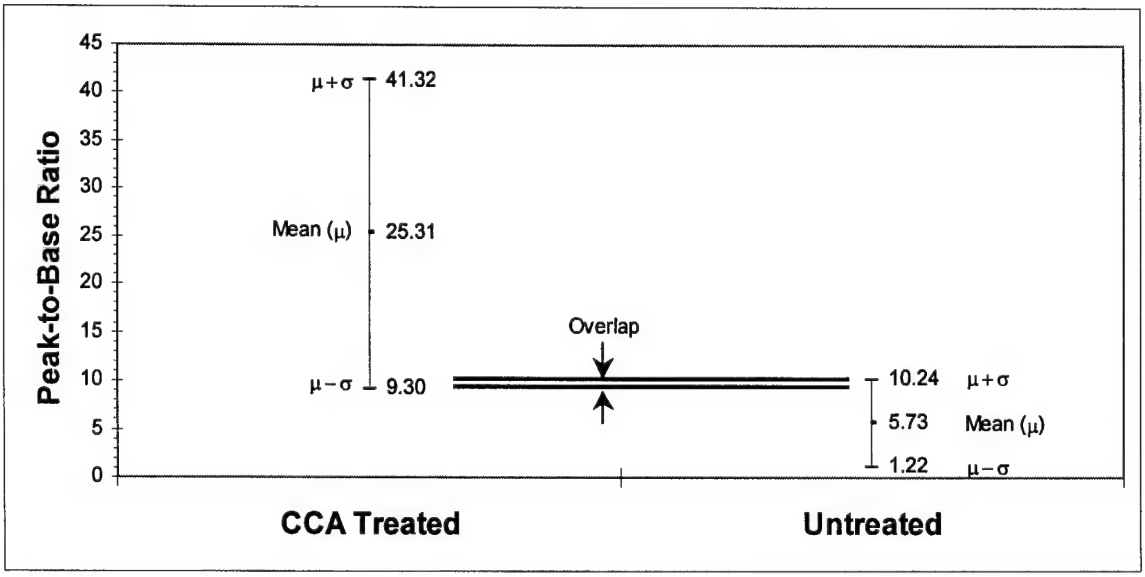

Figure 3.2: Overlap of Peak-to-Base Ratios for Trial 3

Also established was that the optimum threshold for this data set was the mean peak-to-base ratio of CCA treated wood minus one standard deviation. The predictive accuracy of the laser was calculated in the second half of Table 3.3 by first analyzing the number of shots that exceeded this threshold for treated and untreated wood at the three peak widths. While none of the three widths provided satisfactory accuracies on a single-shot basis, analyzing 5 or 10 shots from a single sample provided very accurate results. The same protocol used in the initial sort was applied to this data analysis, if 50% or more of the shots were above the threshold, the sample was predicted to be CCA treated wood. The data indicates that for a 10 shot analysis of wood, the 5 pixel integration had the best results with 100% accuracy in identifying treated wood and 93.3% accuracy in identifying untreated wood. The 3 pixel integration also performed well, but there was concern that if the grating in the spectrometer drifted even slightly, the accuracy of the detector would suffer greatly. Note that initially the 427.50 nm peak was centered on pixel 1538 but eventually shifted to pixel 1539. This shift applied to all peaks across the entire spectra. Therefore, the 5 pixel integration centered on pixel 1539 for a 10 shot analysis was established as the optimum setting.

One issue that was of concern was the larger standard deviation and poorer separation in the peak-to-base ratios than expected. The overlap previously described can be seen on a shot-by-shot basis in Figures 3.3 and 3.4 with the overlaid thresholds. It is noted that 25 shots were recorded for each side of the samples. Therefore, the major tick marks at 50 sample intervals identify new pieces of wood, while the minor tick marks at 25 sample intervals identify changing sides. Little correlation between the sides of the pieces of wood and the ratio was observed.

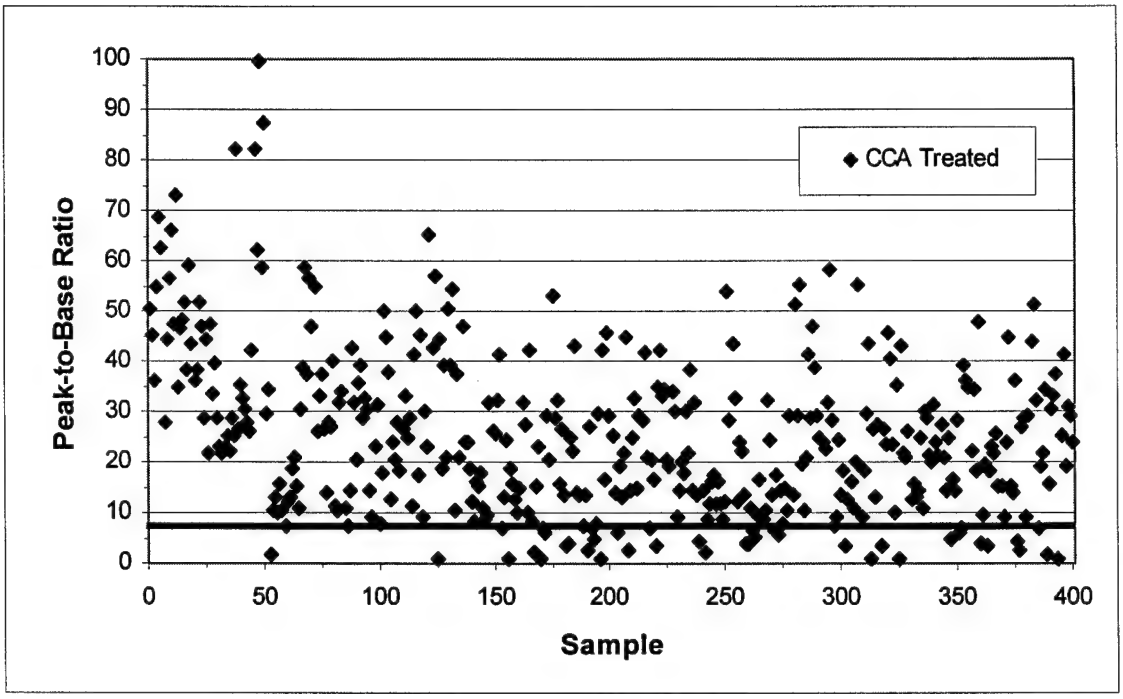

Figure 3.3: Single-Shot Peak-to-Base Ratios for Trial 3 CCA Treated Wood

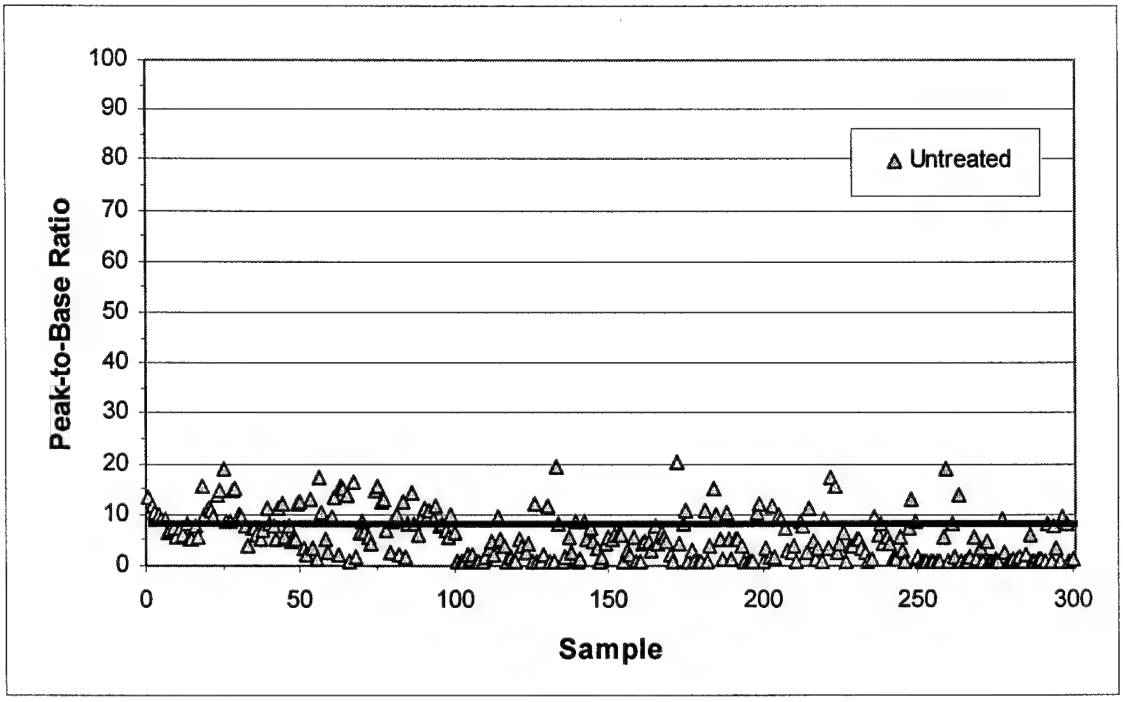

Figure 3.4: Single-Shot Peak-to-Base Ratios for Trial 3 Untreated Wood

When the peak-to-base ratios of this data set were compared to the values recorded during the initial field trial, the ratios were much higher but the standard deviation was also greater. The cause of this was two-fold. The intensity of the pixels corresponding to base 2 (1958 to 1977) was always at zero. This resulted in halving the true continuum intensity, thereby doubling the peak-to-base ratios. The second problem was that with the spectrometer offset equal to zero, the normal fluctuations seen in the continuum spectra were being truncated. The combined effect was that the intensity of the peaks did not scale with the baseline, resulting in an absolute intensity measurement rather than a true peak-to-base measurement. This effect is evident when examining 100 shots for CCA treated wood as shown in Figure 3.5.

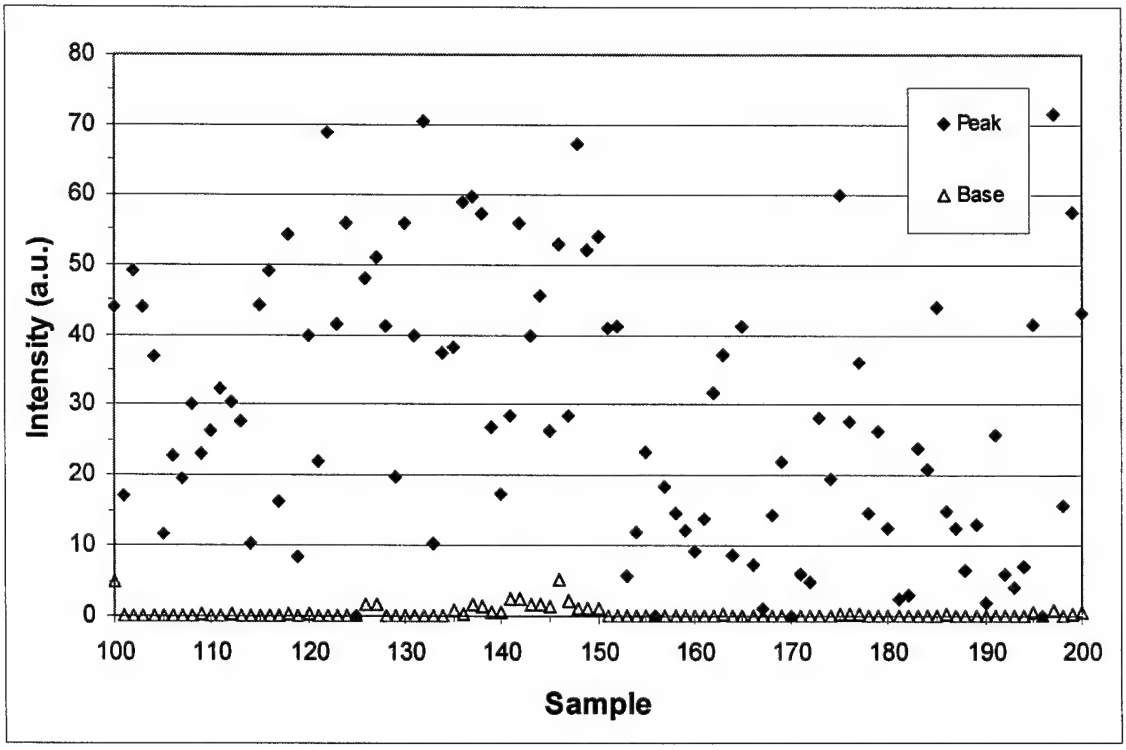

Figure 3.5: Single-Shot Absolute Peak and Base Intensities for CCA Treated Wood

Also interesting was that some shots seemed to "misfire," resulting in weak plasma emission signal and peak-to-base ratios of exactly one. An example of this is seen for shot 167 in Figure 3.4. The calcium peaks were also quenched when these rare events occurred. A related event was observed when the laser struck a painted surface. It was expected that the laser's energy density would be sufficient to either remove enough paint and wood to positively identify the chromium, or the chromium would leach into the paint over time, also resulting in a positive identification. Unfortunately, neither of these occurred, resulting in the inability to tell the difference between CCA treated and untreated wood once it was painted or stained. However, as also seen with the misfires, the calcium emission lines were also quenched. While CCA treated and untreated wood had peak-to-base ratios of approximately 365 and 275 for the 392.64 nm and 395.86 nm calcium lines, the ratios dropped to less than 100 on painted pieces. Therefore, an unexpected benefit was the ability to identify either a misfire or the presence of a painted surface based on the calcium emission lines. By setting thresholds for both the chromium and the calcium emission lines, the software could be programmed to set off a unique trigger through the multi-channel output card whenever both thresholds were not exceeded. This output could then be tied to an alternate color strobe or to mechanical sorting equipment to separate that piece for further analysis.

The alternate analysis could take the following form. The piece could be stopped under another LIBS detector to allow the laser to burn through the paint. It was noticed that as the laser burned through the paint, both the calcium and chromium peak-to-base ratios would climb above the threshold and then taper off once the wood became tempered. These effects on the peak-to-base ratios are shown in Figures 3.6 and 3.7.

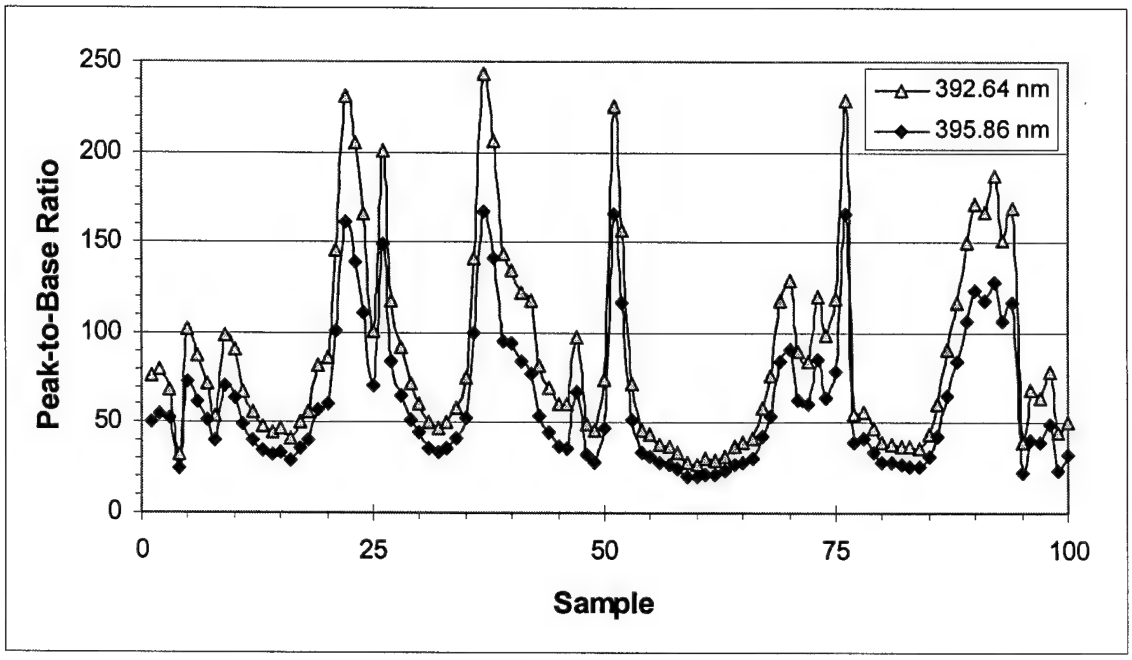

Figure 3.6: Shot-by-Shot Peak-to-Base Ratios for the Calcium Emission Lines when the Freshly Painted Sample is Stationary for 25 Shots

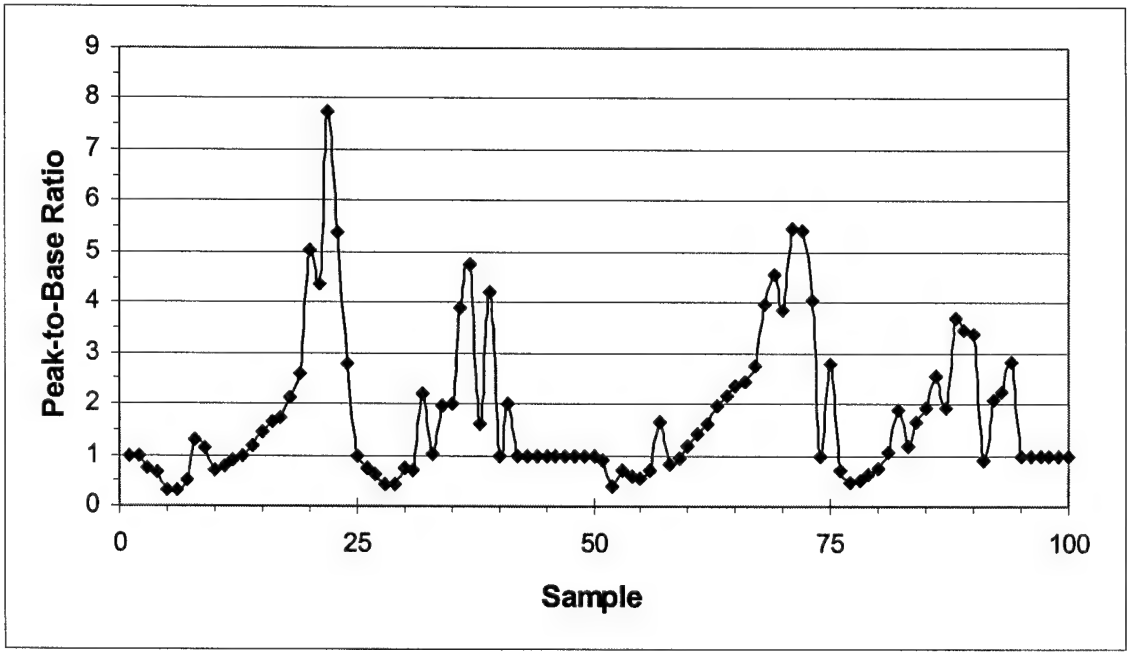

Figure 3.7: Shot-by-Shot Peak-to-Base Ratio for the 425.40 nm Chromium Emission Line when the Freshly Painted Sample is Stationary for 25 Shots

Once tempered, the surface of the wood is less reactive to the incident laser pulse. However, untreated painted wood would not exceed the chromium peak-to-base threshold even after repeated hits. It took between 10 and 25 hits in the same spot to burn through the paint.

As mentioned earlier, alternate wood preserving treatment chemicals were also tested. The chemicals tested included Copper Citrate (CC), Alkaline Copper Quat (ACQ), Copper Dimethyldithiocarbamate (CDDC), Copper Boron Azole (CBA) and Thompson's Water Sealer. The only chemical that tested positive for chromium and therefore would be falsely predicted as CCA, was Copper Boron Azole. This chemical had nearly identical peak-to-base ratios for the analytes as the CCA chemical. Thompson's water sealer did not test positive for chromium but did mask the CCA chemical when applied over CCA treated wood. However, it was considered very unlikely that water sealer would be placed upon any significant percentage of CCA treated wood in the waste stream but rather be used to protect untreated lumber. It is also noted that the heavy coat of water sealer was freshly applied, and had not been weathered or aged, which is expected to reduce the sealer's ability to mask the CCA treated wood.

3.3 Final Field Trial

The final field trial was conducted on July 3, 2001 with the purpose of establishing a true peak-to-base measurement, and enhancing the predictive ability of the laser. This was accomplished by adjusting a potentiometer within the spectrometer to increase the offset to approximately 80 counts. This would eliminate the truncating of the continuum signal at low signal levels. Additional adjustments included increasing the laser power and shortening the delay time, which further aided analysis. The location of

the second base (base 2) was also changed to the same pixels as base 1 to provide a more accurate representation of the continuum intensity. As expected, the peak-to-base ratio dropped to values consistent with the initial trial, but the deviation was also reduced significantly. These revised settings are summarized in Table 3.4.

Table 3.4: Settings for Field Trial 4 in Sarasota County, July 3, 2001

Setting	Value
Flashlamp Energy	11.2 J
Laser Output	196.0 mJ
Frequency	2 Hz
Spectrometer Delay	27.7 μs
Peak 1	Pixels 1537-1541 (~ 425 - 426 nm)
Base 1	Pixels 1385-1404 (~ 417 - 418 nm)
Base 2	Pixels 1385-1404 (~ 417 - 418 nm)
Threshold	2.6
Offset Correction	-75

The threshold value of 2.6 was set after conducting some preliminary trials to determine a value that accurately predicted the presence or absence of the CCA chemical. The optimum value would be determined later in the lab once the single-shot data could be analyzed.

With these settings in place, another sort was conducted to measure the system's accuracy and the sorter's ability to accurately determine if the strobe flashed 5 or more times out of the ten shots analyzed. With 60 pieces of wood sampled, the results were outstanding. The laser operated at 100% accuracy while the human observer only missed a single sample that flashed five times while they thought it was only four. Figure 3.8 identifies each sample as well as the overlaid threshold at 2.6 and the average peak-to-base ratio of all 10 shots. Sample 31 is the one piece that was misidentified by the

observer. In addition to the sort, 1000 single-shot spectra were collected for analysis, with 500 spectra for CCA treated wood and untreated wood each.

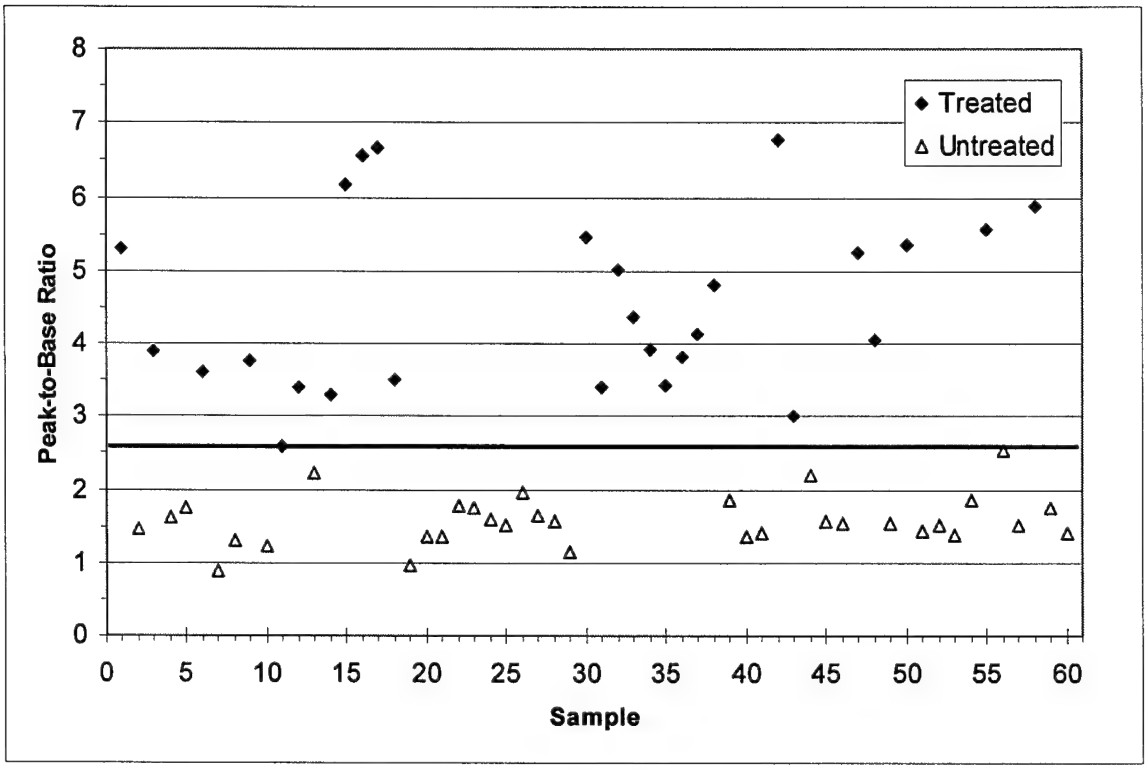

Figure 3.8: Peak-to-Base Ratios (10 shot average) for Trial 4 using the 425.40 nm Chromium Emission Peak

The unique processing applied to the single-shot spectra from this trial was to automatically calculate the offset for each shot. Pixels 2 through 24 are masked from the incoming light, hence they accurately represent the offset. Therefore, averaging these pixels and subtracting one to avoid division by zero errors enabled this value to be used as the offset correction to be subtracted from the entire spectra on a shot-by-shot basis. Pixel 1 was ignored because it is always zero.

During analysis it was immediately noticed that the modifications to the spectrometer and laser settings listed in Table 3.4 solved the problem of the continuum base signal not accurately scaling with the peaks. Figure 3.9 compares the peak and base intensities of trial 4. Only 50 samples are shown to aid resolution.

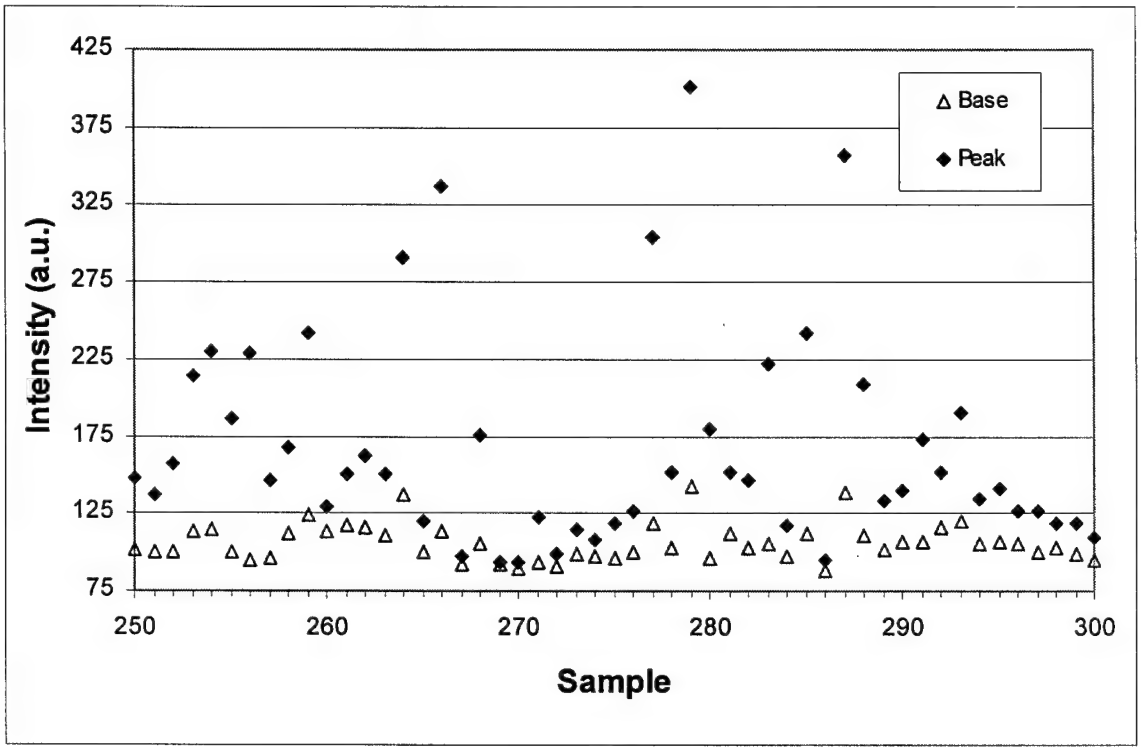

Figure 3.9: Single-Shot Absolute Peak and Base Intensities for Trial 4 CCA Wood

With the improvement in the peak-to-base ratio calculation, and the shot-by-shot calculation of the offset and offset correction factor, the mean and standard deviation were calculated for the peak-to-base ratio of pixel 1539, corresponding to the 425.40 nm chromium emission line, with the peak intensity the calculated average of 5 pixels centered on the peak. As noted above, this peak value was divided by the average of the

base 1 and 2 pixels, both spread from pixels 1385 to 1404. The mean peak-to-base ratios, standard deviation, separation, optimum threshold, and accuracy for CCA treated and untreated wood are shown in Table 3.5.

Table 3.5: Final Statistical Results

Peak	Width	CCA Treated		Untreated		Separation	Threshold
		Mean	σ	Mean	σ		P/B Ratio
1539	5 Pixels	3.98	1.44	1.69	0.35	0.50	2.23

Peak	Width	CCA Treated Wood Accuracy			Untreated Wood Accuracy		
		1 Shot	5 Shots	10 Shots	1 Shot	5 Shots	10 Shots
1539	5 Pixels	91.6%	96.7%	100.0%	95.2%	96.7%	98.9%

The improvements discussed above achieved the desired outcome of decreasing both the mean values of the peak-to-base ratios as well as the standard deviations. While the mean values were much closer than trial 3, the standard deviations were also much less. The small standard deviations had the effect of improving the separation of the CCA treated and untreated peak-to-base ratios to a statistically significant level, as well as lowering the threshold. While the optimum threshold for trial 3 was simply the CCA mean minus one standard deviation, the optimum threshold for the fourth trial was found to be 2.23 rather than 2.54. This was due to the standard deviation for untreated wood having a value much smaller than the standard deviation for CCA treated wood. These effects on the peak-to-base ratios on a shot-by-shot basis are shown in Figures 3.10 and 3.11. Figure 3.12 shows how trial 4 achieved separation of the mean values of the peak-to-base ratios for treated and untreated wood rather than the significant overlap as seen in trial 3.

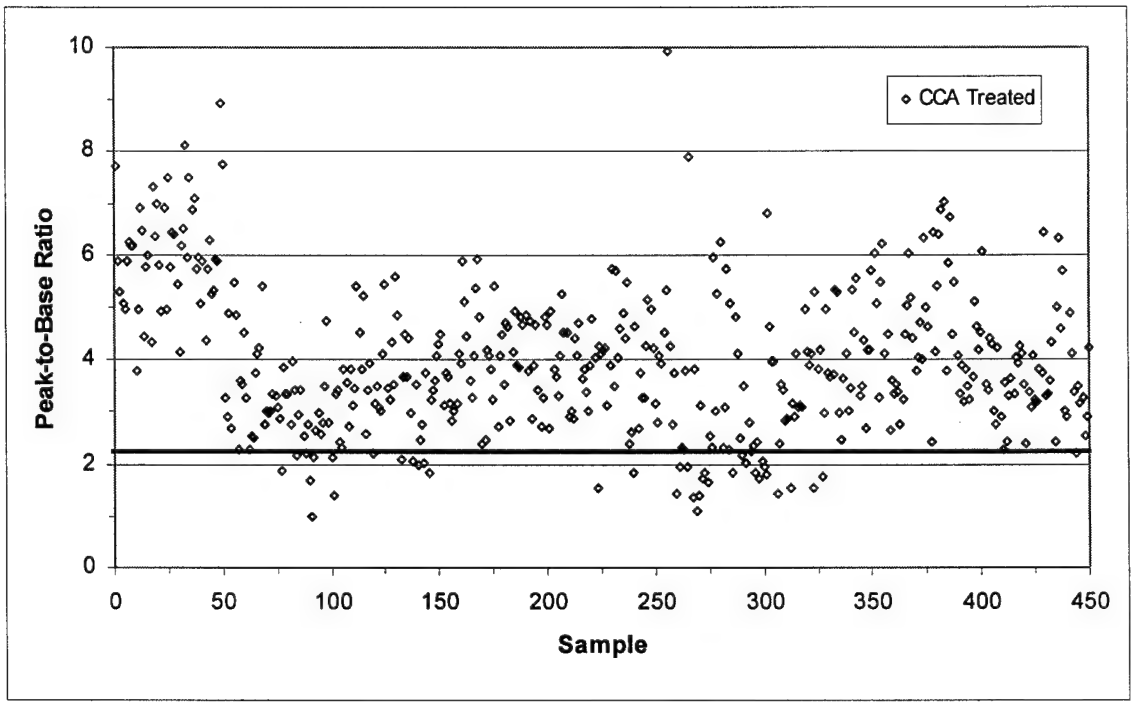

Figure 3.10: Single-Shot Peak-to-Base Ratios for Trial 4 CCA Treated Wood

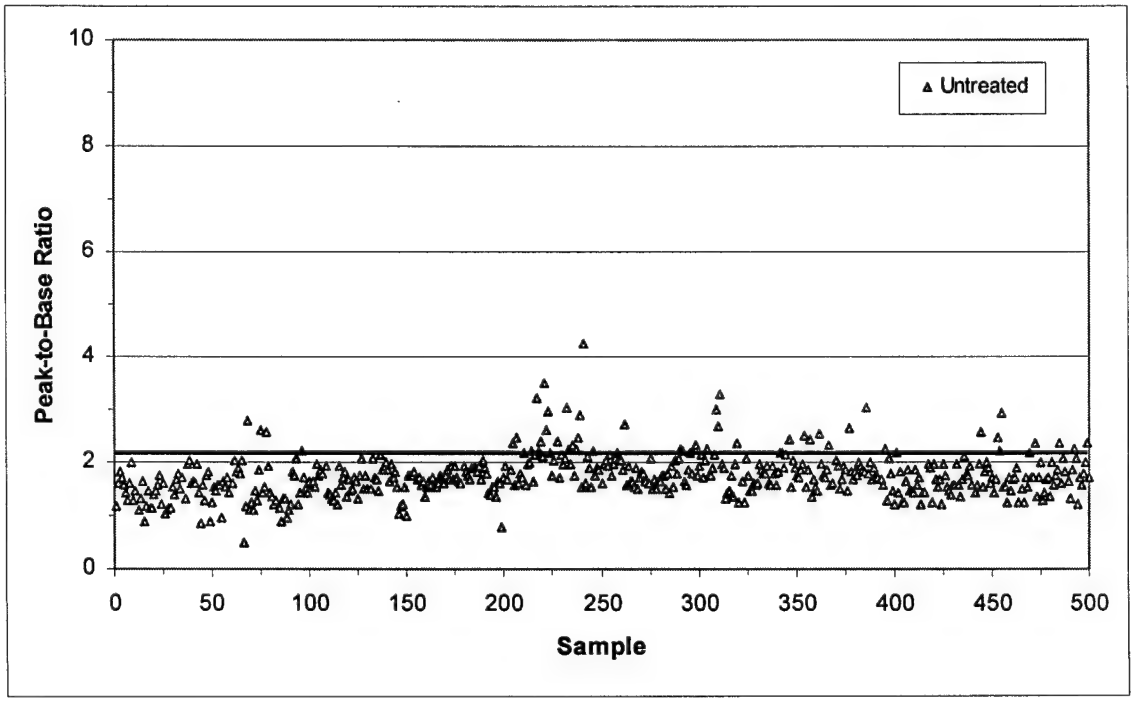

Figure 3.11: Single-Shot Peak-to-Base Ratios for Trial 4 Untreated Wood

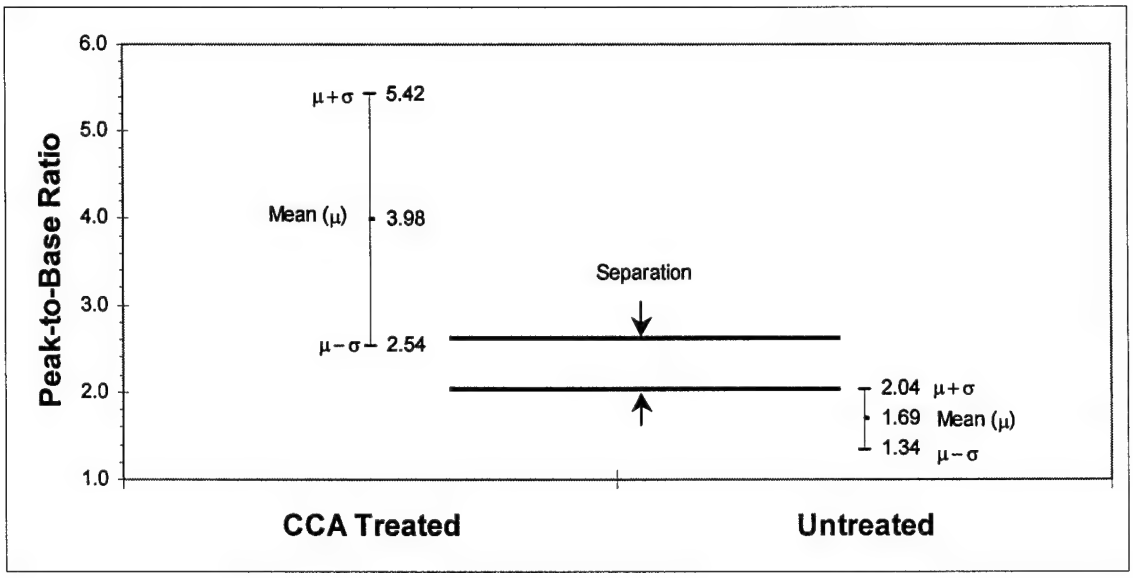

Figure 3.12: Separation of Peak-to-Base Ratios for Trial 4

As seen in Table 3.5, the overall result of the refinements implemented for the fourth field trial was the improved accuracy of the detector. Accuracy of single-shot analysis increased to 91.6% and 95.2% for CCA treated wood and untreated wood respectively. Using 5 shots per sample increased accuracies to 96.7% for both treated and untreated, while a 10 shot analysis perfectly predicted CCA treatment, with 98.9% accuracy for untreated wood.

3.4 Discussion

In addition to the challenges of surface coatings discussed above, striking metal fasteners also required special attention. Fortunately, when the laser pulse struck a metal fastener the peak-to-base ratio for calcium would disappear, allowing the computer to identify metal if the chromium peak-to-base ratio remained high while the calcium peaks

vanished. This algorithm could be implemented with the conditional analysis required for painted surfaces.

Some other observed difficulties that require additional refinement are the effects of moisture content, and heartwood effects on CCA retention level. While the laser was accurate for damp and wet wood, the detector was unable to identify the CCA treated wood after soaking the lumber for 30 minutes. The solution to this challenge is simply to use a higher energy laser in future detectors. It was also observed that in rare occasions some pieces of wood would test positive for the CCA treatment on one side while testing negative on the other. X-Ray fluorescence confirmed that the side of the wood that tested positive had much greater metal concentrations than the side that tested negative. It is believed that the side that tested negative was from the heartwood portion of the tree, a section that is known to have poor CCA retention values, while the side that tested positive was from the sapwood. This effect was recorded in the 500 single-shot spectra taken for CCA treated wood in trial four. Due to the rare nature of these events, the spectra from this piece were not included in the optimum peak-to-base ratio calculation shown in Table 3.5.

Although these difficulties require some additional software programming and hardware upgrades, the results from trial 4 were impressive. The enhanced accuracies, combined with the improved conditional analysis for painted wood and metal, demonstrated the ability of a LIBS based online detector to meet the accuracy required to pass the EPA's leaching tests described in Chapter 1 in order to use wood for fuel or mulch. Two questions arise regarding implementation, namely: what is the optimal value

of the threshold and how many laser shots are required to accurately detect the presence of CCA treated wood?

The answers are that the LIBS based detector has a multitude of settings that can be tailored to almost any application. If speed of detection and ensuring identification of all the CCA wood are the primary concerns, the thresholds can be set low enough to achieve this in only four or five shots. At a laser frequency of 10 Hz, this is about two pieces sorted per second. The drawback is that with the lower thresholds, some untreated wood will test as false positives. If overall accuracy is most important, the thresholds set in trial 4 combined with 10 or more shots is the optimum condition. The drawback here is that that the sorting speed drops to about one piece per second at 10 Hz. These issues are discussed further in Chapter 4.

CHAPTER 4
CONCLUSIONS AND RECOMENDATIONS

4.1 Conclusions

The Environmental Protection Agency and independent researchers continue to evaluate the long term impacts of CCA treated wood on human health and the environment. These studies are examining the leaching characteristics of CCA treated wood with respect to the ash resulting from combustion, the arsenic found under decks and playground structures, potential contamination of groundwater near unlined C&D landfills, as well as calculating the number of tons of arsenic imported into states that have otherwise low concentrations of naturally occurring arsenic.

Added pressures on the wood treatment industry are the increased media attention and several lawsuits, including a class action suit in Florida, resulting from the adverse health effects of arsenic on consumers who purchased and used the product without adequate warning of the composition and hazards of the material. The resultant attention is leading to consumers beginning to ask for the safe and viable alternatives to CCA treated wood, with companies beginning to market these alternatives in new regions.

Furthermore, environmental interest groups are pressuring elected officials and the EPA to review the continued regulatory exemption currently enjoyed by CCA treated wood. Federal regulations regarding the maximum arsenic levels in drinking water are also at the center of a political controversy currently playing out in the nation's capital.

However, even if CCA treated wood is banned or production limited due to consumer demand for alternate products, the inventory of CCA treated wood currently in use needs to be disposed of in an environmentally sound manner. While wood is a natural candidate for combustion to recover the inherent energy or chipping as mulch to reduce the landfill burden, these sources of disposal require the wood stream to be 98% to 100% untreated wood to pass the environmental leaching tests.

To meet these requirements, a system is required to accurately and quickly sort the wood waste stream by differentiating CCA treated from untreated wood or wood treated with an alternate chemical. While chemical stains and X-Ray fluorescence can accurately identify CCA treated wood, neither are ideal candidates for an on-line or *in situ* process that is necessary due to the volume of wood to be sorted.

This research demonstrates that a detector based upon laser induced breakdown spectroscopy can quickly and accurately differentiate unpainted CCA treated, unpainted untreated, and painted woods in the waste stream. By analyzing the chromium emission line at 425.40 nm and either of two calcium emission lines, the laser can determine if the wood is CCA treated if both analytes are above the set thresholds, untreated if the calcium is above the set threshold while the chromium is below, or painted if both analytes are below the set thresholds.

With the proper positioning of the detector above the conveyor, the detector can accurately analyze wood ranging in size from sheet products to 4 x 4 timbers. If a greater range is required, the laser could be placed on its side with the wood placed up against a stop as it passes on the conveyor. This would ensure the wood was always a fixed distance from the focusing optics.

The material costs to reproduce the LIBS detector with the hardware improvements listed below are $25,000 to $30,000 for the laboratory/ field grade hardware. This research has also progressed to the point where this design could be commercially reproduced and immediately implemented with minimal development costs.

4.2 Recommendations

Enhancements to the detector to further increase the accuracy and detection range include improvements in both the hardware and software programming.

4.2.1 Hardware Improvements

1. Use of a Universal Serial Bus (USB) high resolution spectrometer with the grating centered on 425 nm. This would allow the detector to operate at 10 Hz thereby requiring only one second to take a 10 shot analysis of each piece of wood sampled. The higher resolution grating would also reduce the interference of the 427.50 and 428.90 nm chromium peaks. Centering the grating on the chromium peaks would also enhance the sensitivity. This new device is roughly $3,500, approximately the same cost as the current spectrometer used.
2. Replace the laser head with a 400 mJ model. While a 50 mJ laser head was initially used due to much lower costs and smaller size, the price increase from 200 to 400 mJ laser is approximately $20,000 to $22,000 while the physical dimensions are exactly the same. Increased pulse energy will increase the spatial analysis range and increase sensitivity with surface treatments.

3. Replace the focusing/ collection lens with a larger diameter optic. By using a 75 mm or 100 mm diameter lens rather than a 50 mm lens, a greater portion of the plasma emission would be captured by the collection optics.
4. Replace the round pierced mirror with an elliptical pierced mirror. Once the round mirror is rotated 45° to redirect the collected spectral emission, there is light that passes by the sides of the mirror. An elliptical pierced mirror placed at a 45° angle would redirect all of the light collected, increasing the overall signal levels.

4.2.2 Software Improvements

1. Program the software to calculate the offset correction on a shot-by-shot basis.
2. Set up the conditional analysis of the two chromium peaks and one calcium peak to allow the differentiation of painted wood.
3. Set up the signal outputs for metal, as well as painted wood detection.
4. Program the software to recognize when a piece of wood is under the detector. The absence of emission readily enables determination of the start or end of a wood sample; hence the computer could count the number of shots that struck a piece of wood and determine its length. This would allow full use of all shots to calculate the percentage of shots above the threshold. The computer could then provide a single strobe output for each piece of CCA treated wood. Large pieces would have greater accuracy while small pieces could have reasonably accurate analysis down to as few as one or two shots. Another benefit is that this would alleviate the need for the sorter to count flashes. It also is not safe for the strobe to fire at 10 Hz since the frequency range of flashes that induce vertigo or seizure is from 8 to 12 Hz (Viire 2001; Wantland *et al.* 2001).

5. Develop a turnkey system that could be calibrated once a week by passing a couple pieces of CCA treated, painted and untreated wood under the detector. The computer could then automatically ensure the proper threshold values are set, correct for any shift in the spectrometer grating, and predict the conditional probabilities to the operator based on the recent composition of the waste stream. This would eliminate the need for any special training in laser diagnostic equipment for the operators and enhance the reliability of the detector. It is noted that other project team members, with no previous laser experience, operated the current system after minimal training.

APPENDIX A
OPTICS OPTIMIZATION RESULTS

Appendix A includes the complete graphical results of the optics optimization trials for the competing telescope designs. Separate graphs compare beam area and energy density as a function of telescope power and distance from the focusing lens for the 200 and 250 mm focal length optics. The results are only shown for the 50 mJ laser because the larger beam diameter of the 200 mJ laser did not require further expansion. Comparison of the 200 mJ laser energy density characteristics to representative telescope designs for the 50 mJ laser was shown in Figure 2.7.

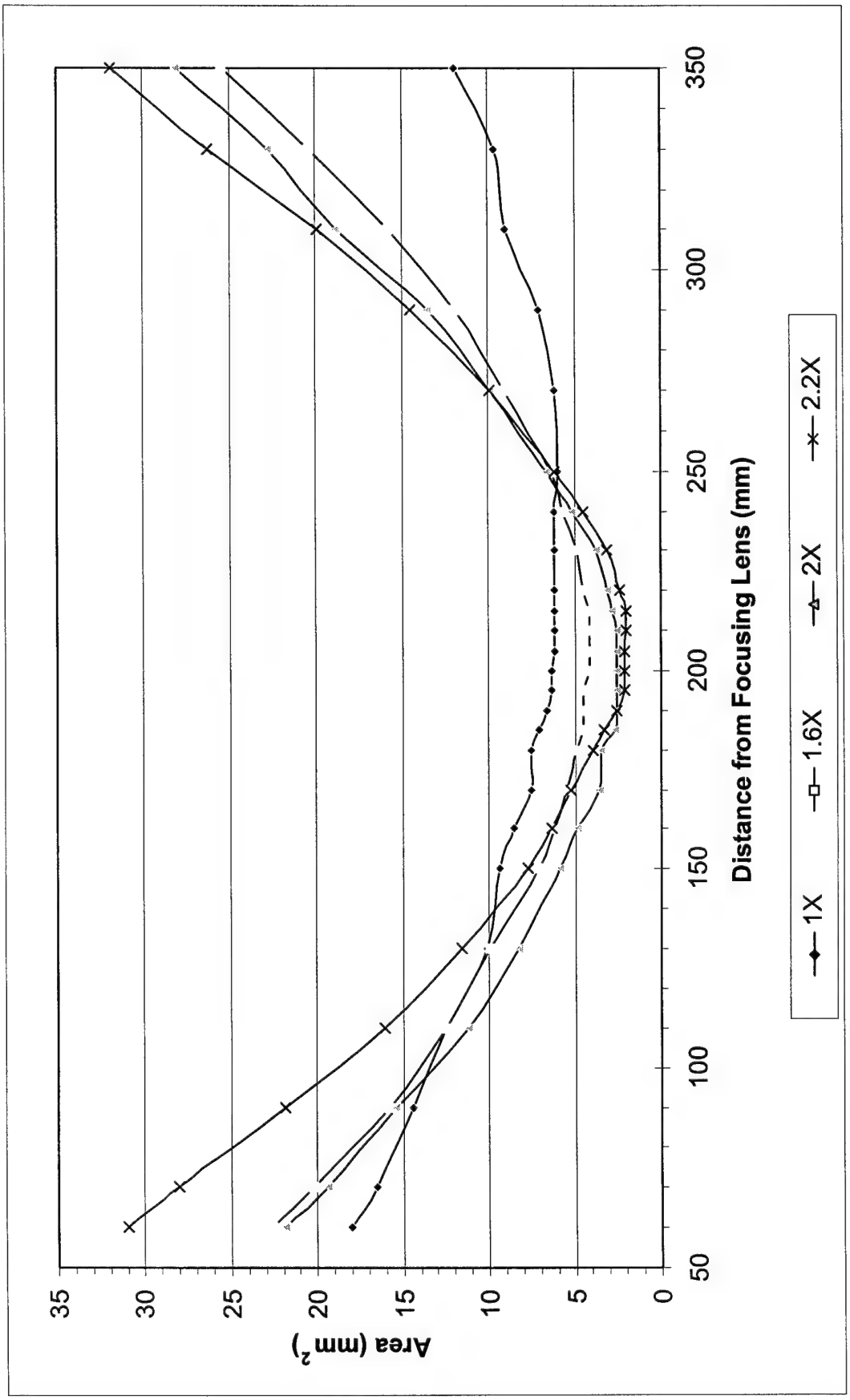

Figure A.1: Laser Beam Area as a Function of the Telescope used and Distance from the Focusing Optic for the 50 mJ Laser with a 200 mm Focal Length Lens

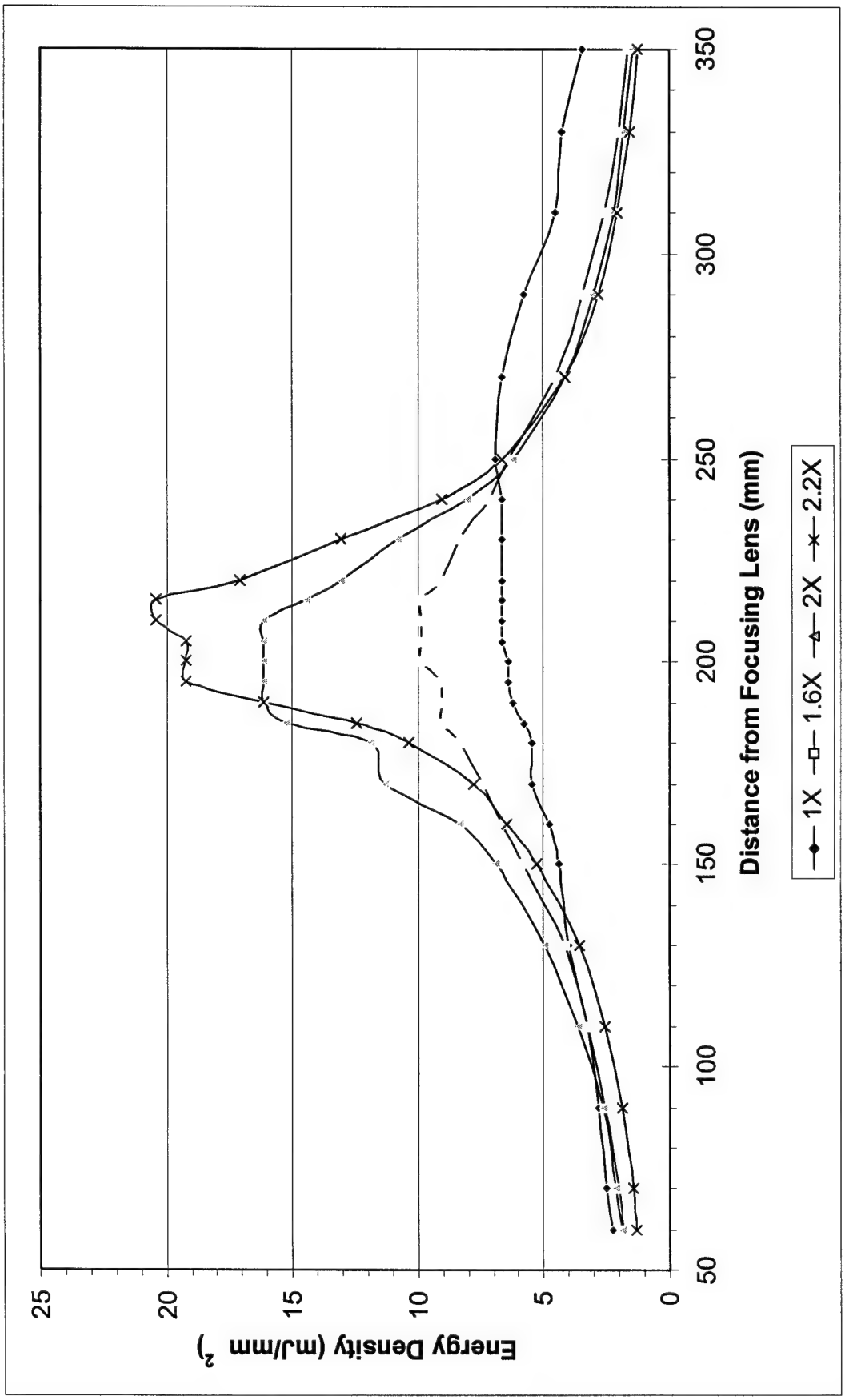

Figure A.2: Laser Beam Energy Density as a Function of the Telescope used and Distance from the Focusing Optic for the 50 mJ Laser with a 200 mm Focal Length Lens

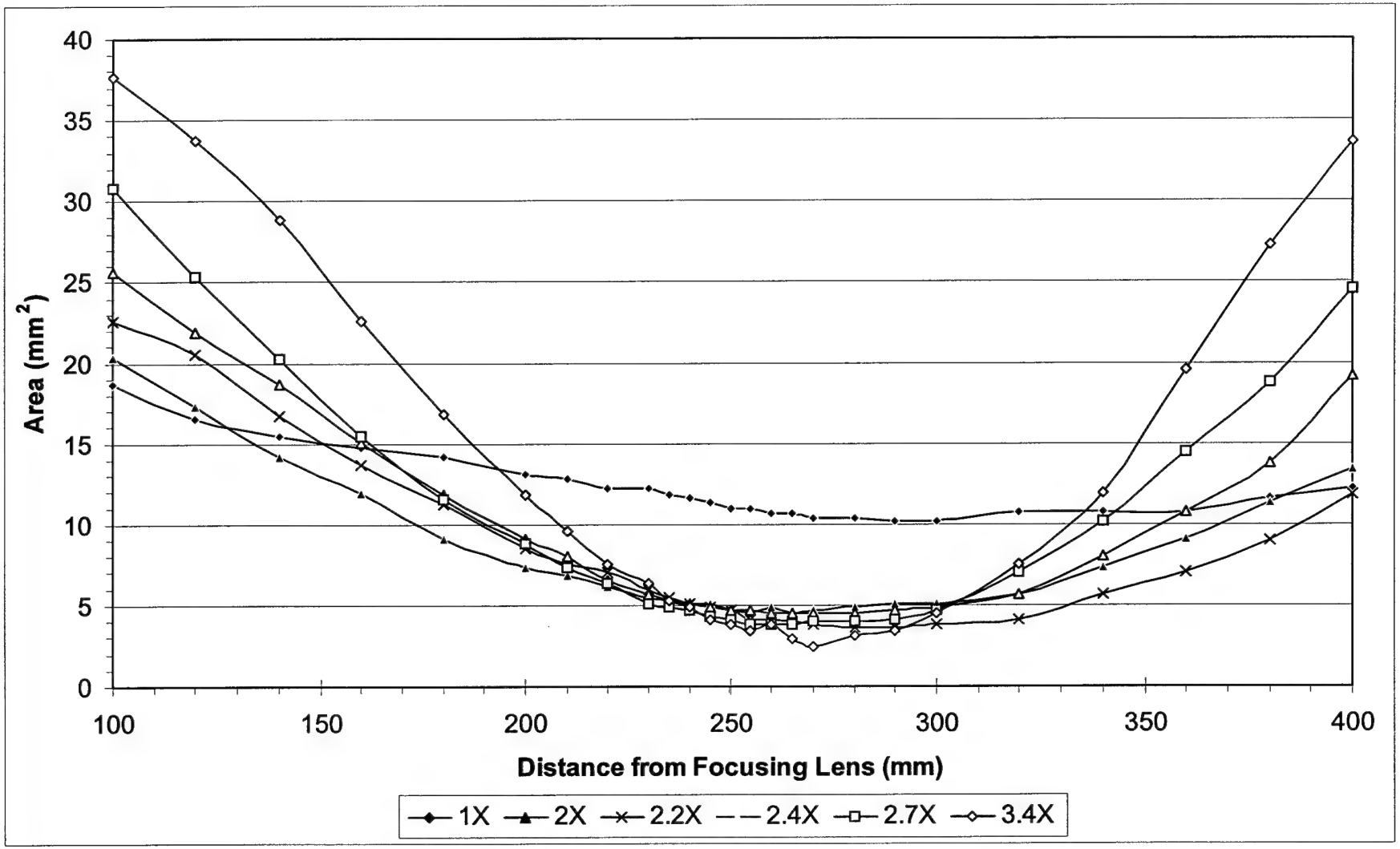

Figure A.3: Laser Beam Area as a Function of the Telescope used and Distance from the Focusing Optic for the 50 mJ Laser with a 250 mm Focal Length Lens

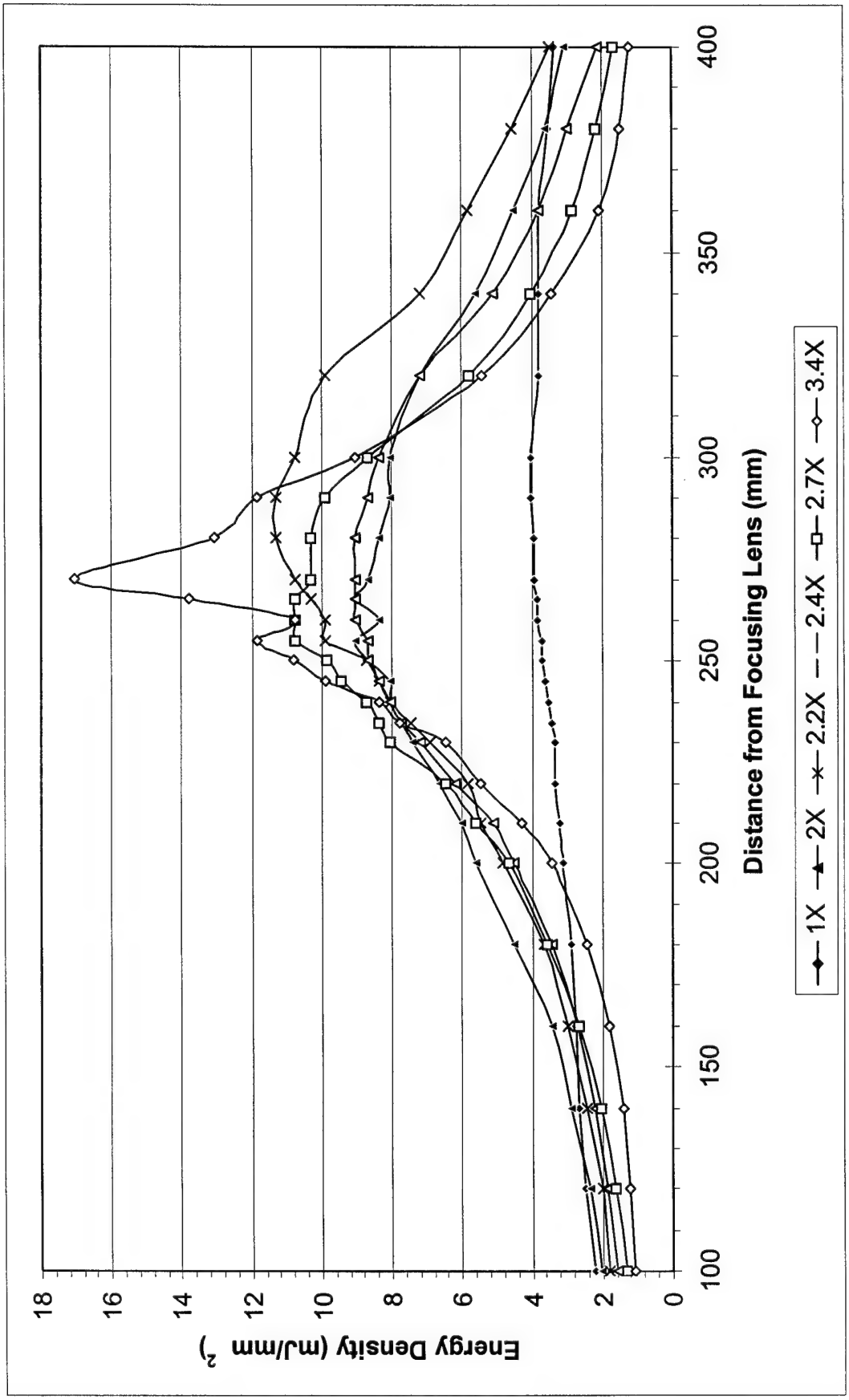

Figure A.4: Laser Beam Energy Density as a Function of the Telescope used and Distance from the Focusing Optic for the 50 mJ Laser with a 250 mm Focal Length Lens

APPENDIX B
BREAKDOWN THRESHOLDS, LASER AREA AND ENERGY CURVES

Appendix B includes graphical representations of the measured values of the laser energy and beam area as a function of power setting for the 50 mJ laser. These values were used to calculate the energy density at the breakdown threshold for various species of wood as shown in Table B.1.

Also included is a comparison of the metals concentrations within wood for the different types of CCA chemical at varying retention levels. Aditionally, Figure B.4 demonstrates the increased pulse energy for a given pump energy for the replacement lamp as discussed in Chapter 3.

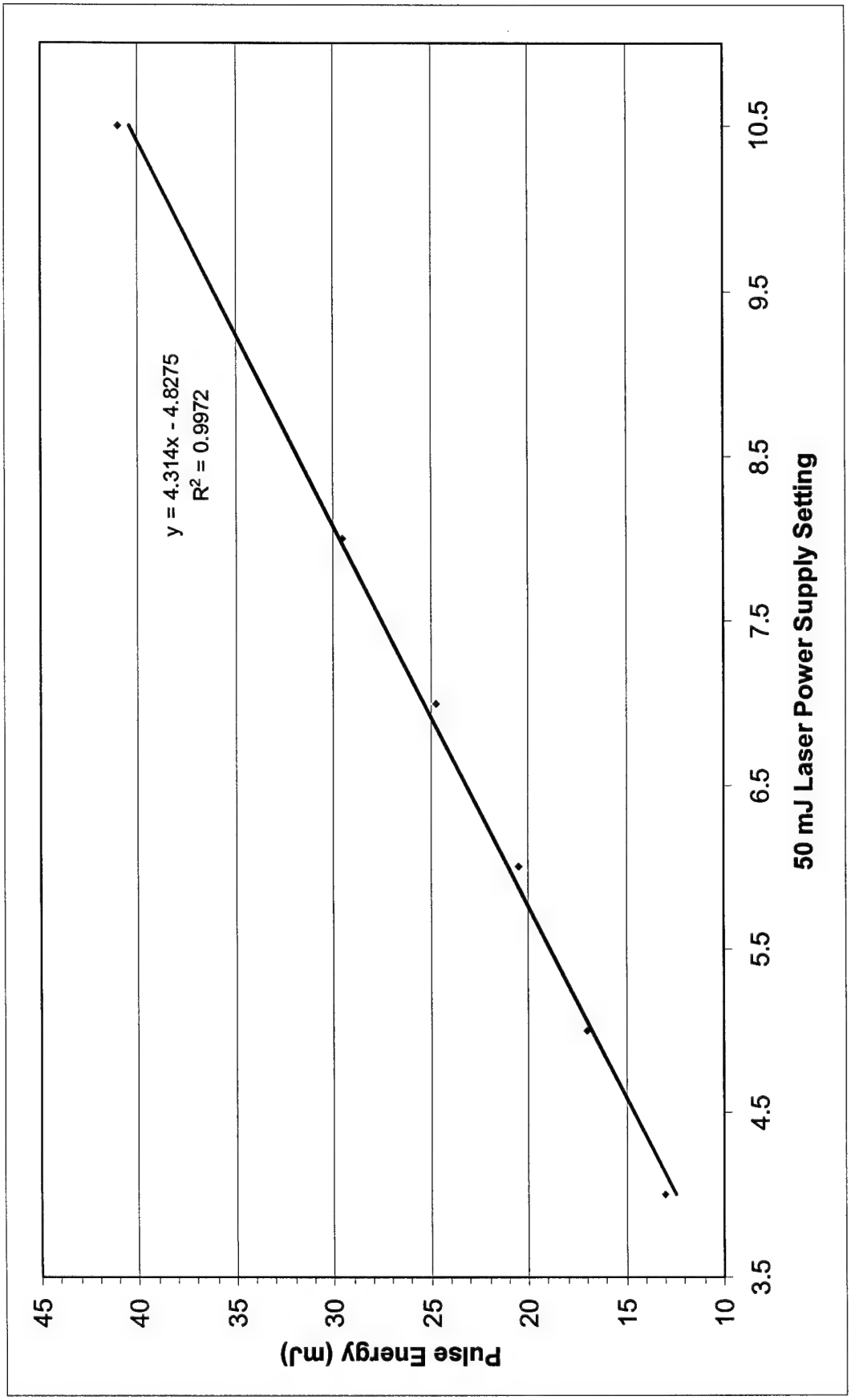

Figure B.1: Pulse Energy vs. Power Supply Setting for the 50 mJ Laser

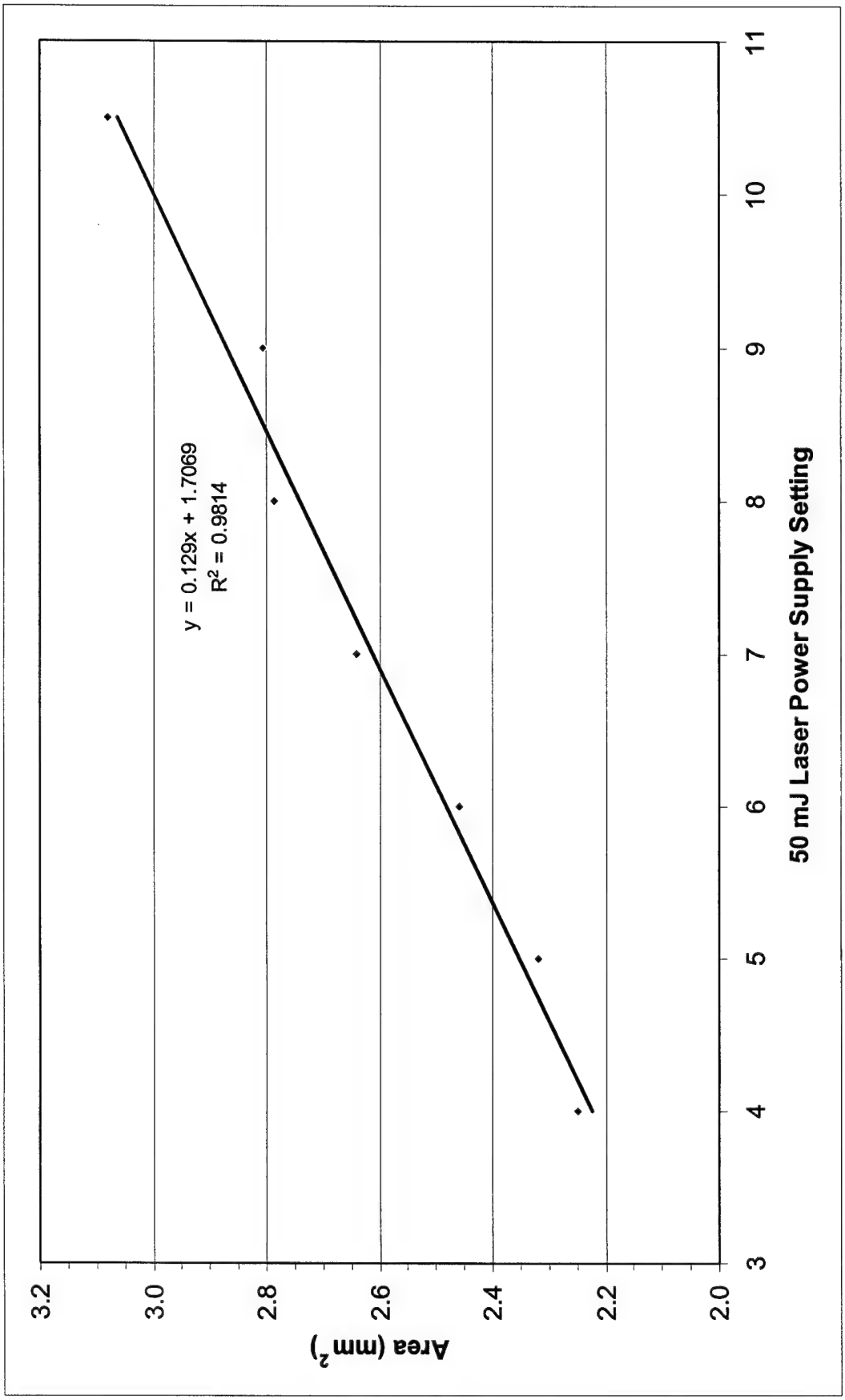

Figure B.2: Beam Area vs. Power Supply Setting for the 50 mJ Laser

Species	Trial 1				Trial 2				Trial 3				Mean Energy Density (mJ/mm^2)	Std. Dev.
	Setting	Energy (mJ)	Beam Area (mm^2)	Energy Density (mJ/mm^2)	Setting	Energy (mJ)	Beam Area (mm^2)	Energy Density (mJ/mm^2)	Setting	Energy (mJ)	Beam Area (mm^2)	Energy Density (mJ/mm^2)		
Ponderosa Pine	8.5	32.0	2.80	11.43	7.0	25.0	2.64	9.47	9.0	33.0	2.81	11.74	10.88	1.23
Poplar	5.5	19.0	2.39	7.95	5.0	16.5	2.32	7.11	6.0	20.5	2.46	8.33	7.80	0.62
Red Oak	7.5	27.5	2.72	10.13	6.0	21.5	2.46	8.74	7.5	27.0	2.72	9.94	9.60	0.75
Multi Layer Scrap	5.5	19.0	2.39	7.95	5.5	19.0	2.39	7.95	5.0	16.5	2.32	7.11	7.67	0.48
Pine 2x4	8.0	29.5	2.79	10.57	7.0	24.5	2.64	9.28	7.5	27.0	2.72	9.94	9.93	0.65
Pine Trim	7.5	27.5	2.72	10.13	7.5	27.5	2.72	10.13	7.5	27.0	2.72	9.94	10.07	0.11
Cedar	7.5	27.5	2.72	10.13	7.5	27.5	2.72	10.13	7.5	27.0	2.72	9.94	10.07	0.11
Partide Board	6.0	20.5	2.46	8.33	5.0	16.5	2.32	7.11	6.5	22.0	2.55	8.63	8.02	0.80
OSB	4.5	14.5	2.29	6.35	4.5	14.5	2.29	6.35	4.5	14.0	2.29	6.13	6.27	0.13
"Water Repellent"	6.5	23.0	2.55	9.02	5.5	18.0	2.39	7.53	5.0	16.0	2.32	6.90	7.82	1.09
.4 CCA 2x4	6.0	20.5	2.46	8.33	6.0	20.5	2.46	8.33	6.0	20.0	2.46	8.13	8.27	0.12
.4 CCA 1x6	7.0	24.5	2.64	9.28	6.5	22.0	2.55	8.63	7.0	23.5	2.64	8.90	8.94	0.33
.25 CCA 1x2	5.5	19.0	2.39	7.95	6.0	20.5	2.46	8.33	6.0	19.0	2.46	7.72	8.00	0.31
.4 CCA 1x6 (wet) (A)	6.5	22.5	2.55	8.82	7.0	24.5	2.64	9.28	6.5	22.0	2.55	8.63	8.91	0.33
.4 CCA 1x6 (wet) (B)	7.0	25.0	2.64	9.47	7.0	24.0	2.64	9.09	7.0	23.5	2.64	8.90	9.15	0.29
.4 CCA 1x6	6.5	22.5	2.55	8.82	6.5	22.0	2.55	8.63	6.5	21.0	2.55	8.24	8.56	0.30
Cypruss	4.5	14.5	2.29	6.35	5.0	16.0	2.32	6.90	5.0	16.0	2.32	6.90	6.71	0.32
Mahogony	4.5	14.5	2.29	6.35	7.0	24.5	2.64	9.28	7.0	23.5	2.64	8.90	8.18	1.60
Panel Board	6.5	22.5	2.55	8.82	7.0	24.5	2.64	9.28	7.0	23.5	2.64	8.90	9.00	0.24
Weathered CCA	4.0	13.0	2.25	5.78	4.5	14.5	2.29	6.35	3.5	10.0	2.25	4.44	5.52	0.98
2.5 CCA 2x4	3.5	10.7	2.25	4.76	3.5	10.5	2.25	4.67	3.5	9.5	2.25	4.22	4.55	0.29
Weathered CCA 2x4	2.5	6.5	2.25	2.89	2.5	6.5	2.25	2.89	2.5	5.0	2.25	2.22	2.67	0.38
Weathered CCA 1x6	2.0	4.5	2.25	2.00	2.5	6.5	2.25	2.89	2.0	4.0	2.25	1.78	2.22	0.59
Melamine	3.0	8.7	2.25	3.87	3.0	8.5	2.25	3.78	3.5	9.0	2.25	4.00	3.88	0.11
.4 CCA Plywood	5.5	18.5	2.39	7.74	5.5	18.0	2.39	7.53	5.5	18.0	2.39	7.53	7.60	0.12
Plywood	8.5	32.0	2.80	11.43	8.0	28.5	2.79	10.22	7.0	23.0	2.64	8.71	10.12	1.36
.25 CCA 2x4	5.0	17.0	2.32	7.33	5.0	16.0	2.32	6.90	5.0	16.0	2.32	6.90	7.04	0.25

Table B.1: Results from Wood Threshold Trials

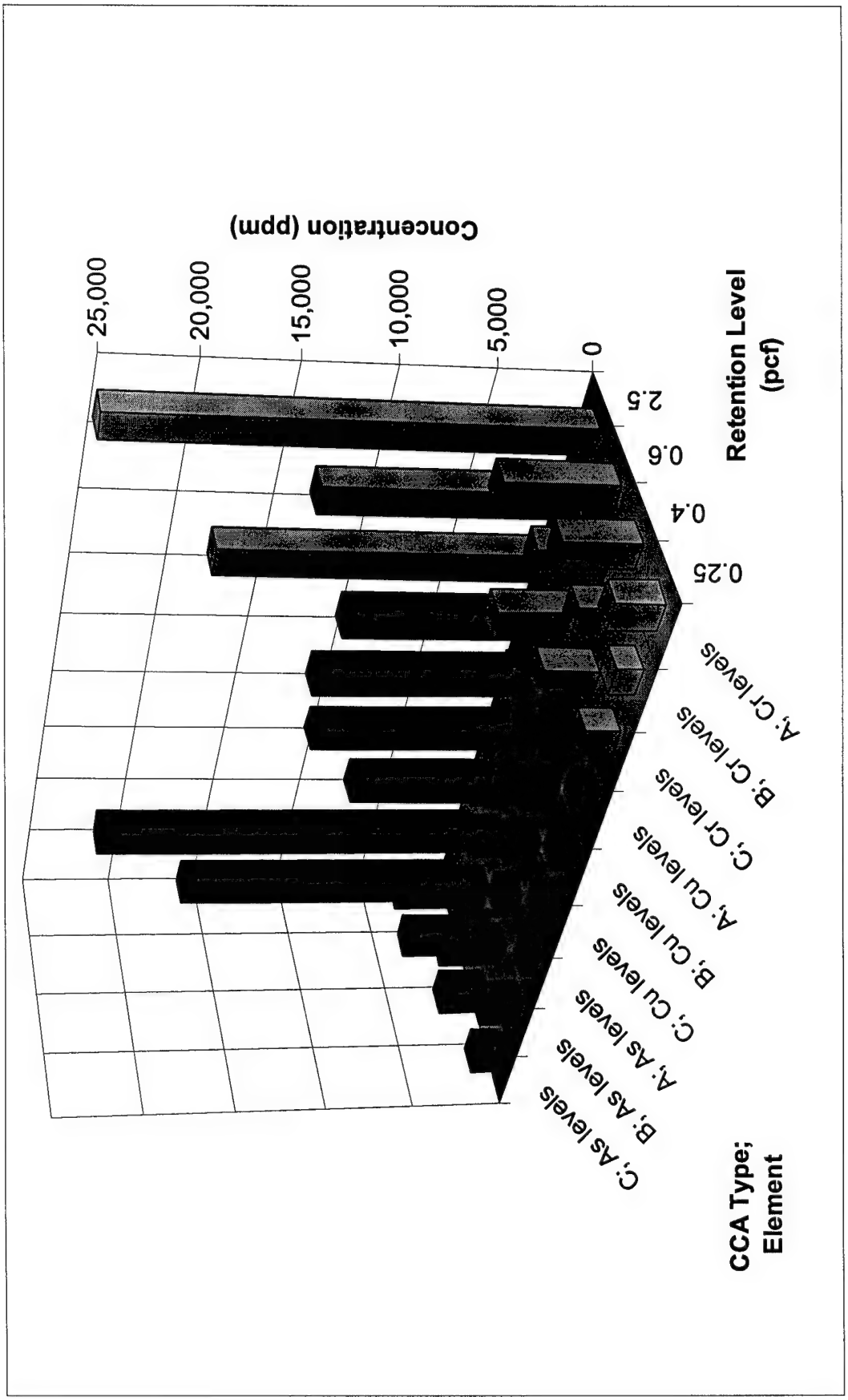

Figure B.3: Metal Concentration as a Function of CCA Type and Retention Level

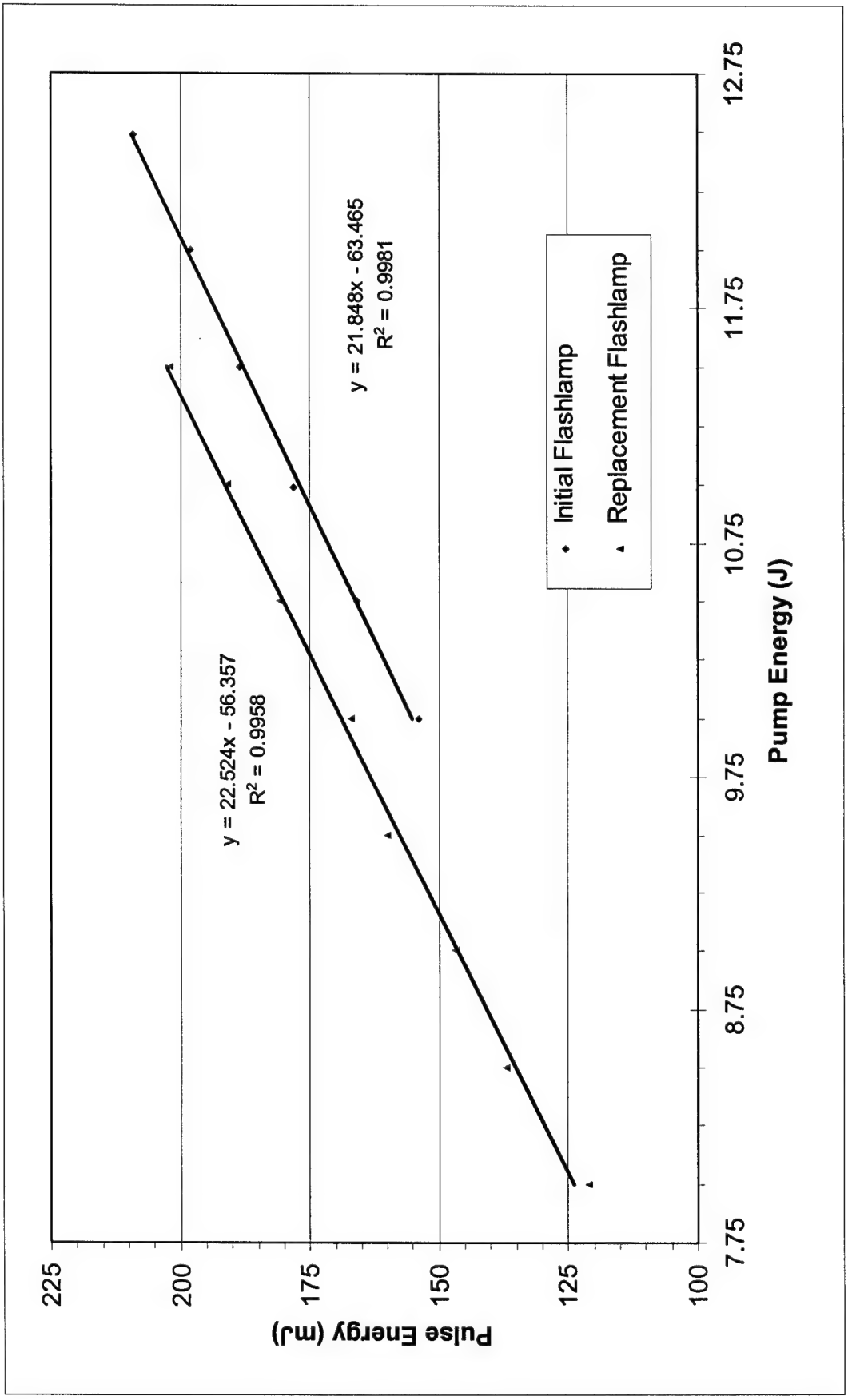

Figure B.4: Comparison of the Initial and Replacement Flashlamp Pulse Energy vs. Pump Energy for the 200 mJ Laser

REFERENCES

American Wood Preservers Association (1996) *Standards*. Granbury, TX.

American Wood Preservers Institute (1996) *Wood Preserving Industry Production Statistical Report*. Fairfax, VA:AWPI.

Andrews, D.L. (1997) *Lasers in Chemistry*, Third Edition. Springer, Berlin.

Atkins, R.S., and Fehrs, J.E. (1992) *Wood Products in the Waste Stream: Characterization and Combustion Emissions*. Energy Authority, Report 92-8, Vol.1. New York State Energy Research and Development Authority, New York.

Barbini, R., Calao, F., Fantoni, R., Palucci, A. and Capitelli, F. (1999) Application of Laser Induced Breakdown Spectroscopy to the Analysis of Metals in Soils. *Applied Physics A-Materials Science & Processing*. 69(7):S175-S178.

Biocycle (1996) Sorting C&D into Wood Products. *Biocycle*, 37(11):39-42.

Buckley, S.G., Johnson, H.A., Hencken, K.R. and Hahn, D.W. (2000) Implementation of Laser Induced Breakdown Spectroscopy as a Continuous Emissions Monitor for Toxic Metals. *Waste Management*. 20 (5-6):455-462.

Environmental Protection Agency (2001) *RCRA Orientation Manual*. U.S. Environmental Protection Agency. Retrieved May 15, 2001 from http://www.epa.gov/epaoswer/general/orientat.

Fehrs, J.E. (1995) *Air Emissions and Ash Disposal at Wood Burning Facilities*. C.T. Donovan Associates, Inc., Burlington, VT.

Fields, S. (2001) Caution-Children at Play: How Dangerous is CCA Treated Wood? *Environmental Health Perspectives*. 109(6):A262-A269.

French, N.B., Haas, W. and Priebe, S. (2000) Status of Multimetal Continuous Emission Monitoring Technologies. *Spectroscopy*. 15(7):24-32.

Gaba, J.M. and Steever, D.W. (1995) *Law of Solid Waste Pollution and Recycling*. Clark Boardman Callaghan/ Thomas Legal Publishing, Inc., Deerfield, IL.

Hahn, D.W., Flower, W.L. and Hencken, K.R. (1997) Discrete Particle Detection and Metal Emissions Monitoring using Laser-Induced Breakdown Spectroscopy. *Applied Spectroscopy*. 51:1836-1844.

Hahn, D.W. and Lunden, M.M. (2000) Detection and Analysis of Aerosol Particles by Laser-Induced Breakdown Spectroscopy. *Aerosol Science and Technology*. 33:30-48 .

Hauserman, J. (2001, March 11) Special Report: The Poison in Your Backyard. *St. Petersburg Times*. Retrieved March 29, 2001 from http://pqasb.pqarchiver.com/sptimes.

Hauserman, J. (2001, March 15) Tarpon Springs Knew of Arsenic. *St. Petersburg Times*. Retrieved March 29, 2001 from http://pqasb.pqarchiver.com/sptimes.

Hauserman, J. (2001, March 16) What to do About Arsenic? *St. Petersburg Times*. Retrieved March 29, 2001 from http://pqasb.pqarchiver.com/sptimes.

Holton, W.C. (2001) Special Treatment: Disposing of CCA-Treated Wood. *Environmental Health Perspectives*. 109(6):A274-A276.

Klein, S., Stratoudaki, T., Zafiropulos, V., Hildenhagen, J., Dickmann, K. and Lehmkuhl, T. (1999) Laser Induced Breakdown Spectroscopy for On-Line Control of Laser Cleaning of Sandstone and Stained Glass. *Applied Physics A-Materials Science & Processing*. 69(4):441-444.

Matus, R. (2001, February 22) Lawmaker Pushes for Landfill Liners. *Gainesville Sun*. Retrieved March 28, 2001 from http://www.sunone.com/articles.

Matus, R. (2001, March 14) Treated Lumber Comes under Fire in Lawsuit. *Gainesville Sun*. Retrieved May 18, 2001 from http://www.sunone.com/articles.

Matus, R. (2001, March 17) State Says Playgrounds Safe for Kids. *Gainesville Sun*. Retrieved March 28, 2001 from http://www.sunone.com/articles.

Matus, R. (2001, March 19) Treated Woods Risks Debated. *Gainesville Sun*. Retrieved May 18, 2001 from http://www.sunone.com/articles.

Matus, R. (2001, March 22) Baby Gator to Tear Down Playground. *Gainesville Sun*. Retrieved May 18, 2001 from http://www.sunone.com/articles.

Matus, R. (2001, March 23) Baby Gator Getting Help. *Gainesville Sun*. Retrieved March 28, 2001 from http://www.sunone.com/articles.

Matus, R. (2001, March 25) Special Report: Wood Worries. *Gainesville Sun*. Retrieved March 28, 2001 from http://www.sunone.com/articles.

Matus, R. (2001, April 1) Fears Rise over Wood Treatment. *Gainesville Sun*. Retrieved May 18, 2001 from http://www.sunone.com/articles.

Matus, R. (2001, April 5) Nelson Expresses Concern about CCA. *Gainesville Sun*. Retrieved May 11, 2001 from http://www.sunone.com/articles.

Matus, R. (2001, April 9) Next Step Weighed for Wood Chemical. *Gainesville Sun*. Retrieved May 18, 2001 from http://www.sunone.com/articles.

Matus, R. (2001, April 21) Arsenic Stances Contradictory. *Gainesville Sun*. Retrieved May 18, 2001 from http://www.sunone.com/articles.

Matus, R. (2001, May 4) Treated Wood Ban Fails to go Through. *Gainesville Sun*. Retrieved May 18, 2001 from http://www.sunone.com/articles.

Matus, R. (2001, May 6) Companies to Produce Safer Wood. *Gainesville Sun*. Retrieved May 18, 2001 from http://www.sunone.com/articles.

Matus, R. (2001, May 9) Nelson to file Bill for Wood Warnings. *Gainesville Sun*. Retrieved May 18, 2001 from http://www.sunone.com/articles.

Matus, R. (2001, May 12) Wood Debate. *Gainesville Sun*. Retrieved May 18, 2001 from http://www.sunone.com/articles.

McGinnis, G. (1995) *Wood Ash in the Great Lakes Region: Production, Characteristics and Regulation*. McGinnis Institute of Wood Research, Houghton, MI.

Monts, D.L., Singh, J.P, Abhilasha, Y.S., Zhang, H., Yueh, F.Y., Jang, P.R., and Singh, S.K. (1998) Toward Development of a Laser Based Continuous Emission Monitor System for Toxic Metals in Off Gasses. *Combustion Science and Technology*. 134(1-6):103-126.

Radziemski, L.J., and Cremers, D.A. (1989) *Laser-Induced Plasmas and Applications*. Marcel Dekker Inc., New York, NY.

Samek, K., Beddows, D.C.S., Telle, H.H., Morris, G.W., Liska, M. and Kaiser, J. (1999) Quantitative Analysis of Trace Metal Accumulation in Teeth using Laser-Induced Breakdown Spectroscopy. *Applied Physics A-Materials Science & Processing*. 69(7):S179-S182.

Samek, K., Beddows, D.C.S., Kaiser, J., Kukhlevsky, S.V., Liska, M., Telle H.H. and Young, J. (2000) Application of Laser Induced Breakdown Spectroscopy to in situ Analysis of Liquid Samples. *Optical Engineering*. 39(8):2248-2262.

Sandell, E.B. and Onishi, H. (1978) *Photometric Determination of Traces of Metals*. John Wiley & Sons, Toronto.

Solo-Gabrielle, H.M., Townsend, T., Penha, J., Tolaymat, T. & Calitu, V., (1998) *Generation, Use, Disposal and Management Options for CCA-Treated Wood, Final Technical Report #98-1.* Florida Center for Solid and Hazardous Waste Management, Gainesville, FL.

Solo-Gabrielle, H.M. and Townsend, T. (1999) Disposal Practices and Management Alternatives for CCA-Treated Wood Waste. *Waste Management Research.* 17:378-379.

Solo-Gabrielle, H.M., Townsend, T., Calitu, V., Messick, B., and Kormienko, M., (1999) *Disposal of CCA-Treated Wood: An Evaluation of Existing and Alternative Management Options. Final Technical Report #99-06.* Florida Center for Solid and Hazardous Waste Management, Gainesville, FL.

Solo-Gabrielle, H.M., Townsend, T., Kormienko, M., Stook, K., Gary, K. and Tolaymat, T.M. (2000) *Alternative Chemicals and Improved Disposal-End Management Practices for CCA-Treated Wood. Final Technical Report #00-03.* Florida Center for Solid and Hazardous Waste Management, Gainesville, FL.

Stilwell, D.E. and Gorny, K.D., (1997) Contamination of Soil with Copper, Chromium and Arsenic under Decks Built from Pressure Treated Wood. *Bulletin of Environmental Contamination and Toxicology.* 58(1):22-29.

Townsend, T., Solo-Gabrielle, H.M., Stook, K., Tolaymat, T.M., Song, J.K., Hosein, N and Khan, B., (2001) *New Lines of CCA-Treated Wood Research: In Service Disposal Issues.* Florida Center for Solid and Hazardous Waste Management, Gainesville, FL.

Uhl, A., Lobe, K., Kreuchwig, L. (2001) Fast Analysis of Wood Preservers using Laser Induced Breakdown Spectroscopy. In Press: *Spectrochemica Act B.* 56(6):795-806.

Vander Wal, R.L., Ticich, T.M., West, J.R. and Householder, P.A. (1999) Trace Metal Detection by Laser Induced Breakdown Spectroscopy. *Applied Spectroscopy.* 53(10):1226-1236.

Van Hecke, G.R. and Karukstis, K.K. (1998) *A Guide to Lasers in Chemistry.* Jones and Bartlett Publishers, Boston, MA.

Viire, E. (2001) A Survey of Medical Issues and Virtual Reality Technology. Retrieved on May 21, 2001 from http://www.hitl.washington.edu/projects/vestibular/article.html.

Wantland, C.A., Gupta, S.C. and Klein, S.A. (2001) Safety Considerations for Current and Future VR Applications. Retrieved on May 21, 2001 from http://www.i-med.com/mi/safety.html.

Williams, K. L. (1987) *An Introduction to X-Ray Spectrometry: X-Ray Fluorescence and Electron Microprobe Analysis.* Allen and Unwin, Inc., London.

BIOGRAPHICAL SKETCH

Thomas M. Moskal was born in Chicago, Illinois, on February 23, 1970. Upon turning 18, he enlisted in the United States Navy Reserves as an Aviation Machinist. After a brief detour to learn to fly light aircraft at Embry-Riddle Aeronautical University, he graduated the University of Illinois at Chicago in December 1994 with a Bachelor of Science in Mechanical Engineering. After completion of Officer Candidate School, he was commissioned into the United States Navy, Civil Engineer Corps, in May 1995. Following additional training at the Civil Engineers Corps Officer School, he reported to the Great Lakes Naval Training Center in October 1995 where he served as an Assistant Public Works Officer. In October 1997 Lieutenant Moskal transferred to the Resident Office in Charge of Construction Contracts, Great Lakes, where he worked as a Construction Project Manager. In August 2000 he began pursuit of a Master of Science in mechanical engineering at the University of Florida, which incorporated the efforts of this master's thesis. He is also a Registered Professional Engineer in the State of Florida.